

Final Report

ERW and Flash Weld Seam Failures

J.F. Kiefner and K.M. Kolovich

September 24, 2012



Kiefner & Associates, Inc.

585 Scherers Court

Worthington, Ohio 43085

(614) 888-8220

www.kiefner.com

Intentionally blank

Final Report

on

ERW AND FLASH WELD SEAM FAILURES

to

BATTELLE

**AS THE DELIVERABLE OF SUBTASK 1.4 ON
U.S. DEPARTMENT OF TRANSPORTATION
OTHER TRANSACTION AGREEMENT NO. DTPH56-11-T-000003**

September 24, 2012

by

J.F. Kiefner and K. M. Kolovich

**Kiefner and Associates, Inc.
585 Scherers Court
Worthington, Ohio 43085**

DISCLAIMER

This document presents findings and/ or recommendations based on engineering services performed by employees of Kiefner and Associates, Inc. The work addressed herein has been performed according to the authors' knowledge, information, and belief in accordance with commonly accepted procedures consistent with applicable standards of practice, and is not a guaranty or warranty, either expressed or implied.

The analysis and conclusions provided in this report are for the sole use and benefit of the Client. No information or representations contained herein are for the use or benefit of any party other than the party contracting with KAI. The scope of use of the information presented herein is limited to the facts as presented and examined, as outlined within the body of this document. No additional representations are made as to matters not specifically addressed within this report. Any additional facts or circumstances in existence but not described or considered within this report may change the analysis, outcomes and representations made in this report.

EXECUTIVE SUMMARY

This report presents an analysis of the causes of 280 ERW (high-frequency-welded, low-frequency-welded, and DC-welded) and Flash Weld seam failures in natural gas and hazardous liquid pipelines. The objectives of this report are to:

- Present examples of the various kinds of defects that have caused in-service and hydrostatic test failures in ERW and Flash Weld line pipe materials,
- Determine which kinds of ERW and Flash Weld seam defects remain stable throughout the life of a pipeline,
- Determine which kinds of ERW and Flash Weld seam defects may tend to grow during the life of a pipeline,
- Determine whether or not manufacturers' hydrostatic tests (mill tests) have prevented ERW and Flash Weld seam defects from failing in service,
- Determine whether prior hydrostatic tests have prevented ERW and Flash Weld seam defects from failing in service,
- Determine whether or not ductile fracture initiation models could have predicted the failure stress levels of the various kinds of defects,

Analysis of the 280 seam failures in the database produced the following findings. The types of ERW and Flash Weld anomalies that have caused failures in-service and/or during hydrostatic tests are:

- | | |
|---------------------------------------|------------|
| • Cold Welds | (99 cases) |
| • Penetrators (a short cold weld) | (8 cases) |
| • Hook Cracks | (76 cases) |
| • Cold Weld, Hook Crack Combinations | (5 cases) |
| • Stitching | (7 cases) |
| • Woody Fracture | (6 cases) |
| • Selective Seam Weld Corrosion | (24 cases) |
| • Fatigue Enlargement of Seam Defects | (37 cases) |
| • Other Cracking | (4 cases) |
| • Miscellaneous | (14 cases) |

The failure circumstances of some of these types of anomalies have important implications for pipeline integrity, and for the manner in which the remaining strength of the pipe is calculated. The failure circumstances of other types of anomalies suggest that they can be expected to have little or no impact on pipeline integrity. The details of these findings are as follows.

Cold Welds and Penetrators

Sixteen cold welds and five penetrators caused leaks in operating pipelines within their normal operating pressure ranges. These anomalies were through-wall defects as-manufactured, but they apparently were plugged with the oxide formed at high-temperatures immediately after welding (Fe_3O_4). It is reasonable to assume that all of the pipes containing these defects had been subjected to manufacturers' hydrostatic tests and/or subsequent in-situ hydrostatic tests to stress levels well in excess of their operating stress levels. It can be argued that these tests actually contributed to the formation of the leaks by causing the oxide to crack or disbond. So, hydrostatic testing cannot be relied upon to eliminate this threat. Within the current state of the art in ILI crack detection, it is likely that these kinds of anomalies are too short to be reliably detected and repaired.

Seven cold welds caused ruptures at stress levels in the range of 51 to 71 percent of SMYS. These anomalies had previously survived manufacturers' hydrostatic tests at stress levels of 75 or 85 percent of SMYS. No evidence of crack growth had been identified in conjunction with these anomalies. An explanation for these failures is that they represent pressure reversals.

Thirty-five of the 99 cold weld anomalies leaked or ruptured at hoop stress levels ranging from 85 to 100 percent of SMYS. That implies that pipelines that have been tested to such levels are less likely to exhibit an in-service rupture from a cold weld anomaly, but it does not change the fact that hydrostatic testing is not expected to prevent leaks from short, through-wall cold welds or penetrators.

Where dimensions of non-through-wall cold welds were determinable, predictions of the failure stress levels using a ductile crack initiation model (the Modified Ln-Sec model) gave unsatisfactory estimations of the actual failure pressures of most of the anomalies. In 16 of 27 cases the actual failure stress levels were less than 80 percent of the model-predicted failure stress levels. It should be noted that the other widely-used ductile fracture initiation models, API 579 Level II, PAFFC and CorLAS would be expected to produce predictions similar to that of the Modified Ln-Sec model, so it is not likely that these methods would give reliable predictions of the failure stress levels of most cold weld anomalies.

It is speculated that the reason for the inability of ductile fracture initiation models to reliably predict the failure stresses of cold welds is that most of the cold weld anomalies failed in a brittle manner. The implication of the inability of a ductile fracture model to predict the failure stress levels for most cold weld anomalies is that, even if an ILI crack tool arises that can reliably find and characterize these types of anomalies, a reliable algorithm for calculating anomaly failure stress levels will have to be discovered or developed.

Hook Cracks

All but one of the 76 hook crack failures occurred during hydrostatic tests. Because the remaining hook crack failed at a hoop stress level of 56.6 percent of SMYS, it is reasonable to assume that it failed in-service. The information provided by the contributor suggests that the failure of this defect most likely was the result of crack extension from several large pressure applications leading to a pressure reversal.

Of the 75 hook cracks that failed in hydrostatic tests, 74 failed as ruptures and only one failed as a leak. A few of the hook cracks failed at stress levels more than 5 percent below those of the manufacturers' hydrostatic tests. Because the manufacturers' tests were of only 5 to 10-second duration, it is not a stretch to believe that a 5-percent pressure reversal would be fairly common for an anomaly that barely survives the mill test.

When the failure stress level of a seam manufacturing defect is more than 5 percent below that of the mill test, it is reasonable to suspect that some factor in its test or service history has had an influence on its failure stress level even if direct evidence of such influence cannot be found. One such anomaly failed at 68.3 percent of SMYS (about 80 percent of the mill test pressure). This hook crack had undergone some ductile tearing before failing, but its final fracture path involved a sideways jump from the ductile tearing to a brittle fracture in the bondline. It is considered significant that this behavior was similar to the fracture behavior of the hook crack that is believed by many to have been the origin of the November 1, 2007 failure of the Dixie Pipeline at Carmichael MS. The latter defect, if it was indeed the origin of the failure, failed at a hoop stress level of 80 percent of the hydrostatic test it had survived 23 years prior to its failing in service.

Twelve hook cracks failed in hydrostatic tests at stress levels ranging from 80.8 to 83.8 percent of SMYS, all at stress levels below their 85-percent-of-SMYS mill test levels and in two cases at stress levels below levels of 85.2 and 88.3 percent of SMYS applied during in-situ hydrostatic tests. It is reasonable to speculate that these occurrences are attributable to pressure-cycle-induced fatigue or pressure reversals. Only one of these cases involved a gas pipeline, the other eleven cases involved liquid pipelines.

Fifty-nine of the 76 hook cracks failed at stress levels above the mill test stress levels. Most of these failed at the highest stress levels they had ever experienced. This suggests that for pipelines that have been tested to hoop stress levels of 90% of SMYS or more, any remaining hook cracks are unlikely to fail in service at the allowable operating stress level unless they become enlarged by pressure-cycle-induced fatigue.

Calculations of failure stresses were made using the Modified Ln-Sec model for 61 of the hook cracks. In 23 cases the actual failure stresses exceeded the predicted failure stresses by factors ranging from 1.03 to 1.8. In 22 cases the actual failure stresses ranged from 0.57 to 0.94 percent of the predicted values. There was essentially no correlation between the predicted and the actual failure stress levels. It should be noted that the other widely-used ductile fracture initiation models, API 579 Level II, PAFFC and CorLAS would be expected to produce predictions similar to that of the Modified Ln-Sec model, so it is not likely that these methods would give reliable predictions of the failure pressures of most hook crack anomalies.

The implication of the inability of ductile fracture models to predict the failure stress levels for hook crack anomalies is that, even if an ILI crack tool arises that can reliably find and characterize these types of anomalies, a reliable algorithm for calculating anomaly failure stress levels will have to be discovered or developed.

Cold Weld + Hook Crack

The five cases involving a combination of a cold weld and a hook crack illustrate that such combinations constitute risks to pipeline integrity that are about the same as those posed by cold welds and hook cracks separately.

Stitching

Seven failures in the database were said to have been caused by stitching. All 7 occurred at stress levels of 89.5 percent of SMYS or more. Stitching is a phenomenon associated with the fracture of low-frequency-welded ERW seams. The presence of stitching on a fracture surface is indicative of sub-optimum bonding. In the cases examined herein, it was not a threat to seam integrity. However, it is believed that stitching on occasion has been so severe as to have caused failures at stress levels below those of the stitched weld failures discussed herein.

Woody Fracture

Six failures in the database were said to have been caused by woody fracture. A woody fracture is indicative of an ERW seam region that is affected by clusters of inclusions and/or small discontinuous hook cracks. It describes the appearance of a fracture created in such a material. In the absence of some other defect such as a hook crack or a cold weld, woody fractures appeared in the database only in conjunction with hydrostatic test failures at stress levels of 94.7 percent of SMYS or more. Hence, woody fractures are not a threat to seam integrity.

Selective Seam Corrosion

Twenty-four failures in the database were caused by selective seam weld corrosion. Fourteen of the failures occurred in-service, and the stress level in one case was only 7.3 percent of SMYS. Selective seam weld corrosion failures occurred in both gas and liquid pipelines. The ability of ILI tools to detect and characterize selective seam corrosion anomalies is not as reliable as the ability to detect and characterize corrosion in the pipe body. Therefore, if ILI is used to assess a potential selective seam weld corrosion problem, an adequate number of anomalies should be examined and characterized to establish confidence in the particular ILI tool. The use of ILI is complicated by the fact that neither the models normally used to predict the remaining strength of corroded pipe nor the models used to predict failure stress levels of cracks in ductile materials can be used to predict the failure stress levels of selective seam weld corrosion anomalies.

Hydrostatic testing, if used on a periodic basis, could prevent failures from selective seam weld corrosion, but the times to failure observed for some of the anomalies in the database suggest that the maximum rate of corrosion must be known for testing to be done at the required interval to be effective. The Fessler-Rapp approach to scheduling retests for controlling SCC is probably applicable for scheduling retests for selective seam weld corrosion.

Fatigue Enlargement of Seam Defects

Thirty-seven cases of failures from fatigue enlargement of ERW and flash-weld seam defects are contained in the database. All of these occurred in liquid pipelines; none occurred in a gas pipeline. Thirteen of the failures occurred in service; 24 occurred in hydrostatic tests. Most of the fatigue cracks initiated at hook cracks (28 cases). Other fatigue initiators included mismatched edges (6 cases), one case of lack of fusion (a cold weld in a high-frequency-welded pipe), one case of a damaged edge, and one case where the initiator was referred to as an ID feature.

Pipeline operators who have identified fatigue enlargement of ERW seam defects as a threat to pipeline integrity manage the threat either by means of periodically running an appropriate ILI crack-detection tool or by conducting periodic hydrostatic tests. Scheduling of re-assessment for a fatigue threat is typically done using a “Paris-Law” model of fatigue crack growth.

It was noted in the cases of two of the failures by fatigue enlargement that ILI crack tools failed to identify the relevant anomalies as being significant. It was also seen that some of the fatigue-enlargement failures occurred at relatively short times (3 and 5 years) after a hydrostatic test.

Other Cracking

Causes of failures categorized as “other cracking” included sulfide stress cracking starting at a hook crack in a flash-welded seam in a gas pipeline, two cases of SCC starting at hook cracks in ERW seams, and a case of hydrogen stress cracking starting at a small hook crack in the excessively hard heat-affected zone of a 1949-vintage Youngstown pipe. These occurrences were the result of unique circumstances and are not considered a systematic risk.

Miscellaneous Causes

Fourteen failures in the database were attributed to miscellaneous causes. To the extent that most of these appeared to be similar to cold welds or hook cracks the miscellaneous defects constitute risks to pipeline integrity that are about the same as those posed by cold welds or hook cracks.

Significance of the Pipe Vintages Involved in the Failures

The vintages of pipe involved in cold weld, hook crack, selective seam weld corrosion, and fatigue failures were analyzed to see if the year of installation had a significant influence on the numbers of failures.

The year 1970 is seen to be significant. Only 6 of 96 cold weld failures occurred in pipe manufactured after 1970. Only two hook crack failures out of 77 occurred in pipe manufactured after 1970. None of the 24 selective seam weld failures occurred in pipe manufactured after 1970, and only 3 of 37 fatigue failures occurred in pipe manufactured after 1970. While it is true that somewhere around 80 percent of the pipelines in the U.S. were installed prior to 1970, the track record of failures involving pipe of pre-1970 vintage is clearly not as good as that of pipe manufactured after 1970.

These findings do not mean that seam integrity is not an issue for ERW pipe made after 1970, but they certainly indicate that the focus should be on pre-1970 pipe in order to gain significant improvements in seam integrity.

Recap

The main findings of this study are as follows.

1. The primary threats to the seam integrity of ERW and Flash-Welded pipe arise from cold welds, hook cracks, selective seam weld corrosion, and enlargement of seam defects by pressure-cycle-induced fatigue. On the basis of the failures analyzed, only liquid pipelines, not gas pipelines, exhibited failures from the fatigue crack growth phenomenon. Defects in gas pipelines are not necessarily immune to fatigue crack

- growth, but because of the relatively non-aggressive rate of pressure cycling both in terms of frequency and amplitude compared to the typical rates observed in liquid pipelines, one can expect that such failures in gas pipelines are not likely to occur as soon after pipeline commissioning as they do in liquid pipelines.
2. In-service leaks from short cold welds and/or penetrators cannot be prevented by hydrostatic testing. The evidence suggests that testing has probably contributed to such leakage.
 3. Cold weld failures in LF-ERW and DC-ERW materials tended to be initiated in a brittle manner. Failures at stress levels well below that of a previous test have occurred.
 4. Commonly used ductile fracture initiation models gave unsatisfactory predictions of the failure stress levels of cold weld defects. The model predictions nearly always overestimated the actual failure stress by a significant amount. The reason is believed to be associated with the tendency of cold welds to fail in a brittle manner.
 5. Hydrostatic tests eliminated many cold weld defects though not the type of short, through-wall, oxide-filled cold weld that becomes a leak when the oxide becomes degraded.
 6. Hook cracks appeared not to be a significant cause of in-service failures unless they were enlarged by fatigue crack growth.
 7. One hook crack failure in the database seems to be very similar to the presumed failure of the hook crack that many believe was the origin of the Carmichael failure.
 8. Hydrostatic tests eliminated many hook cracks.
 9. Commonly used ductile fracture initiation models gave unsatisfactory predictions of the failure stress levels of hook crack defects. There was essentially no correlation between the predicted and the actual failure stress levels.
 10. Neither the models normally used to predict the remaining strength of corroded pipe nor the models used to predict failure stress levels of cracks in ductile materials can be used to predict the failure stress levels of selective seam weld corrosion anomalies.
 11. Commonly used ductile fracture initiation models appeared to be usable for the assessment of defects enlarged by fatigue crack growth.
 12. The inability of ductile fracture initiation models to predict failure stress levels for cold welds, hook cracks, and selective seam weld corrosion means that the current use of such models to predict the failure stress levels of these types of anomalies detected and sized by ILI crack tools is unreliable.
 13. Serious fatigue-enlarged anomalies were not identified as such by ILI crack tools in two of the cases reviewed.

14. Hydrostatic testing to levels in excess of 90 percent of SMYS appears to be a satisfactory means of controlling seam-integrity threats even though it is not helpful in eliminating leaks at short cold welds or penetrators.
15. Setting the proper interval for periodic hydrostatic tests is essential. In-service failures of both selective seam weld corrosion and fatigue-enlarged seam defects could have been prevented by a timely hydrostatic test.
16. The means of establishing appropriate retest intervals to prevent in-service failures from ERW and flash-welded seam anomalies are available. Techniques for predicting such intervals are presented herein for anomalies that might grow by fatigue or by selective seam weld corrosion.
17. Pre-1970 materials pose by far the greatest risk of seam failures.
18. While hydrostatic testing appears to be an effective means of preventing some failures from various types of ERW seam anomalies, the short duration of the manufacturers' hydrostatic test (mill test 5 or 10 seconds) appears to limit its effectiveness. Data presented herein suggest that mill test level is probably no more than 95% as effective as an in-situ hydrostatic test where the same pressure level is held for minutes to hours.
19. The risk of hard heat-affected zone cracking associated with late 1940s through the 1950s Youngstown pipe has been known for some time. One such failure was included in the database of ERW seam failures presented herein. Operators who have that vintage of Youngstown pipe have to take steps to minimize the chances of atomic hydrogen being generated at the ID surface of the pipe from internal sour components or from excess cathodic protection at the OD surface.

Recommended responses are as follows.

1. Review other fracture initiation models such as brittle fracture initiation models to determine whether or not they can be used for more accurate assessments of ILI data. (Will be addressed under Subtask 2.4.)
2. Evaluate techniques to determine the effective toughness levels and flow stress levels of the bondlines and heat-affected zones of ERW and flash-welded seams. (Will be addressed under Subtask 2.3.)
3. Evaluate the effectiveness of fatigue crack growth models. (Will be addressed under Subtask 2.5.)
4. Continue to collect and analyze ERW and flash-welded seam failure data. (Could be done if renewed funding for Subtask 1.4 becomes available.)
5. Evaluate effectiveness of ILI crack tools based on actual examples of tool runs and follow-up inspections. (Will be addressed under Subtask 1.3.)

6. Evaluate effectiveness of hydrostatic testing for preventing in-service failures from ERW and flashed-welded seam anomalies based on actual examples. (Will be addressed under Subtask 1.2.)

Intentionally blank

TABLE OF CONTENTS

EXECUTIVE SUMMARY	ES-1
Cold Welds and Penetrators.....	ES-2
Hook Cracks.....	ES-3
Cold Weld + Hook Crack	ES-4
Stitching	ES-4
Woody Fracture	ES-4
Selective Seam Corrosion	ES-5
Fatigue Enlargement of Seam Defects.....	ES-5
Other Cracking.....	ES-6
Miscellaneous Causes	ES-6
Significance of the Pipe Vintages Involved in the Failures	ES-6
Recap.....	ES-6
INTRODUCTION	1
Acknowledgements.....	1
BACKGROUND.....	2
Line Pipe Steel	2
ERW Pipe Manufacturing.....	3
Low-Frequency-Welded ERW (LF-ERW) Pipe.....	4
Direct-Current-Welded ERW (DC-ERW) Pipe.....	6
High-Frequency-Welded ERW (HF-ERW) Pipe.....	7
Electric Flash-Welded (EFW) Pipe	8
DESCRIPTION OF THE DATABASE OF ERW AND FLASH-WELDED SEAM FAILURES	10
ANALYSIS OF THE SEAM FAILURES BY TYPE OF DEFECT	13
Cold Welds.....	13
CW Case Number 1	26
CW Case Number 2	26
CW Case Number3	27
CW Case Number 4	27
CW Case Number 5	27
CW Case Number 6	27
CW Case Number 7	28

CW Case Number 8	28
CW Case Number 9	28
CW Case Number 10	29
CW Case Number 11	29
CW Case Number 12	29
CW Case Number 14	30
CW Case Number 15 and CW Case Number 29	30
CW Case Number 16	31
CW Case Number 20	31
CW Case Number 22	32
CW Case Number 31	32
CW Case Number 33 and Case Number 34	32
CW Case Number 45	33
CW Case Number 53	33
CW Case Number 54 and CW Case Number 55	33
Summary of Cold Weld Failures	34
Penetrators	37
Hook Cracks	39
HC Case Number 1	48
HC Case Number 2	48
HC Case Number 3	50
HC Case Number 4	50
HC Case Numbers 11 and 12	51
HC Case Number 5	51
HC Case Numbers 6, 14, and 16	51
HC Case Numbers 7 and 10	52
HC Case Numbers 8	52
HC Case Number 9	52
HC Case Number 13	53
HC Case Number 15	53
Summary of Hook Crack Failures	53
Cold Weld + Hook Crack	56
CW+HC Case Number 1	57

Stitching	59
Woody Fracture	61
Selective Seam Weld Corrosion	63
Overview	63
Selective Seam Weld Corrosion Incidents in the Database	66
Details of Selected Individual Failures	71
A Method for Determining Re-Assessment Intervals for Selective Seam Weld Corrosion if Hydrostatic Testing is the Method of Re-Assessment	78
Summary of the Findings on Selective Seam Weld Corrosion.....	79
Pressure-Cycle-Induced-Fatigue	79
Details of Selected Individual Failures	85
Summary of Fatigue Failures.....	118
Other Cracking.....	119
OC Case Number 1 (Hook Crack + Sulfide Stress Cracking).....	119
OC Case Number 2 (HC+SCC).....	122
OC Case Number 3 (Hook Crack + SCC)	122
OC Case Number 4 (Hydrogen Induced Cracking).....	123
Summary of Other Cracking Failures	126
Miscellaneous Causes	126
DISCUSSION	128
Cold Welds and Penetrators.....	129
In-Service Leaks	129
In-Service Ruptures	130
Ruptures and Leaks at Stress Levels above Operating Stress Ranges.....	130
Failure Stress Prediction	130
Hook Cracks.....	131
In-Service Ruptures	131
Hydrostatic Test Failures	131
Ruptures at Stress Levels above the Mill Test Stress Levels.....	133
Failure Stress Prediction	133
Cold Weld + Hook Crack	134
Stitching	134
Woody Fracture	134

Selective Seam Corrosion	134
Fatigue Enlargement of Seam Defects.....	135
Other Cracking.....	136
Miscellaneous Causes	136
Significance of the Pipe Vintages Involved in the Failures	137
REFERENCES	141

LIST OF FIGURES

Figure 1. A Low-Frequency Welder	5
Figure 2. Metallographic Section across a Low-Frequency-Welded ERW Seam.....	6
Figure 3. Metallographic Section across a DC-ERW Seam	6
Figure 4. A High-Frequency Welder	7
Figure 5. Metallographic Section across a High-Frequency-Welded ERW Seam	8
Figure 6. Appearance of a Flash-Welded Seam as seen at the OD Surface of a Piece of Flash-Welded Pipe.....	8
Figure 7. Metallographic Section across a Flash-Welded Seam.....	10
Figure 8. Through-wall Cold Weld on a Fracture Surface of Leak in a LF-ERW Pipe that was Broken Open after Being Chilled in Liquid Nitrogen (repetitive pattern is “stitching”).....	14
Figure 9. Appearance of the Cold Weld on a Metallographic Section across the Weld shown in Figure 8 (taken at the location of the yellow line in Figure 8)	14
Figure 10. Section across an Intact Portion of the Seam Shown in Figure 8.....	15
Figure 11. Another Section across a Cold Weld in LF-ERW Pipe.....	15
Figure 12. Periodic Cold Welds (coincident with the stitch pattern) on a Surface Broken After Chilling (LF-ERW Pipe).....	15
Figure 13. Part-Through Cold Weld in LF-ERW Pipe	16
Figure 14. Appearance of a “Penetrator” on a Surface Broken after Chilling (HF-ERW Pipe)..	16
Figure 15. Surface Broken After Chilling Showing a Cold Weld Leak in DC-ERW Pipe	17
Figure 16. Cross Section of the Cold Weld Shown in Figure 15 Showing Evidence of Strain Possibly Produced by a Hydrostatic Test to a Stress Level of 96.6% of SMYS	17
Figure 17. Cold Weld in LF-ERW Pipe Containing Melted Material	17
Figure 18. Fracture Surface of a Rupture at a Cold Weld in HF-ERW Pipe Showing Relatively Ductile Behavior	18
Figure 19. Cross Section of the Cold Weld Shown in Figure 18.....	18
Figure 20. Fracture Surface of a Rupture at a Cold Weld in HF-ERW Pipe Showing Relatively Brittle Behavior.....	18

Figure 21. Cross Section of the Cold Weld Shown in Figure 20.....	18
Figure 22. Stress at Failure for CW Leaks.....	34
Figure 23. Stress at Failure for CW Ruptures.....	35
Figure 24. Actual Failure Stress Levels of Cold Welds Compared to Failure Stress Levels Predicted Using Base Metal Properties.....	36
Figure 25. A Penetrator Shown on a Surface Created by Chilling and Breaking the Sample.....	38
Figure 26. Hook Crack Seen on a Fracture Surface.....	39
Figure 27. Cross Section of Hook Crack Shown in Figure 26 (Note that the end of the hook crack was close to the bondline and that the fracture jumped into the bondline.).....	40
Figure 28. Cross Section of Hook Crack Where End of Hook Crack Was Not Close to the Bondline (Note that the fracture propagated in the heat-affected zone of the base metal.)....	40
Figure 29. Cross Section of a Flash-Welded Seam Where the Hook Crack Extended Far From the Bondline (Failure is in the base metal.)	41
Figure 30. Cross Section of a Small Hook Crack near a Low-Frequency-Welded Seam	41
Figure 31. Cross Section across HC Case Number 2 Defect.....	49
Figure 32. Metallographic Section across Likely Origin of the Carmichael failure.....	50
Figure 33. Stress Levels of Hook Crack Failures	54
Figure 34. Ratio of Actual Failure Stress to Predicted Failure Stress	55
Figure 35. Depths of Hook Cracks	56
Figure 36. Leak Associated with an OD-connected Hook Crack and ID-connected Cold Weld	58
Figure 37. Metallographic Section across Leak Associated with a Cold Weld and a Hook Crack Showing that the Leak Path was the Result of Ductile Tearing Between the Two Anomalies	58
Figure 38. Stitch Pattern on a Fracture of the Bondline of a LF- ERW Seam.....	59
Figure 39. Fracture Surface of a Woody Fracture – Case Number W2.....	61
Figure 40. Metallographic Section across Woody Fracture – Case Number W2.....	61
Figure 41. Fracture Surface of a Woody Fracture – Case Number W3.....	62
Figure 42. Metallographic Section across Woody Fracture – Case Number W3.....	62
Figure 43. Selective Seam Weld Corrosion.....	65
Figure 44. Selective Seam Corrosion with a Grooving Ratio of About 2 in a High-Frequency- Welded Seam	66
Figure 45. Failure Stress Levels of Selective Seam Weld Corrosion Failures	69
Figure 46. Times to Failure after Pipeline Installation for Selective Seam Corrosion Anomalies	69

Figure 47. Times to Failure after the Most Recent Hydrostatic Test for Selective Seam Corrosion Anomalies	70
Figure 48. Actual Failure Stress Levels of Selective Seam Weld Corrosion Anomalies Compared to Failure Stress Levels Predicted Using Base Metal Properties	71
Figure 49. Selective Seam Weld Corrosion Case Number 1	71
Figure 50. Close-up of the Selective Seam Corrosion in Case Number 1 Showing that it Was Not Centered on the Bondline.....	72
Figure 51. Selective Seam Weld Corrosion in Case Number 2 showing a Relatively Blunt Corrosion Tip	73
Figure 52. SSWC Case Number 9 Anomaly as It Appeared on the Fracture Surfaces	74
Figure 53. Cross Section of SSWC Case Number 9 Anomaly	74
Figure 54. Cross Section of a Nearby Intact SSWC Anomaly	75
Figure 55. SSWC Case Number 12 Anomaly as it Appeared on the Fracture Surfaces	75
Figure 56. Cross Section of SSWC Case Number 12 Anomaly	76
Figure 57. Cross Section of SSWC Case Number 14 Anomaly	77
Figure 58. Cross Section of SSWC Case Number 15 Anomaly	78
Figure 59. Failure Stress Levels for Fatigue-Enlarged Anomalies that Failed in Hydrostatic Tests	82
Figure 60. Failure Stress Levels for Fatigue-Enlarged Anomalies that Failed In-Service	83
Figure 61. Times to Failure After Pipeline Installation for Fatigue-Enlarged Anomalies	83
Figure 62. Times to Failure In Service after a Hydrostatic Test for Fatigue-Enlarged Anomalies	84
Figure 63. Ratios of Actual to Predicted Failure Stresses for Fatigue-Enlarged Anomalies.....	85
Figure 64. Cross Section of Fatigue Case Number 1 Anomaly	86
Figure 65. Fracture Surfaces of Fatigue Case Number 2 Anomaly	87
Figure 66. Cross Section of Fatigue Case Number 2 Anomaly	88
Figure 67. Cross Section of Fatigue Case Number 3 Anomaly	89
Figure 68. Fracture Surfaces of Fatigue Case Number 4 Anomaly	90
Figure 69. Cross Section of Fatigue Case Number 4 Anomaly	91
Figure 70. SEM Image of Possible Fatigue Crack Area, 6500X	92
Figure 71. Fracture Surfaces of Fatigue Case Number 5 Anomaly	93
Figure 72. Cross Section of Fatigue Case Number 5 Anomaly	93
Figure 73. Fracture Surfaces of Fatigue Case Number 6 Anomaly	94
Figure 74. Cross Section of Fatigue Case Number 6 Anomaly	94

Figure 75. Fracture Surfaces of Fatigue Case Number 7 Anomaly	95
Figure 76. Cross Section of Fatigue Case Number 7 Anomaly	95
Figure 77. Fracture Surfaces of Fatigue Case Number 8 Anomaly	97
Figure 78. Cross Section of Fatigue Case Number 8 Anomaly	98
Figure 79. Cross Section of Fatigue Case Number 9 Anomaly	99
Figure 80. Fracture Surfaces of Fatigue Case Number 10 Anomaly	100
Figure 81. Cross Section of Fatigue Case Number 10 Anomaly	100
Figure 82. Fracture Surfaces of Fatigue Case Number 11 Anomaly	102
Figure 83. Cross Section of Fatigue Case Number 11 Anomaly	103
Figure 84. Fracture Surfaces of Fatigue Case Number 12 Anomaly	104
Figure 85. Cross Section of Fatigue Case Number 15 Anomaly	107
Figure 86. Cross Section of Fatigue Case Number 18 Anomaly	108
Figure 87. Fracture Surfaces of Fatigue Case Number 19 Anomaly	110
Figure 88. Cross Section of Fatigue Case Number 19 Anomaly	111
Figure 89. Cross Section of Fatigue Case Number 23 Anomaly	112
Figure 90. One Fracture Surface of the Anomaly that Raises Doubts about Fatigue Being the Crack Growth Mechanism	112
Figure 91. A Metallographic Section that Raises Doubts about Fatigue Being the Crack Growth Mechanism	113
Figure 92. Pipe Surface Showing Anomalies in the Flash-Welded Seam of the Pipe in Fatigue Case Number 24.....	114
Figure 93. Cross Section of Fatigue Case Number 27 Anomaly	116
Figure 94. Fracture Surface of Fatigue Case Number 36 Anomaly	117
Figure 95. Close-up of Fracture Surface Showing Ratchet Marks and Beach Marks	117
Figure 96. Cross Section of Fatigue Case Number 36 Anomaly	118
Figure 97. Fracture Surfaces of the Sulfide Stress Cracking that Took Place at an ID-Surface- Connected Hook Crack	120
Figure 98. Metallographic section across the weld showing the various stages of cracking.....	121
Figure 99. Combination of SCC and Hook Crack the Caused a Hydrostatic Test Rupture	122
Figure 100. Fracture Surface Showing SCC on the Same Plane as Hook Cracks	123
Figure 101. Fracture Surface Showing Markings Indicating the Origin to be a Small Hook Crack	124
Figure 102. Metallographic Section across the Fracture	125

Figure 103. 400X SEM Image of Fracture Surface Showing Into-the-Plane Cracks often Associated with Hydrogen Embrittlement Cracking	126
Figure 104. Pipe Vintages in Failures of Cold Welds	137
Figure 105. Pipe Vintages in Failures of Hook Cracks	138
Figure 106. Pipe Vintages in Failures of Selective Seam Weld Corrosion	138
Figure 107. Pipe Vintages in Fatigue Failures	139

LIST OF TABLES

Table 1. Number of Incidents by Cause.....	11
Table 2. Number of Failures by Pipe Manufacturer	12
Table 3. Number of Failures by Type of Fluid	12
Table 4. In-Service or Hydrostatic Test Failures	12
Table 5. Leak or Rupture Failures	13
Table 6. Number of Failures by Type of Seam.....	13
Table 7. Listing of the Cases CW1 through CW35	20
Table 8. Failure Modes and Failure Stresses of Cases CW1 through CW35	23
Table 8. (continued) Failure Modes and Failure Stresses of Cases CW36 through CW70.....	24
Table 8. (continued) Failure Modes and Failure Stresses of Cases CW71 through CW99	25
Table 9. Listing of Cases Arising from Penetrators.....	38
Table 10. Failure Modes and Failure Stresses of Cases P1 through P8.....	38
Table 11. Listing of the Cases HC1 through HC38.....	43
Table 11. (continued) Listing of the Cases HC39 through HC76.....	44
Table 12. Failure Modes and Failure Stresses of Cases HC1 through HC38	46
Table 12. (continued) Failure Modes and Failure Stresses of Cases HC39 through HC76.....	47
Table 13. Listing of Cases Arising from Combinations of a Cold Weld and a Hook Crack.....	56
Table 14. Failure Modes and Failure Stresses of Cases Arising from Combinations of a Cold Weld and a Hook Crack	57
Table 15. Listing of Cases Arising from Stitching	60
Table 16. Failure Modes and Failure Stresses of Failures Attributed to Stitching	60
Table 17. Listing of Cases Involving Woody Fracture.....	63
Table 18. Failure Modes and Failure Stresses of Cases of Woody Fractures.....	63
Table 19. Pipe Attributes, Failure Mode, and Type of Incident (in-service or test) for Incidents that were Attributed to SSWC (highlighted cells indicate where a reasonable guess was made where data were not available)	67

Table 20. Date of Failure, Failure Mode, Failure Stress Level, and Time-Relevant Information for Incidents That Were Attributed to SSWC (highlighted cells indicate where a reasonable guess was made where data were not available).....	68
Table 21. List of Fatigue Failures, Pipe Attributes and Type of Initiating Anomaly	80
Table 22. Failure Modes, Failure Stresses and Times to Failure for Fatigue Failure.....	81
Table 23. Pipe Attributes and Primary Causes of Failure for Miscellaneous Causes.....	127
Table 24. Failure Stress Levels and Test Histories Associated with Miscellaneous Causes.....	127

Intentionally blank

ERW and Flash Weld Seam Failures

J.F. Kiefner and K.M. Kolovich

INTRODUCTION

This report presents an analysis of the causes of 280 electric-resistance welded (ERW) and electric Flash Welded (EFW) longitudinal seam failures in natural gas and hazardous liquid pipelines. The objectives of this report are to:

- Present examples of the various kinds of defects that have caused in-service and hydrostatic test failures in ERW and EFW line pipe materials,
- Determine which kinds of ERW and EFW seam defects remain stable throughout the life of a pipeline,
- Determine which kinds of ERW and EFW seam defects may tend to grow during the life of a pipeline,
- Determine whether or not manufacturers' hydrostatic tests (mill tests) have prevented ERW and EFW seam defects from failing in service,
- Determine whether prior hydrostatic tests have prevented ERW and EFW seam defects from failing in service,
- Determine whether or not ductile fracture initiation models could have predicted the failure stress levels of the various kinds of defects.

Acknowledgements

The authors are grateful for the contributions of data by numerous pipeline operators who choose to remain anonymous. The authors are also grateful for the contributions of data by DNV.

BACKGROUND

The main thrust of this report is to address ERW and EFW pipe problems associated with older manufacturing processes. The following sections briefly describe the steels used to make these pipes and the manufacturing processes employed prior to 1980 for low-frequency-welded ERW (LF-ERW), direct-current-welded ERW (DC-ERW), high-frequency-welded ERW (HF-ERW), and electric Flash Welded (EFW) Line Pipe made in accordance with API Specifications 5L and 5LX.¹ In more recent times much has changed in the steel-making and pipe-manufacturing processes for producing ERW pipe. EFW pipe is no longer manufactured. As a result some of the problems alluded to herein have been largely eliminated. However it is important to note that the types of seam-quality issues that early ERW pipe manufacturers experienced can occur in modern ERW pipe-making facilities if quality control measures fail.

Line Pipe Steel

In the time period of primary interest to this document (the late 1920s to 1980), line pipe materials were typically fabricated from low-carbon steels made by the open-hearth furnace process or the electric-arc-melting process. Following either of these processes the molten steel was cast into ingots where some de-oxidation was attempted through the addition of silicon or aluminum. The point of de-oxidation was to minimize effervescence of gases that tended to distribute non-metallic substances throughout the molten metal where they would create laminations and non-metallic inclusions in the final product. Fully-de-oxidized steels were referred to as “fully-killed” steels; partially-de-oxidized steels were referred to as “semi-killed” steels.

The line pipe steels made prior to 1980 had carbon contents ranging from 0.2 to 0.3 percent by weight and sulfur contents ranging from 0.03 to 0.05 percent by weight. With that range of carbon, the steels tended to have a pearlite-ferrite microstructure at ambient temperatures. In conjunction with the conventional rolling practices at the time and the lack of micro-alloying additions, the resulting steels tended to have relatively large grains sizes (ASTM grain sizes 5 through 8) that are characterized by high ductile-to-brittle fracture transition temperatures. With the range of sulfur given above, the steels also tended to contain manganese-sulfide inclusions. The latter were detrimental to ductile fracture resistance.

¹ The reference for the pipe-manufacturing processes described in this section is *History of Line Pipe Manufacturing in North America* by J.F. Kiefner and E.B. Clark. ASME, 1996, New York, New York. ISBN 0791812332.

ERW Pipe Manufacturing

ERW pipe typically was made from hot-rolled strip steel. The strip was usually rolled to a width for a particular pipe diameter. The final wall thickness of the strip was intended to be the wall thickness of the finished pipe. Following rolling, the strip was coiled while still red hot. The coils were allowed to cool to room temperature. Subsequently, the coils were shipped to a pipe mill for the making of ERW pipe.

Typically, the coils were unrolled at room temperature and fed into a continuous processing line that begins with the leveling mill that flattens the strip. The strip at this point is referred to as pipe “skelp”. Most pipe mills had a “traveling looper” of some sort at the beginning of the line that periodically was activated to allow one end of the strip to continue to move into the pipe forming stand while the other end was held stationary so that a new coil could be flash-welded to the end of the skelp. Skelp welds were later removed as they were not intended to be left in a finished pipe. For small-diameter pipe (8.625 inch or less) wider coils were typically slit in half or into thirds. Slit skelp was usually re-coiled so that it could be moved from the slitter to the forming and welding line.

The uncoiled skelp was first leveled. Then, the edges were trimmed or skived to bring the skelp to the proper width for the intended pipe diameter and to properly prepare the edges for welding. The skelp proceeded into the forming stand where it was cold-formed in stages into a round “can”. The last stage of forming usually consisted of a “fin” pass, that is, a set of rollers, one of which has a narrow ridge against which the edges of the skelp were firmly pressed to align them for welding. The can then passed through the welding stand where electric current was employed to heat and soften the edges as they were mechanically forced together between a set of rollers. It was intended that the edges should bond together without actual melting of the steel². Material was extruded towards the inside and outside pipe surfaces during this welding process. Immediately upon completion of the weld, the excess material that was radially extruded was trimmed away. The weld was then given a post-weld heat treatment via induced electric current. The weld location was then sprayed with water to cool it. As the welded can moved out from the cooling stand it was usually subjected to sets of sizing and straightening rolls. Finally, a traveling cut-off saw was employed to cut the can into the desired lengths, usually, 40, 60, or 80-foot lengths.

After the ERW pipes had been cut into 40, 60, or 80-foot-lengths, the ends were typically beveled at the pipe mill for subsequent welding in the field, and then each piece was subjected to a hydrostatic test for 5 or 10 seconds to a stress level ranging from 60 percent of the specified

² The melting temperature of a low-carbon steel is about 2730°F. Bonding can be achieved at slightly lower temperatures.

minimum yield strength (SMYS) to 90 percent of SMYS depending on the size and grade of the pipe. The finished and tested pipes were then measured, weighed, and marked with certain required information such as wall thickness, grade, and mill test pressure. Prior to 1962, seam inspection by the manufacturer may or may not have been limited to visual inspection. A few manufacturers also used techniques such as magnetic particle inspection or ultrasonic inspection to examine the ERW seams. After 1962, manufacturers were required by API specification 5L to provide non-destructive examination of the entire seam of each piece of pipe. Most chose to do that by means of ultrasonic angle-beam inspection.

Manufactures of API 5L Line Pipe were required to provide mechanical test results and chemical analyses for the pipe made from each heat³ of steel or for subsets of large heats of steel. The tests included evaluating the yield strength, ultimate strength, and elongation of the base metal, tensile strength perpendicular to the seam weld, and flattening tests of ring specimens to evaluate bondline quality. The chemical analyses for percent by weight of the elements, carbon, manganese, phosphorus, and sulfur were compared to maximum allowable limits. Materials that did not pass any one of these tests or limits were to be rejected. A significant loop hole in these specifications was created by the fact only the pipe associated with failure to meet one of the limits was rejected if test results on a second pipe passed. Beyond that, a manufacturer was permitted to test each piece and reject only those that failed one or more tests. It is unlikely that a whole heat was ever rejected.

Low-Frequency-Welded ERW (LF-ERW) Pipe

ERW pipe was introduced by Republic Steel in 1929 and variations of the original process are still in use today. Cans were formed continuously as described above, and welding was done with low-frequency alternating current (typically 120 cycles per second). A schematic of a low-frequency welder is show in Figure 1. By the late 1940s other manufacturers of LF- ERW pipe had emerged using essentially the same process.

³ A heat of steel may range from 50 to 300 or more tons depending on the steel-making process.

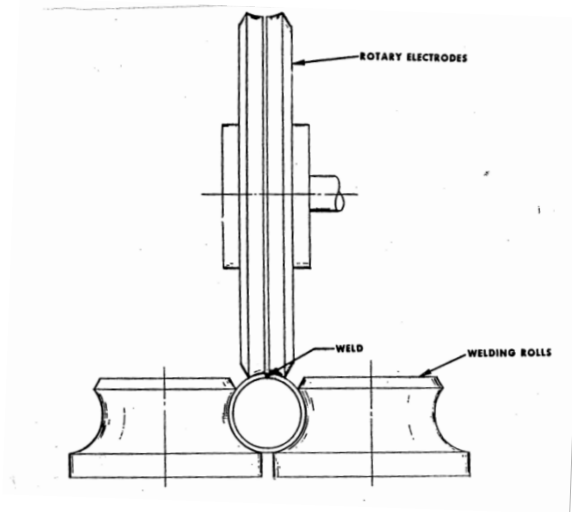


Figure 1. A Low-Frequency Welder

The low-frequency alternating current tended to penetrate deeply into the edges of the pipe. A metallographic section across a low-frequency-welded seam is shown in Figure 2. Note the rectangular shape of the heat-affected zone and the “contact marks” at the outside pipe surface on either side of the seam where the wheels shown in Figure 1 introduced current into the pipe (contact marks may not always appear in a metallographic section across a low-frequency-welded pipe – they may not appear in cases where post-weld heat treatment is applied over a wide area). Also note the grain-coarsening of the central region of the weld caused by the heat of welding and subsequent rapid cooling. This region typically possessed a ductile-to-brittle fracture transition temperature higher than that of the base metal. A ferrite-rich portion of the weld, referred to as the “bondline”, denotes the location where the two edges of the skelp or plate came together. On either side of this bondline, material flow lines can often be observed. The flow lines are parallel to the pipe surfaces outside the weld zone, and become upturned and nearly perpendicular to the pipe surfaces at the bondline. When the steel was rolled into strips, the microstructure became elongated and parallel with the rolling direction. As the weld was formed and material was extruded towards the outside and inside pipe surfaces, the orientation of microstructure changed to follow the flow of the material.

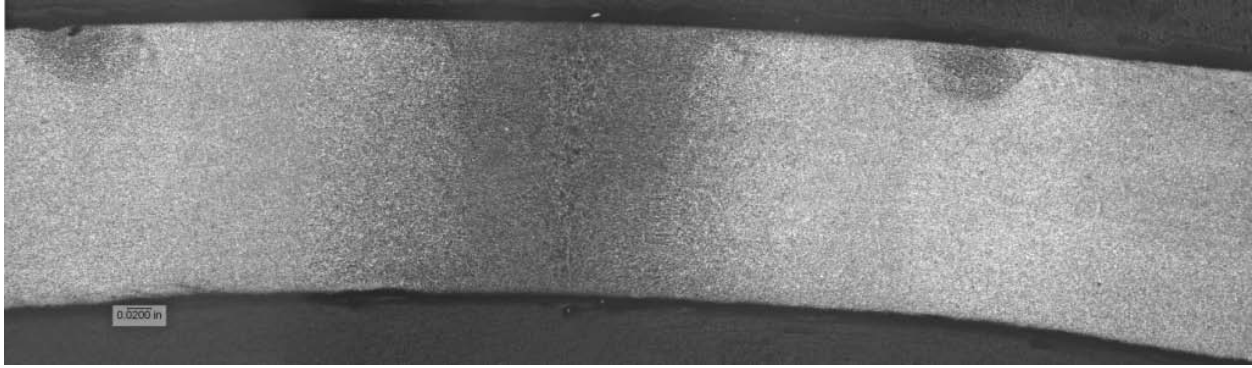


Figure 2. Metallographic Section across a Low-Frequency-Welded ERW Seam

Direct-Current-Welded ERW (DC-ERW) Pipe

ERW pipe made with direct current was introduced around 1930 by Youngstown Sheet & Tube Company. Individual cans were cold formed from hot-rolled plates of more than 50 feet in length. Each pipe was thus welded as a separate unit compared to the continuous process described above. A least one other manufacturer, Page-Hersey Tube, adopted this process for some time, but the DC-ERW pipe market was dominated by Youngstown until 1980 when the mill was closed. The welding electrodes used for the DC process were identical to those shown in Figure 1 above. Only the nature of the welding current was different. A metallographic section across a DC-ERW seam is shown in Figure 3. Note the similarity of the DC-welded pipe microstructure to that of the low-frequency weld, particularly the grain-coarsening and the contact marks. The DC current tended to provide a higher heat input and therefore created a wider heat affected zone than low-frequency current. Also, contact marks tended to be larger and present on every pipe.

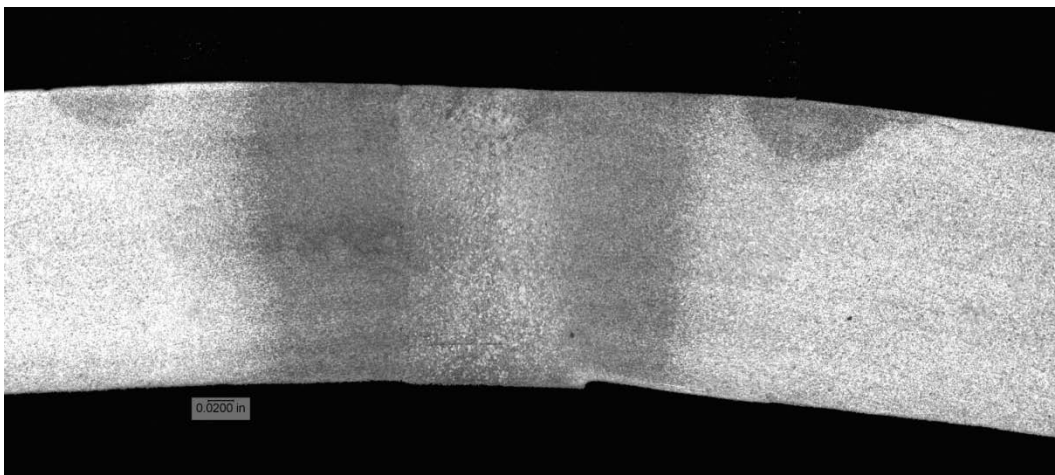


Figure 3. Metallographic Section across a DC-ERW Seam

High-Frequency-Welded ERW (HF-ERW) Pipe

Between about 1960 and 1970, most manufacturers of low-frequency-welded ERW pipe either converted to high-frequency welding (450 kilocycles per second) or went out of business. The high-frequency welding process was easier to control, the equipment was easier to maintain, and it produced weld zones with better resistance to brittle fracture than the low-frequency process. A schematic of a high-frequency welder is shown in Figure 4.

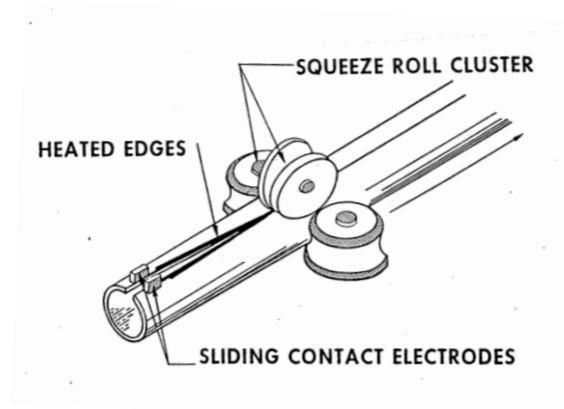


Figure 4. A High-Frequency Welder

A metallographic section across a HF-ERW seam is shown in Figure 5. The narrow, hour-glass-shaped heat affected zone is typical of a high-frequency-welded ERW seam. The contact marks are much smaller than in the case of low-frequency welding. The smaller heat-affected zone and contact marks relative to those of a low-frequency or DC-welded seam are consequences of the fact that the high-frequency current does not penetrate deeply into the material and tends to heat only the material near the bondline sufficiently to change the microstructure. The fact that little or no grain coarsening took place with high-frequency welding meant that the fracture resistance of such seams was generally superior to those formed by low-frequency welding or dc welding. As will be shown, however, the early high frequency welds often exhibited much the same kinds of manufacturing defects that tended to affect LF-ERW and DC-ERW seams.

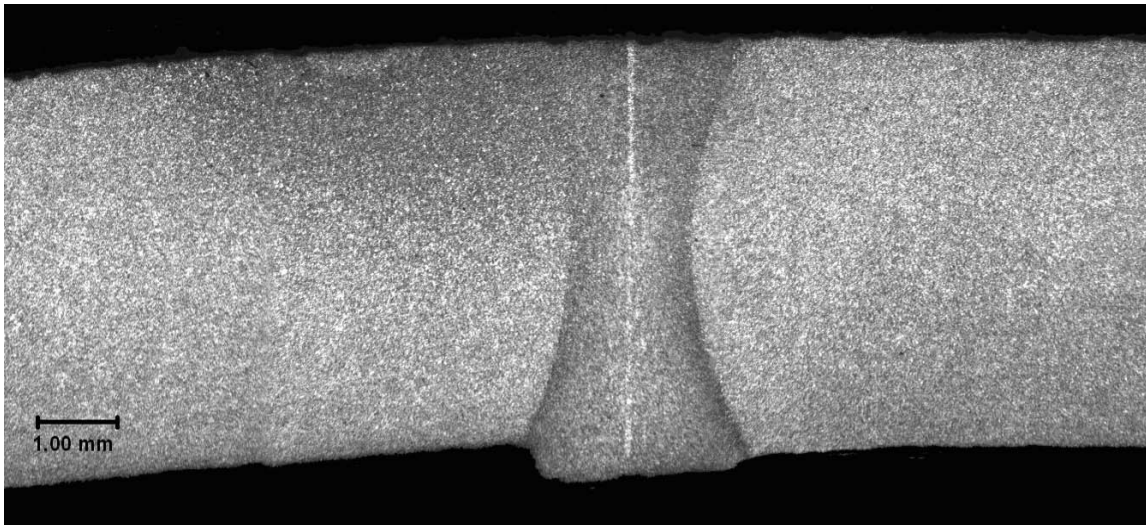


Figure 5. Metallographic Section across a High-Frequency-Welded ERW Seam

Electric Flash-Welded (EFW) Pipe

Flash-welded line pipe was made by only one manufacturer, A.O. Smith Corporation. It was made by cold-forming hot-rolled plates into round cans by “U-ing” and “O-ing” and using a flash-welding process to join the longitudinal edges of the can. The entire weld was formed in one stage. As the edges were forced together, direct electrical current was applied to heat the abutting edges. When the heated edges attained the proper temperature, the can was “bumped” to extrude excess heat-softened metal, bonding them together at the interface. Some, but not all of the extruded material at both the OD and ID surfaces was then trimmed away leaving a flat-topped ridge visible at both surfaces. The appearance of a typical flash-welded seam as viewed from the OD side of a piece of flash-welded pipe is shown in Figure 6. Because the hot-rolled plates tended to be about 40 feet in length, flash-welded pipe was supplied in 40-foot lengths.



Figure 6. Appearance of a Flash-Welded Seam as seen at the OD Surface of a Piece of Flash-Welded Pipe

After welding, the ends of each pipe were beveled, and each was sized by cold expansion initially by internal water pressure, and at a later time by mechanical means. Then, similar to ERW pipe manufacturing, each pipe was subjected to a 5 or 10-second hydrostatic test to stress levels ranging from 60 to 90 percent of SMYS depending on the size and grade of the material. Finally, each piece was measured, weighed, inspected, and marked in accordance with the edition of the API Specification 5L specification in effect at the time.

Flash-welded pipe was made between 1930 and 1968 at one of two pipe mills operated by A.O. Smith Corporation. Flash-welded pipe was initially made in sizes ranging from 8.625-inch OD to 26-inch OD. Later, 30 and 36-inch OD pipes were made as well. Pipe grades ranged from Grade B through Grade X65.

A metallographic section through a flash weld is shown in Figure 7. As was fairly typical for a flash weld, no distinct bondline is visible, but the grain-coarsening in the center of the weld is quite visible. The amount of heating needed to make the weld was sufficient to create a wide heat-affected zone. Flash Welds were not given a post-weld heat treatment until the large-diameter mill was opened. At that mill when the higher grades of pipe such as X60 and X65 were introduced, a system of gas-flame post-weld heat treatment was established. Flash-welded pipe was always made with fully-killed steel.

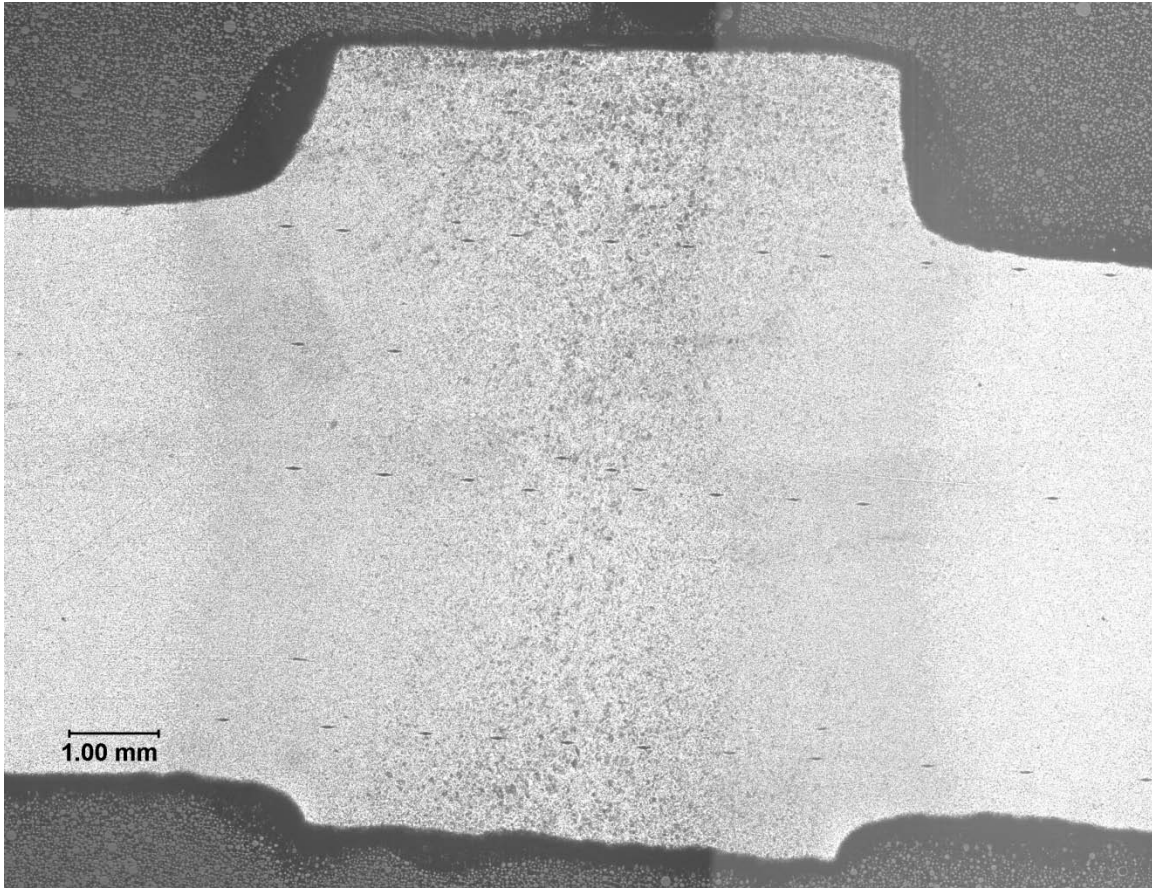


Figure 7. Metallographic Section across a Flash-Welded Seam

DESCRIPTION OF THE DATABASE OF ERW AND FLASH-WELDED SEAM FAILURES

The database contains 280 examples of ERW seam failures. Each case has been assigned a database number. The complete database is available in a spreadsheet. The numbers of failures by cause are presented in Table 1. Those highlighted in blue are consolidated into a category of “Other Cracks”. Those highlighted in purple are consolidated into a category of “Miscellaneous Causes”. The manufacturers are presented in Table 2. Other characteristics of the database are presented in Table 3 through Table 6.

Table 1. Number of Incidents by Cause

Cause	Number of Failures
Cold Weld	99
Hook Crack	76
Fatigue-Enlarged Seam Defect	37
Selective Seam Weld Corrosion	24
Penetrator	8
Stitching	7
Woody Fracture	6
Cold Weld + Hook Crack	5
Hook Crack +SCC	2
Hook Crack +Sulfide Stress Cracking	1
Hydrogen-Induced Cracking	1
Foreign Material in Weld	2
Weak Plane	2
Weld Inclusions	2
Contact Burn	1
Dent and Hook Crack	1
Lamination + Hook Crack +Cold Weld	1
Hot tear cracks	1
Unbonded layer	1
Weld Flash	1
LOF defect SW, HAC RW	1
Layers of voids and inclusions	1

Table 2. Number of Failures by Pipe Manufacturer

Manufacturer	Number of ERW Pipe Failures
A.O. Smith Corporation	37
Acme Steel Company	1
Bethlehem Steel Corporation	10
Cal-Metal Pipe Corporation	2
Huludao City Steel Pipe Industrial Co., Ltd.	1
Jones & Laughlin Steel Corporation	35
Kaiser Steel Corporation	2
Lone Star Steel Company	30
Maverick Tube Corporation	2
Newport Steel Corporation	1
Page Hersey Iron Tube & Lead Company	2
Republic Steel Corporation	42
Stupp Corporation	3
Tenaris Prudential Steel	2
TexTube Company	4
U.S. Steel Corporation	6
Youngstown Sheet and Tube Company	41
Manufacturer not specified	60

Table 3. Number of Failures by Type of Fluid

Type of Fluid	Number of Failures
Liquid	225
Gas	25
HVL	23
NGL	3
Not specified	4

Table 4. In-Service or Hydrostatic Test Failures

In-Service or Test	Number of Failures
Hydrostatic test	219
In-service	55
Not specified	6

Table 5. Leak or Rupture Failures

Leak or Rupture	Number of Failures
Leak	71
Rupture	206
Not specified	3

Table 6. Number of Failures by Type of Seam

Type of Seam	Number of Failures
Low-Frequency	153
High-Frequency	48
Direct Current	40
Flash-Welded	37
Not specified	2

ANALYSIS OF THE SEAM FAILURES BY TYPE OF DEFECT

Cold Welds

The database contains 99 incidents where the cause of failure was attributed primarily to a cold weld (CW). Cold weld refers to a localized area of a weld where no bonding has occurred between the two skelp or plate edges. Cold welds may alternatively be referred to as lack-of-fusion (LOF), however, the term cold weld will be used herein.

The non-bonded region where a complete bondline would be expected consists of a high-melting-temperature oxide that was not sufficiently heated and extruded out of the weld zone. Contamination of the skelp edges, upsets in the welding process (such as current interruptions), or non-optimal welding parameters (too low of heat input, too high a travel speed, or incorrect approach angle) are believed to be factors contributing to the creation of cold welds. Some cold welds extend entirely through the wall thickness while others do not. Those that extend entirely through the wall for only a short length of weld ($\ll 1$ inch) are sometimes referred to as “penetrators”. Penetrators are, in fact, a form of cold weld albeit a very short one. It will be seen that they are indistinguishable from cold welds in terms of their characteristics, aside from length. The 8 cases of penetrators that appear in the database are discussed separately at the end of this section on cold welds. It is expected that cold welds (or penetrators) will fail in the manufacturer’s hydrostatic test if they are large enough. However, cold welds and penetrators that are small in size will not be eliminated by the mill test.

The appearances of cold welds in metallographic cross section and fractographic examination are typified by the following photographs (Figure 8 through Figure 21).

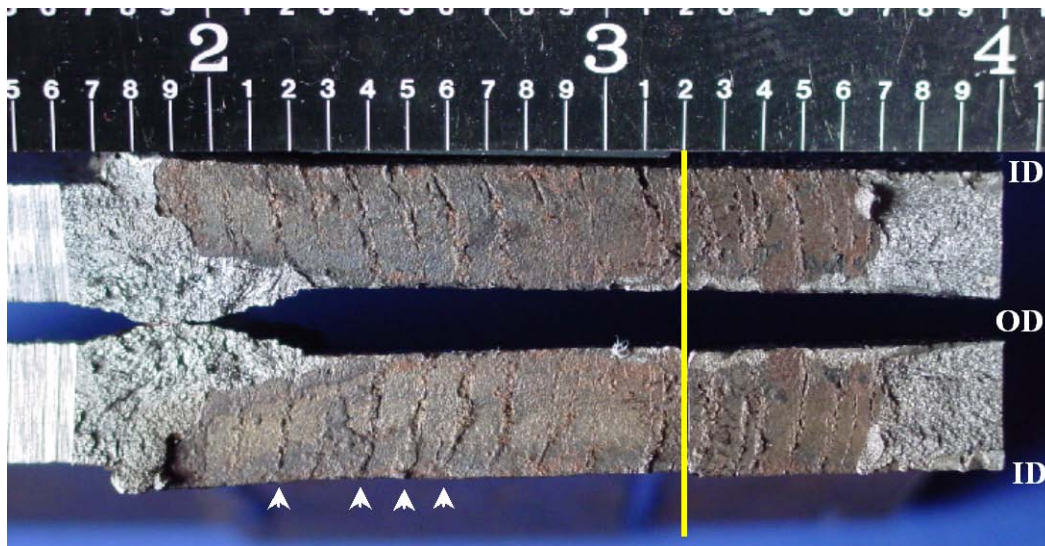


Figure 8. Through-wall Cold Weld on a Fracture Surface of Leak in a LF-ERW Pipe that was Broken Open after Being Chilled in Liquid Nitrogen (repetitive pattern is “stitching”)

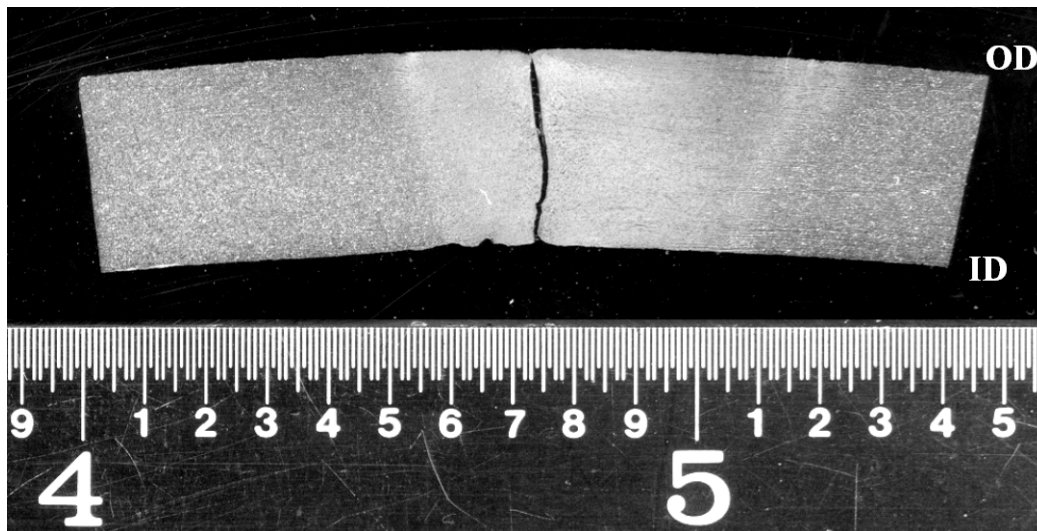


Figure 9. Appearance of the Cold Weld on a Metallographic Section across the Weld shown in Figure 8 (taken at the location of the yellow line in Figure 8)

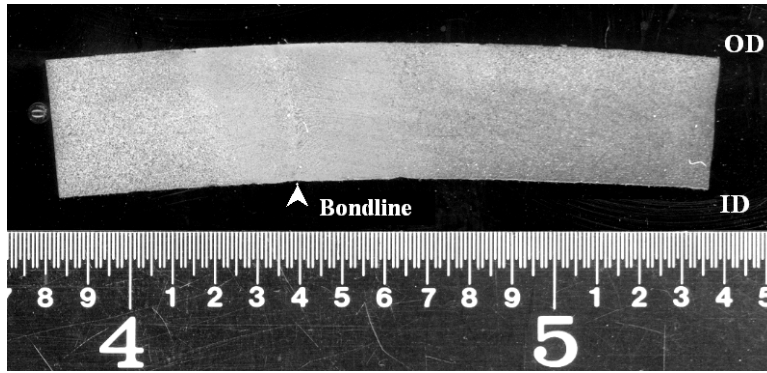


Figure 10. Section across an Intact Portion of the Seam Shown in Figure 8

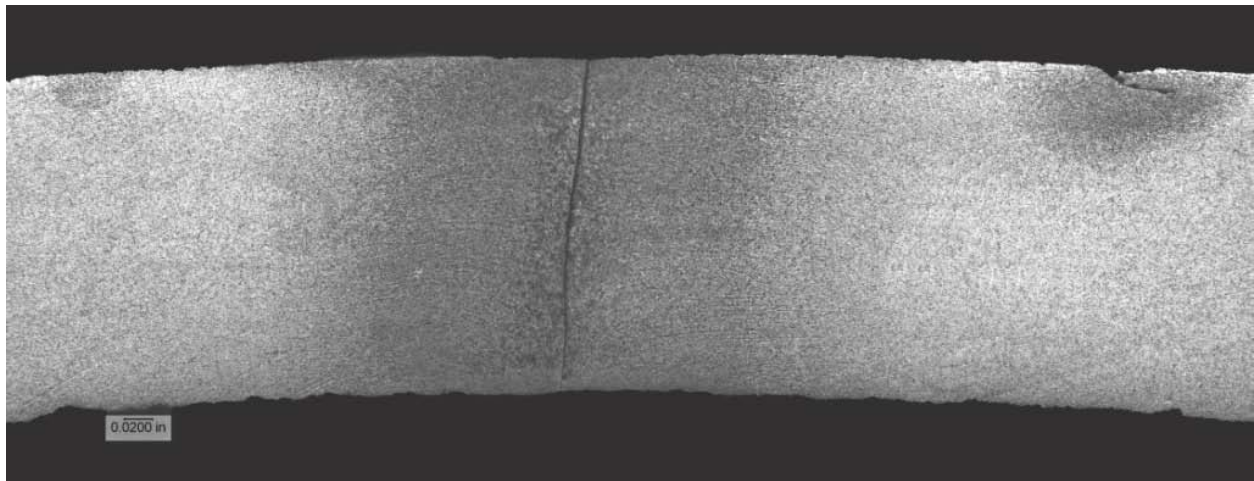


Figure 11. Another Section across a Cold Weld in LF-ERW Pipe



Figure 12. Periodic Cold Welds (coincident with the stitch pattern) on a Surface Broken after Chilling (LF-ERW Pipe)

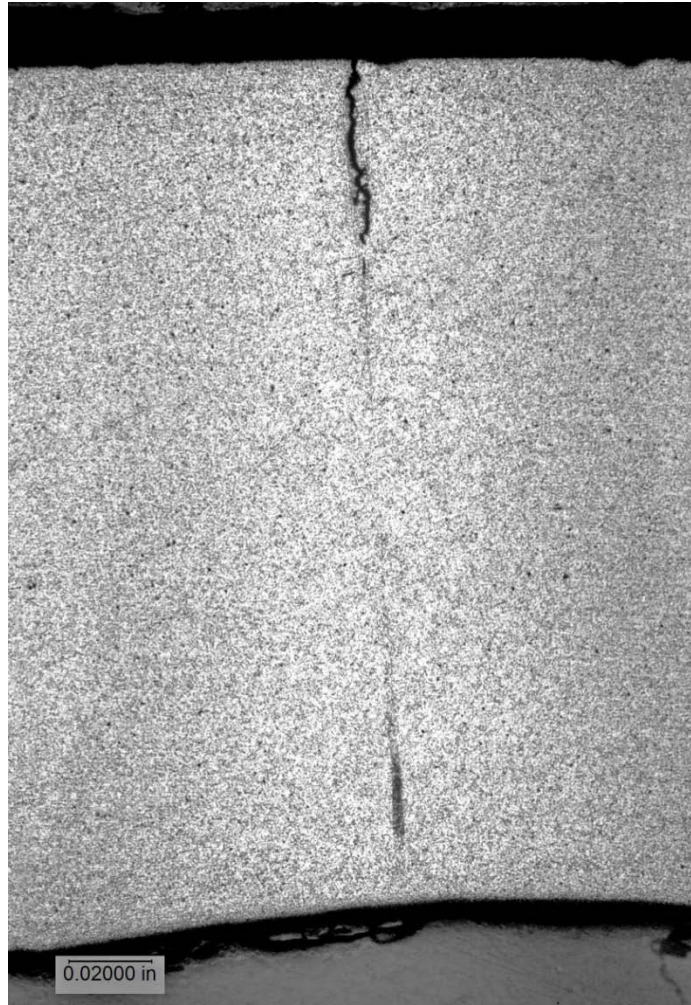


Figure 13. Part-Through Cold Weld in LF-ERW Pipe

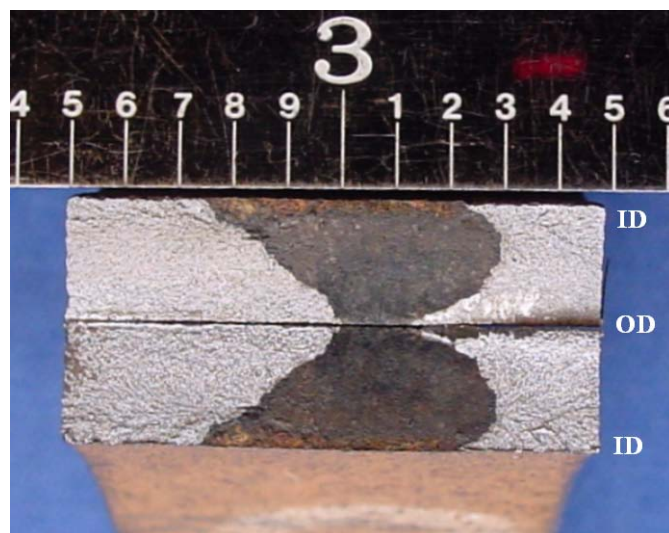


Figure 14. Appearance of a "Penetrator" on a Surface Broken after Chilling (HF-ERW Pipe)

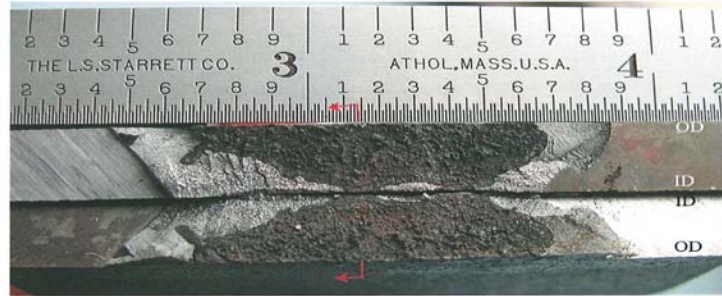


Figure 15. Surface Broken After Chilling Showing a Cold Weld Leak in DC-ERW Pipe

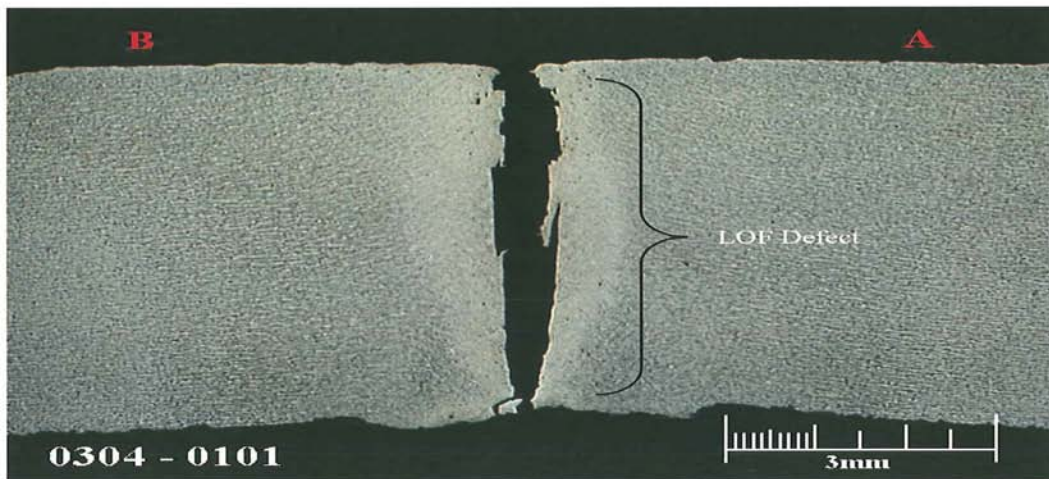


Figure 16. Cross Section of the Cold Weld Shown in Figure 15 Showing Evidence of Strain Possibly Produced by a Hydrostatic Test to a Stress Level of 96.6% of SMYS

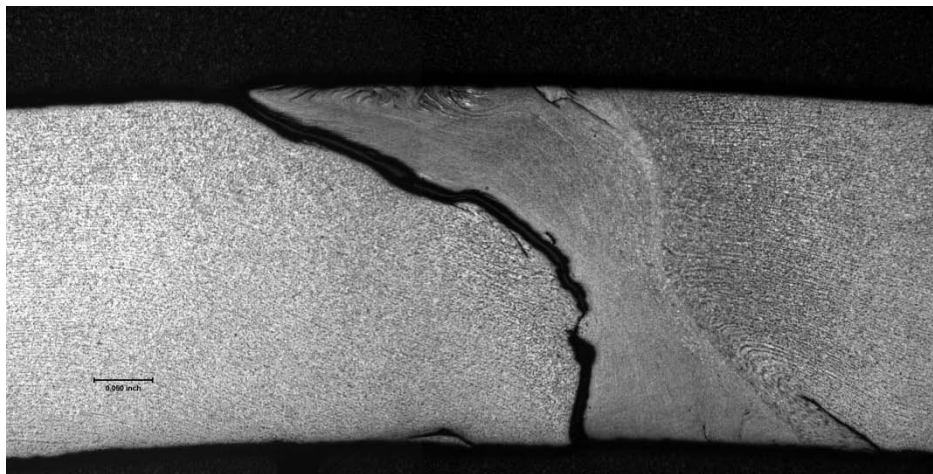


Figure 17. Cold Weld in LF-ERW Pipe Containing Melted Material



Figure 18. Fracture Surface of a Rupture at a Cold Weld in HF-ERW Pipe Showing Relatively Ductile Behavior

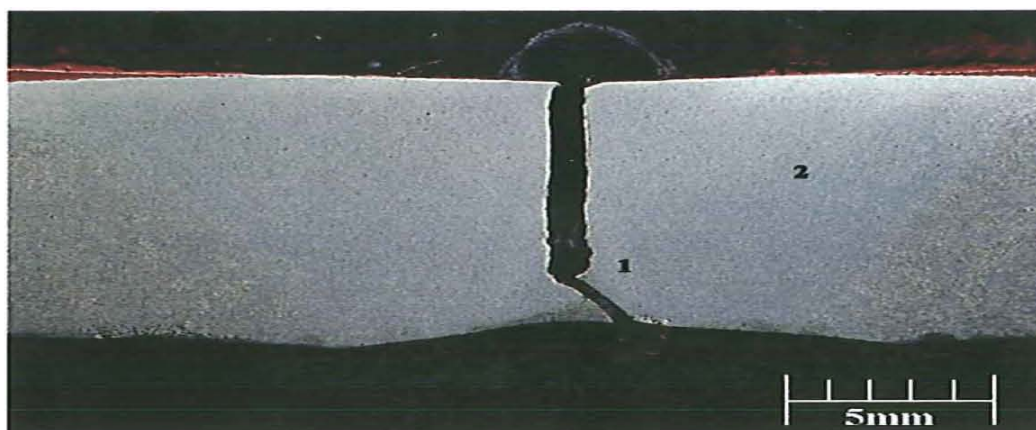


Figure 19. Cross Section of the Cold Weld Shown in Figure 18



Figure 20. Fracture Surface of a Rupture at a Cold Weld in HF-ERW Pipe Showing Relatively Brittle Behavior

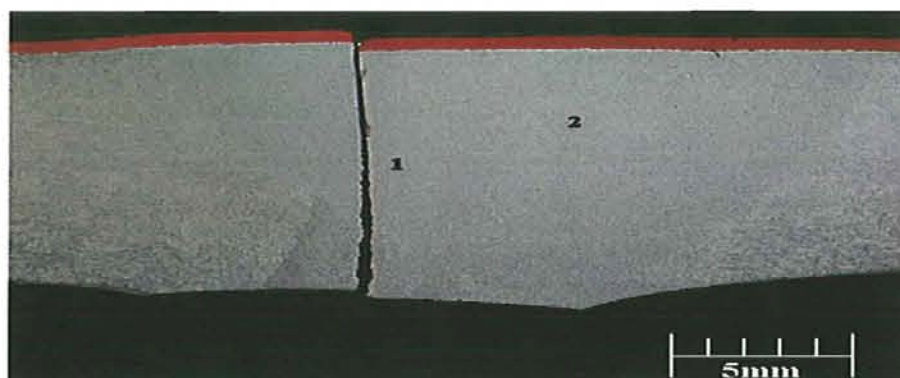


Figure 21. Cross Section of the Cold Weld Shown in Figure 20

Through-thickness cold welds often show no evidence of leakage for long periods of time after the pipes are manufactured and put into service. They are characteristically short; otherwise they would be eliminated by pressure testing conducted in the pipe mill or by the pipeline operator. It is believed that the oxide that typically is formed on the non-bonded surfaces at high temperature (probably Fe_3O_4) tends to prevent leakage. However, pressure cycles and particularly high-pressure hydrostatic tests may crack the oxide leading to a leakage path. It is also feasible that products transported in the pipe may deteriorate or dissolve portions of the oxide. Alternatively, the high-melting-temperature oxide may become oxidized to a less competent material over time leading to a leak path.

The pipe attributes, manufacturers, and failure stress levels are listed for the 99 cold weld failures in Table 7 (a three-page table). Note that the database number of each case is given in the second column. The failures are listed in order by failure stress level starting with lowest failure stress level. The failure stress levels of cold weld (CW) Case Numbers 18, 30, and 31 are highlighted in yellow to indicate that the values are uncertain. The failure stress levels for CW Case Numbers 18 and 30 were taken as the maximum operating pressure (MOP) of the pipeline because the actual failure stress levels when these two leaks occurred are unknown. The anomaly in the CW Case Number 31 failed during a surge event, and the highlighted value is the minimum possible internal pressure at the location of the anomaly when it failed. The stress level could have been higher, but the rapid pressure change during a surge event was not captured by the pressure-recording equipment. “Liquid” is highlighted in yellow in the last two cases because liquid pipelines were thought to be involved.

**Table 7. Listing of the Failures Caused by Cold Welds, Cases CW1 through CW35
(highlighted cases indicate instances where the failure stress level was uncertain)**

CW Case Number	Database Number	Liquid/Gas	Pipe OD, inches	Pipe WT, inch	SMYS, psi	Type of Seam	Manufacturer	Failure Pressure, %SMYS
1	110	Liquid	12.75	0.25	46,000	ERW - LF	Republic	11.1
2	202	Liquid	12.75	0.25	46,000	ERW - LF	Republic	20.6
3	245	Liquid	12.75	0.250	42,000	ERW - LF	J&L	27.3
4	207	Liquid	16	0.312	52,000	ERW - LF	Republic	29.6
5	206	Gas	10.75	0.25	42,000	ERW - HF	Republic	30.7
6	85	Liquid	12.75	0.25	42,000	ERW - LF	J&L	33.7
7	122	Liquid	10.75	0.307	35,000	ERW - LF	NS	34.5
8	156	Liquid	12.75	0.25	42,000	ERW - LF	Republic	35.5
9	147	Gas	20	0.25	35,000	ERW - DC	Youngstown	40.0
10	150	Liquid	6.625	0.188	35,000	ERW - LF	Republic	41.9
11	149	NGL	16	0.25	35,000	ERW - LF	NS	45.7
12	1	Liquid	12.75	0.375	60,000	ERW - HF	Newport Steel	51.0
13	222	NGL	8.625	0.188	52,000	ERW - LF	Lone Star	52.9
14	246	Gas	8.625	0.190	52,000	ERW - HF	Stupp	59.1
15	50	Gas	12.75	0.375	52,000	ERW - HF	Maverick Tube	59.2
16	248	Liquid	8.625	0.160	52,000	ERW - HF	Lone Star	63.3
17	19	Liquid	6.625	0.156	52,000	ERW - LF	NS	63.3
18	157	Liquid	12.75	0.25	42,000	ERW - LF	Republic	63.8
19	133	Liquid	12.75	0.203	46,000	ERW - LF	NS	64.9
20	130	Liquid	8.625	0.25	42,000	ERW - LF	NS	65.5
21	228	HVL	6.625	0.156	46,000	ERW - LF	Lone Star	66.5
22	23	Liquid	6.625	0.188	42,000	ERW - LF	ACME	67.4
23	151	Liquid	6.625	0.188	35,000	ERW - LF	Republic	70.5
24	152	Liquid	6.625	0.188	35,000	ERW - LF	Republic	70.5
25	153	Liquid	6.625	0.188	35,000	ERW - LF	Republic	70.5
26	154	Liquid	6.625	0.188	35,000	ERW - LF	Republic	70.5
27	155	Liquid	6.625	0.188	35,000	ERW - LF	Republic	70.5
28	214	Liquid	34	0.281	52,000	Flash-weld	A.O. Smith	71.1
29	51	Gas	12.75	0.375	52,000	ERW - HF	Maverick Tube	71.2
30	176	Liquid	6.625	0.156	42,000	ERW - LF	Lone Star	72.0
31	18	Liquid	8.625	0.156	52,000	ERW - HF	Lone Star	72.4
32	54	Gas	20	0.375	35,000	ERW - DC	Youngstown	73.5
33	219	Gas	10.75	0.219	46,000	ERW - LF	NS	74.7
34	218	Gas	10.75	0.219	46,000	ERW - LF	NS	75.5
35	221	Gas	10.75	0.219	46,000	ERW - LF	NS	75.5

Table 7. (continued) Listing of the Failures Caused by Cold Welds, Cases CW36 through CW70

CW Case Number	Database Number	Liquid/Gas	Pipe OD, inches	Pipe WT, inch	SMYS, psi	Type of Seam	Manufacturer	Failure Pressure, %SMYS
35	221	Gas	10.75	0.219	46,000	ERW - LF	NS	75.5
36	28	Liquid	8.625	0.322	42,000	ERW - LF	NS	76.6
37	21	Liquid	8.625	0.322	42,000	ERW - LF	NS	77.0
38	128	Liquid	8.625	0.219	52,000	ERW - LF	J&L	77.3
39	20	Liquid	8.625	0.322	42,000	ERW - LF	NS	77.4
40	53	Gas	20	0.375	35,000	ERW - DC	Youngstown	77.8
41	52	Gas	20	0.375	35,000	ERW - DC	Youngstown	78.5
42	118	Liquid	8.625	0.219	46,000	ERW - LF	Bethlehem	78.5
43	220	Gas	10.75	0.219	46,000	ERW - LF	NS	79.0
44	2	Liquid	8.625	0.203	52,000	ERW - LF	NS	79.1
45	211	Liquid	16	0.25	52,000	ERW - LF	Lone Star	79.4
46	119	Liquid	8.625	0.219	46,000	ERW - LF	Bethlehem	79.4
47	223	Liquid	8.625	0.219	46,000	ERW - LF	Bethlehem	79.7
48	120	Liquid	8.625	0.219	46,000	ERW - LF	Bethlehem	80.3
49	131	Liquid	8.625	0.265	35,000	ERW - NS	NS	80.6
50	22	Liquid	8.625	0.322	42,000	ERW - LF	NS	81.0
51	66	Liquid	20	0.312	42,000	ERW - DC	Youngstown	81.3
52	27	Liquid	10.75	0.344	35,000	ERW - LF	NS	82.8
53	64	Liquid	20	0.312	42,000	ERW - DC	Youngstown	83.3
54	49	HVL	10.75	0.219	52,000	ERW - LF	J&L	83.4
55	48	HVL	10.75	0.219	52,000	ERW - LF	J&L	83.8
56	136	Liquid	6.625	0.188	42,000	ERW - HF	NS	83.9
57	44	HVL	10.75	0.219	52,000	ERW - LF	J&L	85.6
58	43	HVL	10.75	0.219	52,000	ERW - LF	J&L	85.8
59	32	HVL	8.625	0.188	52,000	ERW - HF	Stupp	86.0
60	112	Liquid	22	0.344	46,000	ERW - DC	Youngstown	86.2
61	111	Liquid	22	0.344	46,000	ERW - DC	Youngstown	86.8
62	61	Liquid	20	0.312	42,000	ERW - DC	Youngstown	87.7
63	146	Liquid	10.75	0.25	42,000	ERW - LF	Republic	88.0
64	84	Liquid	12.75	0.25	42,000	ERW - LF	J&L	88.6
65	65	Liquid	20	0.312	42,000	ERW - DC	Youngstown	89.2
66	195	Liquid	12.75	0.25	52,000	ERW - LF	Lone Star	89.4
67	185	Liquid	10.75	0.219	52,000	ERW - LF	J&L	89.4
68	107	Liquid	12.75	0.25	46,000	ERW - LF	Republic	93.1
69	81	Liquid	12.75	0.25	42,000	ERW - LF	J&L	93.2
70	108	Liquid	12.75	0.25	46,000	ERW - LF	Republic	93.2

Table 7. (continued) Listing of the Failures Caused by Cold Welds, Cases CW71 through CW99 (highlighted cells indicate case where the fluid type was uncertain)

CW Case Number	Database Number	Liquid/Gas	Pipe OD, inches	Pipe WT, inch	SMYS, psi	Type of Seam	Manufacturer	Failure Pressure, %SMYS
71	109	Liquid	12.75	0.25	46,000	ERW - LF	Republic	93.2
72	172	Liquid	12.75	0.25	46,000	ERW - LF	Republic	93.8
73	83	Liquid	12.75	0.25	42,000	ERW - LF	J&L	94.0
74	97	Liquid	12.75	0.25	46,000	ERW - LF	Republic	94.5
75	82	Liquid	12.75	0.25	42,000	ERW - LF	J&L	94.6
76	101	Liquid	12.75	0.25	46,000	ERW - LF	Republic	94.6
77	98	Liquid	12.75	0.25	46,000	ERW - LF	Republic	94.7
78	92	Liquid	12.75	0.25	46,000	ERW - LF	NS	94.8
79	94	Liquid	12.75	0.25	46,000	ERW - LF	NS	94.8
80	80	Liquid	12.75	0.25	42,000	ERW - LF	J&L	95.5
81	229	Liquid	12.75	0.375	35,000	ERW - HF	Huludao City Steel	95.6
82	89	Liquid	12.75	0.25	46,000	ERW - LF	NS	95.9
83	79	Liquid	12.75	0.25	42,000	ERW - LF	J&L	96.4
84	33	HVL	12.75	0.25	52,000	ERW - LF	Lone Star	96.4
85	124	Liquid	20	0.312	46,000	ERW - DC	Youngstown	97.1
86	99	Liquid	12.75	0.25	46,000	ERW - LF	Republic	97.2
87	78	Liquid	12.75	0.25	42,000	ERW - LF	J&L	97.4
88	100	Liquid	12.75	0.25	46,000	ERW - LF	Republic	97.9
89	123	Liquid	20	0.312	46,000	ERW - DC	Youngstown	98.2
90	121	Liquid	12.75	0.25	46,000	ERW - LF	Republic	98.2
91	17	Liquid	12.75	0.281	60,000	ERW - HF	US Steel	98.8
92	125	Liquid	20	0.312	46,000	ERW - DC	Youngstown	99.1
93	164	Liquid	10.75	0.188	52,000	ERW - HF	NS	100.4
94	169	Liquid	10.75	0.188	52,000	ERW - HF	NS	103.0
95	166	Liquid	10.75	0.188	52,000	ERW - HF	NS	103.4
96	163	Liquid	10.75	0.188	52,000	ERW - HF	NS	104.2
97	170	Liquid	10.75	0.188	52,000	ERW - HF	NS	105.1
98	274	Liquid	20	0.312	52,000	Flash-weld	A.O. Smith	131.0
99	275	Liquid	20	0.312	52,000	Flash-weld	A.O. Smith	137.1

As seen in Table 7, cold welds have occurred across large ranges of pipe sizes, material grades, and manufacturers. They have caused failures in both gas and liquid pipelines, and they have appeared in all types of non-filler-metal seams (i.e., LF-ERW, DC-ERW, HF-ERW, and EFW).

Along with the failure stress levels of the 99 cold weld failures, Table 8 (also given in three parts) presents the mode of failure (leak or rupture), whether the event occurred in service or during a hydrostatic test, and the stress levels reached in the most recent hydrostatic test and the

mill hydrostatic test. The vintage of the pipe is included, and whether or not the failure occurred below the mill test pressure is noted.

Table 8. Failure Modes and Failure Stresses of Cases CW1 through CW35

CW Case Number	Failure Mode	In-service or Hydrostatic Test	Failure Pressure, %SMYS	Pressure in last hydrostatic test, % SMYS	Pipe Vintage	Mill Test Pressure, SMYS	Failure Pressure less than Mill Test Pressure
1	Leak	In-service	11.1	97.0	1958	85	yes
2	Leak	In-service	20.6	83.9	1958	85	yes
3	Leak		27.3	93.9	1957	85	yes
4	Leak	In-service	29.6	61.5	1959	85	yes
5	Leak	In-service	30.7		NS	85	yes
6	Leak	In-service	33.7		1957	85	yes
7	Leak	In-service	34.5	80.0	1959	60	yes
8	Leak	In-service	35.5	84.3	1950	85	yes
9	Leak	In-service	40.0	96.6	1969	90	yes
10	Leak	In-service	41.9	73.0	1946	60	yes
11	Leak	In-service	45.7	83.3	1940	60	yes
12	Rupture	Hydrostatic test	51.0	51.0		85	yes
13	Leak	In-service	52.9		1962	75	yes
14	Rupture		59.1	85.2	1961	75	yes
15	Rupture	Hydrostatic test	59.2		2001	85	yes
16	Rupture		63.3	89.0	1971	75	yes
17	Leak	Hydrostatic test	63.3		1962	75	yes
18	Leak	In-service	63.8	84.3	1950	85	yes
19	Leak	In-service	64.9	90.0	1966	85	yes
20	Rupture	Hydrostatic test	65.5		1956	75	yes
21	Leak	Hydrostatic test	66.5	92.0	1967	75	yes
22	Rupture	Hydrostatic test	67.4		1960	75	yes
23	Leak	Hydrostatic test	70.5		1946	60	no
24	Leak	Hydrostatic test	70.5		1946	60	no
25	Leak	Hydrostatic test	70.5		1946	60	no
26	Leak	Hydrostatic test	70.5		1946	60	no
27	Leak	Hydrostatic test	70.5		1946	60	no
28	Leak	In-service	71.1	88.9	1967	90	yes
29	Rupture	Hydrostatic test	71.2		2001	85	yes
30	Leak	In-service	72.0		1964	60	no
31	Rupture	In-service	72.4	89.4	1971	75	yes
32	Rupture	Hydrostatic test	73.5	45.7	1942	60	no
33	Rupture	Hydrostatic test	74.7		1957	85	yes
34	Rupture	Hydrostatic test	75.5		1957	85	yes
35	Leak	Hydrostatic test	75.5		1957	85	yes

Table 8. (continued) Failure Modes and Failure Stresses of Cases CW36 through CW70

CW Case Number	Failure Mode	In-service or Hydrostatic Test	Failure Pressure, %SMYS	Pressure in last hydrostatic test, % SMYS	Pipe Vintage	Mill Test Pressure, SMYS	Failure Pressure less than Mill Test Pressure
36	Rupture	Hydrostatic test	76.6		1952	75	no
37	Rupture	Hydrostatic test	77.0		1952	75	no
38	Rupture	Hydrostatic test	77.3		1960	75	no
39	Rupture	Hydrostatic test	77.4		1952	75	no
40	Rupture	Hydrostatic test	77.8		1942	60	no
41	Rupture	Hydrostatic test	78.5		1942	60	no
42	Rupture	Hydrostatic test	78.5		1963	75	no
43	Leak	Hydrostatic test	79.0		1957	85	yes
44	Rupture	Hydrostatic test	79.1	75.2	1961	75	no
45	Rupture	Hydrostatic test	79.4		1961	85	yes
46	Rupture	Hydrostatic test	79.4		1963	75	no
47	Rupture	Hydrostatic test	79.7		1963	75	no
48	Rupture	Hydrostatic test	80.3		1963	75	no
49	Rupture	Hydrostatic test	80.6			75	no
50	Rupture	Hydrostatic test	81.0		1952	75	no
51	Leak	Hydrostatic test	81.3	80.8	1944	85	yes
52	Rupture	Hydrostatic test	82.8		1948	60	no
53	Rupture	Hydrostatic test	83.3	85.2	1944	85	yes
54	Rupture	Hydrostatic test	83.4		1961	85	yes
55	Rupture	Hydrostatic test	83.8		1961	85	yes
56	Leak	Hydrostatic test	83.9	76.4	1994	75	no
57	Rupture	Hydrostatic test	85.6		1961	85	no
58	Rupture	Hydrostatic test	85.8		1961	85	no
59	Rupture	Hydrostatic test	86.0		1961	75	no
60	Rupture	Hydrostatic test	86.2		1949	85	no
61	Rupture	Hydrostatic test	86.8		1949	85	no
62	Rupture	Hydrostatic test	87.7	74.9	1944	85	no
63	Leak	Hydrostatic test	88.0		1954	85	no
64	Rupture	Hydrostatic test	88.6	90.1	1957	85	no
65	Rupture	Hydrostatic test	89.2	89.8	1944	85	no
66	Leak	Hydrostatic test	89.4	94.4	1961	85	no
67	Rupture	Hydrostatic test	89.4	87.6	1961	85	no
68	Leak	Hydrostatic test	93.1	94.2	1958	85	no
69	Rupture	Hydrostatic test	93.2	90.1	1957	85	no
70	Leak	Hydrostatic test	93.2	94.2	1958	85	no

Table 8. (continued) Failure Modes and Failure Stresses of Cases CW71 through CW99

CW Case Number	Failure Mode	In-service or Hydrostatic Test	Failure Pressure, %SMYS	Pressure in last hydrostatic test, % SMYS	Pipe Vintage	Mill Test Pressure, SMYS	Failure Pressure less than Mill Test Pressure
71	Leak	Hydrostatic test	93.2	94.2	1958	85	no
72	Rupture	Hydrostatic test	93.8	95.9	1964	85	no
73	Leak	Hydrostatic test	94.0	90.1	1957	85	no
74	Rupture	Hydrostatic test	94.5	93.0	1958	85	no
75	Rupture	Hydrostatic test	94.6	90.1	1957	85	no
76	Rupture	Hydrostatic test	94.6	94.2	1958	85	no
77	Rupture	Hydrostatic test	94.7	93.0	1958	85	no
78	Rupture	Hydrostatic test	94.8	93.0	1964	85	no
79	Leak	Hydrostatic test	94.8	93.0	1964	85	no
80	Rupture	Hydrostatic test	95.5	90.1	1957	85	no
81	Rupture	Hydrostatic test	95.6		2010	60	no
82	Rupture	Hydrostatic test	95.9	93.0	1964	85	no
83	Rupture	Hydrostatic test	96.4	90.1	1957	85	no
84	Rupture	Hydrostatic test	96.4		1961	85	no
85	Leak	Hydrostatic test	97.1	91.0	1950	85	no
86	Leak	Hydrostatic test	97.2	93.0	1958	85	no
87	Leak	Hydrostatic test	97.4	90.1	1957	85	no
88	Rupture	Hydrostatic test	97.9	93.0	1958	85	no
89	Leak	Hydrostatic test	98.2	91.0	1950	85	no
90	Rupture	Hydrostatic test	98.2	94.2	1958	85	no
91	Leak	Hydrostatic test	98.8	94.2	1967	85	no
92	Leak	Hydrostatic test	99.1	91.0	1950	85	no
93	Rupture	Hydrostatic test	100.4		1970	85	no
94	Rupture	Hydrostatic test	103.0		1970	85	no
95	Rupture	Hydrostatic test	103.4		1970	85	no
96	Rupture	Hydrostatic test	104.2		1970	85	no
97	Rupture	Hydrostatic test	105.1		1970	85	no
98	NS	Hydrostatic test	131.0		1950s	90	no
99	NS	Hydrostatic test	137.1		1950s	90	no

As seen in Table 8 by the “yes” in the last column, many of the cold weld failures occurred at hoop stress levels below the mill test stress levels, some well below those levels. Further examination of the table indicates that the failure stresses in some cases were also well below the hoop stress levels employed in in-situ hydrostatic tests to levels exceeding the mill test stress levels.

The failure of cold welds associated with in-service failures, with one exception, occurred as leaks at stress levels below 72 percent of SMYS. One in-service rupture occurred during a surge event where the hoop stress was believed to be at least 72.4 percent of SMYS. However, as can be seen, five cold welds failed as ruptures in hydrostatic tests at stress levels below 72 percent of SMYS and several more failed as ruptures in hydrostatic tests at stress levels below the mill test stress levels.

The occurrences of leaks and ruptures of cold welds at stress levels well within the range of pipeline operating stress levels and at levels well below stress levels previously imposed on the materials, is a matter of concern. These occurrences suggest that the threat of a cold weld failure at typical pipeline operating stress levels cannot be eliminated by means of a pre-service hydrostatic test. It is necessary to examine some of the individual failures in more detail in order to understand the significance of cold welds and whether or not the concern about their not being manageable by hydrostatic testing is real.

CW Case Number 1

CW Case Number 1 involved a 12.75-inch-OD, 0.250-inch-wall, X46 low-frequency-welded pipe manufactured by Republic in 1958. The failure mode was a leak in service. The leak may have developed at a hoop stress level higher than the 11.1 percent of SMYS value listed in Table 8. The stress level of 11.1 percent of SMYS existed at the anomaly at the time it was excavated, examined, and repaired. A pressure-containing sleeve was installed over the anomaly to keep it from leaking until the operator was able to drain the line and remove the leaking piece of pipe. The most recent hydrostatic test conducted a year prior to the discovery of the leak was carried out at a hoop stress level of 97.0 percent of SMYS. This level is even higher than the 85-percent-of-SMYS mill test that was likely performed on the pipe. This 1-inch-long cold weld was entirely through the wall along a portion of its length. The leak may have been facilitated by the increased hoop stress arising during the recent hydrostatic test.

CW Case Number 2

CW Case Number 2 involved a 12.75-inch-OD, 0.250-inch-wall, X46 low-frequency-welded pipe manufactured by Republic in 1958. The failure mode was a leak in-service. The failure stress level of 20.6 percent of SMYS was about the normal operating stress level at the location of the leak. The most recent hydrostatic test conducted a year prior to the discovery of the leak was carried out at a hoop stress level of 83.9 percent of SMYS. The anomaly had survived not only this latter test but a mill test to a stress level of 85 percent of SMYS. This anomaly was less than half an inch long and was entirely through the wall thickness.

CW Case Number 3

CW Case Number 3 involved a 12.75-inch-OD, 0.250-inch-wall, X42 low-frequency-welded pipe manufactured by J&L in 1957. The failure mode was a leak in service discovered while the pipeline was being operated at a hoop stress level of 27.3 percent of SMYS. The most recent hydrostatic test was conducted 13 years prior to the discovery of the leak. The test stress level was 74.8 percent of SMYS. Also, the pipe was supposed to have been subjected to a mill test to a stress level of 85 percent of SMYS.

CW Case Number 4

CW Case Number 4 involved a 16-inch-OD, 0.312-inch-wall, X52 low-frequency-welded pipe manufactured by Republic in 1959. The failure mode was a leak in-service discovered while the pipeline was being operated at a hoop stress level of 29.6 percent of SMYS. The most recent hydrostatic test conducted 1 year prior to the discovery of the leak was carried out at a hoop stress level of 61.5 percent of SMYS. The anomaly had survived not only this latter test but a mill test to a stress level of 85 percent of SMYS.

This 1.8-inch-long cold weld anomaly was revealed for examination by chilling the sample containing the leak in liquid nitrogen and breaking it open. Its appearance is illustrated in Figure 8 and Figure 9. The black surfaces illustrate the area of no bonding. The stitch pattern of this low-frequency weld is evident (stitching is explained later in this report). The anomaly extended to the girth weld at one end of the piece.

CW Case Number 5

CW Case Number 5 involved a 10.75-inch-OD, 0.250-inch-wall, X42 high-frequency-welded pipe manufactured by Republic. The year of manufacturing was not known although metallography revealed the seam to be high-frequency welded. The failure mode was a leak in service discovered while the pipeline was being operated at a hoop stress level of 30.7 percent of SMYS. No hydrostatic test data were available, but the anomaly had survived a mill test to a stress level of 85 percent of SMYS. The appearance of this anomaly was revealed after chilling the sample in liquid nitrogen and breaking it open. The relatively short, non-bonded area is the black-oxide-coated area shown in Figure 14. These short, through-wall cold welds are sometimes referred to as “penetrators”.

CW Case Number 6

CW Case Number 6 involved a 12.75-inch-OD, 0.250-inch-wall, X42 low-frequency-welded pipe manufactured by J&L in 1957. The failure mode was a leak in-service discovered while the pipeline was being operated at a hoop stress level of 33.7 percent of SMYS. No hydrostatic test data were available, but the anomaly had survived a mill test to a stress level of 85 percent of

SMYS. The leaking anomaly consisted of two very narrow curved penetrations of the wall thickness separated by solid material.

CW Case Number 7

CW Case Number 7 involved a 10.75-inch-OD, 0.307-inch-wall, Grade B low-frequency-welded pipe manufactured in 1959. The manufacturer was not known. The failure mode was a leak in-service discovered while the pipeline was being operated at a hoop stress level of 34.5 percent of SMYS. The pipeline had been subjected to hydrostatic test to 80 percent of SMYS 18 years prior to the time the leak was discovered, and the anomaly had survived a mill test to a stress level of 60 percent of SMYS.

The 1-inch-long anomaly had a very unusual appearance which suggested that metal in the vicinity of the seam may have actually melted but did not bond to the adjacent material leaving a path for leakage that must have remained blocked by oxide until the time the leak was discovered (see Figure 17).

CW Case Number 8

CW Case Number 8 involved a 10.75-inch-OD, 0.188-inch-wall, X52 high-frequency-welded pipe manufactured by Republic in 1970. The failure mode was a leak in-service discovered while the pipeline was being operated at a hoop stress level of 40.0 percent of SMYS. The anomaly had survived a hydrostatic test to 90 percent of SMYS 7 years prior to the discovery of the leak, and it had survived a mill test to a stress level of 85 percent of SMYS. The through-wall anomaly was about 0.5 inch in length.

CW Case Number 9

CW Case Number 9 involved a 20-inch-OD, 0.250-inch-wall, Grade B DC-welded pipe manufactured by Youngstown in 1969. The failure mode was a leak in-service discovered while the pipeline was being operated at a hoop stress level of 40 percent of SMYS. The anomaly had survived a pre-service hydrostatic test to 96.6 percent of SMYS. The anomaly was about 1 inch long at the OD surface and 0.5 inch long at the ID surface (see Figure 15). Note that no stitching is present because this seam was DC-welded. The anomaly is believed to have extended 100 percent through the wall initially. The stretched-open appearance of the anomaly (see Figure 16) suggests that the original pre-service hydrostatic test caused some extension of the anomaly but not enough to cause it to leak during the test. It is possible that the leak developed later as the result of a pressure reversal.

CW Case Number 10

CW Case Number 10 involved a 6.625-inch-OD, 0.188-inch-wall, Grade B low-frequency-welded pipe manufactured by Republic in 1946. The failure mode was a leak in-service discovered while the pipeline was being operated at a hoop stress level of 41.9 percent of SMYS. The anomaly had survived a hydrostatic test to 73.0 percent of SMYS 14 years prior to the discovery of the leak, and it had survived a mill test to a stress level of 60 percent of SMYS. The through-wall anomaly was about 0.2 inch in length at the OD surface and about 0.1 inch in length at the ID surface.

CW Case Number 11

CW Case Number 11 involved a 16-inch-OD, 0.250-inch-wall, Grade B low-frequency-welded pipe manufactured in 1940. The manufacturer of the pipe was not known. The failure mode was a leak in-service discovered while the pipeline was being operated at a hoop stress level of 45.7 percent of SMYS. The anomaly had survived a hydrostatic test to 83.3 percent of SMYS 3 years prior to the discovery of the leak. The mill test stress level likely did not exceed 60 percent of SMYS.

The anomaly consisted of a few intermittent cold welds, one of which appeared to have been repaired by the manufacturer.

Non-uniqueness of Cold Welds that Leak at Hoop Stress Levels Well Below the Level of a Previous Hydrostatic Test

In view of the number of leaks at low stress levels discussed above, it should be clear that in-service leaks from through-wall cold welds at hoop stress levels well below that of a prior higher pressure hydrostatic test are not all that unusual. It is believed these cases are explainable in terms of cracking of the oxide by a previous pressure spike such as during a prior hydrostatic test or in terms of deterioration of the high-temperature oxide into a less coherent material that eventually allows leakage. These anomalies are characteristically too short to cause the pipe to rupture at typical in-service stress levels. Examples of cold welds which are believed to have leaked in this manner were shown previously in Figure 8 and Figure 14. The remaining discussion of cold weld failures is confined to those cold welds associated with the rupture mode of failure at stress levels below that of the mill test stress levels.

CW Case Number 12

This case involved a hydrostatic test rupture in a new piece of pipe. The pipe was a 12.75-inch-OD, 0.375-inch-wall, X60 high-frequency-welded material manufactured by Newport Steel sometime after 1995. The failure mode was a hydrostatic test rupture at a hoop stress level of

51.0 percent of SMYS. The pipe had presumably been tested by the manufacturer to 85 percent of SMYS, so it is hard to understand how it could rupture in its next pressurization to a level 40 percent below the mill test pressure.

The technical report on this failure indicates that the seam that failed was located at the extrados of a cold bend. More likely, this was actually a hot bend. The pipe had been bent to a radius of 62.375 inches. For a 12.75-inch-OD pipe this is a 5D bend whereas a cold bend is limited by ASME B31.4 to a minimum bend radius of 18D. More evidence suggests that this probably was a hot bend. The fact that the full-scale transition temperature of the base metal was determined to be 180°F for this modern material is one reason. The chemistry of the material suggests that it was a modern, micro-alloyed steel. Its carbon content was 0.074 percent by weight, and sulfur content was 0.006 percent by weight. It should have had a much lower base metal transition temperature. Also, the wall thickness measured at the extrados at the center of the bend was only 0.306 inch, whereas the wall thickness measured at 8 points around the circumference of the straight portion of the bend ranged from a minimum of 0.359 inch to 0.367 inch. These circumstances strongly suggest that the material had been subjected to hot bending in an inappropriate manner that degraded the properties of the pipe and the seam. As such the failure should not be considered indicative of cold weld behavior.

The anomaly which served as the origin of the rupture was a part-through cold weld 2.5 inches in length and 55 percent through the wall in depth. Because the full-size equivalent upper shelf Charpy energy of the seam was determined to be 68 ft lb, the predicted failure stress level of this anomaly, if it had failed in a ductile manner, would have been 110.4 percent of SMYS. The anomaly failed in a brittle manner at a hoop stress level of about half that amount. Therefore, it is reasonable to conclude that this failure is uniquely attributable to the misapplication of a hot bending procedure which resulted in excessive wall-thinning and which failed to properly heat treat the material after bending.

CW Case Number 14

This case involved a hydrostatic test rupture in a piece of 8.625-inch-OD, 0.190-inch-wall, X52 high-frequency-welded material manufactured by Stupp Corporation in 1961. The failure mode was a hydrostatic test rupture at a hoop stress level of 59.1 percent of SMYS. The pipe had presumably been tested by the manufacturer to 75 percent of SMYS, so it is hard to understand how it could rupture at a level 21 percent below the mill test pressure.

CW Case Number 15 and CW Case Number 29

These two cases involved two successive hydrostatic test ruptures in two pieces of new pipe in the same pipeline. The pipe was a 12.75-inch-OD, 0.375-inch-wall, X52 high-frequency-welded

material manufactured by Maverick Tube Corporation in 2001. This material was a micro-alloyed steel with a base metal toughness equivalent to more than 240 ft lb of full-size-equivalent, Charpy upper shelf energy. The first hydrostatic test rupture occurred at a hoop stress level of 59.2 percent of SMYS. The second hydrostatic test rupture occurred at a hoop stress level of 71.2 percent of SMYS. The pipe had been tested by the manufacturer to 85 percent of SMYS, and mill certificates so stated. Therefore, it is hard to understand how these pipes could rupture at stress levels 30 percent and 16 percent, respectively, below the mill test stress level. The likely explanation is that the mill test duration (only 5 seconds) was not long enough to cause these defects to fail. These two cases may represent extreme cases of pressure reversals if each piece was indeed subjected to the mill test. Additionally, the seams were required to be ultrasonically inspected. If the inspections actually took place, the results do not provide much confidence in the mill's ultrasonic inspection.

Both failures propagated in a brittle manner, although it is clear the first failure initiated in a ductile mode (see Figure 18 and Figure 19). In this failure, the OD-surface-connected anomaly was 8.5-inches long and 66% through the wall thickness. It failed at 59.2 percent of SMYS just about the level that one would predict for a rectangular-shaped flaw using the Modified Ln-Sec Equation with 240 ft lb of Charpy energy.

The other failure originated at one or both of a pair of OD-surface-connected defects both about 3 inches long and 33 percent through the wall, separated by about 0.5 inch. This combination of cold welds ruptured at a stress level of 71.2 percent of SMYS which is only about 50 percent of the level that one would predict for a rectangular-shaped flaw using the Modified Ln-Sec Equation with 240 ft lb of Charpy energy. This failure appeared to have occurred in a brittle manner (see Figure 20 and Figure 21).

CW Case Number 16

This case involved a hydrostatic test rupture in a piece of 8.625-inch-OD, 0.160-inch-wall, X52 high-frequency-welded material manufactured by Lone Star in 1971. The failure mode was a hydrostatic test rupture at a hoop stress level of 63.3 percent of SMYS. The pipe had presumably been tested by the manufacturer to 75 percent of SMYS, so it is hard to understand how it could rupture in its next pressurization to a level 16 percent below its mill test pressure.

CW Case Number 20

CW Case Number 20 involved an 8.625-inch-OD, 0.250-inch-wall, X42 low-frequency-welded pipe manufactured in 1956. The manufacturer of the pipe is unknown. The piece of pipe ruptured in a hydrostatic test at a hoop stress level of 65.5 percent of SMYS. No mention of a

prior hydrostatic test was made. The pipe was supposed to have been subjected to a mill test to a stress level of 75 percent of SMYS.

The shapes of the multiple, closely-spaced cold welds make it difficult to analyze this test failure. The small sizes of the defects and brittle appearance of the fracture surface strongly suggest that the failure initiated in a brittle manner at a stress level that was well below what one would predict using the sizes of the flaws and the base metal Charpy value to represent toughness.

CW Case Number 22

CW Case Number 22 involved a 6.625-inch-OD, 0.188-inch-wall, X42 low-frequency-welded pipe manufactured by ACME in 1960. The piece of pipe ruptured in a hydrostatic test at a hoop stress level of 67.4 percent of SMYS. No mention of a prior hydrostatic test was made. The pipe was supposed to have been subjected to a mill test to a stress level of 75 percent of SMYS.

The OD-surface-connected defect was 1.1 inch long and 70 percent through the wall. The rupture propagated along the seam in a brittle manner. The failure having occurred at a stress level of 67.4 percent of SMYS indicates a brittle fracture initiation as well. On the basis of the parent metal full-size-equivalent upper shelf energy of 50 ft lb, one predicts that a defect this size would have been expected to fail at a hoop stress level of 122 percent of SMYS.

CW Case Number 31

This case involved an in-service rupture where the hoop stress was known to have been at least 72.4 percent of SMYS and could have been higher as the event took place during a surge. The pipe which failed was an 8.625-inch-OD, 0.156-inch-wall, X52 high-frequency-welded ERW material. An ID-surface-connected cold weld extended over a distance of 60 inches along the seam. The defect had an average depth of 45 percent of the wall thickness. The pipe was supposed to have been subjected to a mill test to a stress level of 75 percent of SMYS.

CW Case Number 33 and Case Number 34

These two cases involved two successive hydrostatic test ruptures during a test of an existing pipeline. The pipe was a 10.75-inch-OD, 0.219-inch-wall, X46 low-frequency-welded material manufactured in 1957. The first hydrostatic test rupture occurred at a hoop stress level of 74.7 percent of SMYS. The second hydrostatic test rupture occurred at a hoop stress level of 75.5 percent of SMYS. Presumably the pipe had been tested by the manufacturer to 85 percent of SMYS. Therefore, it is hard to understand how these pipes could rupture in at stress levels 12 percent and 11 percent, respectively, below the mill test stress level. The likelihood is that the mill test duration (only 5 seconds) was not long enough to cause these defects to fail. These two

cases may represent cases of pressure reversals if each piece was indeed subjected to the mill test.

The anomaly associated with CW Case Number 33 was about one-half inch long and 20 percent through the wall. The predicted hoop stress level at failure for an anomaly this size based on a base metal toughness corresponding to 50 ft lb (full-size-equivalent) upper shelf energy is 132% of SMYS. The rupture of the anomaly at a hoop stress level of 74.7 percent of SMYS indicates that the failure of the anomaly initiated in a brittle manner.

CW Case Number 45

This case involved an in-service rupture where the hoop stress at failure was 79.4 percent of SMYS. The pipe that failed was a 16-inch-OD, 0.250-inch-wall, X52 low-frequency-welded ERW material manufactured by Lone Star in 1961. An OD-surface-connected cold weld extended over a distance of 1.75 inches along the seam. The initial cold weld defect had an average depth of 25 percent of the wall thickness. However, a crack with varying depth along its length extended from the cold weld near but not in the bondline to an average depth of about 60 percent of the wall thickness. The crack and the cold weld were coated with coal tar enamel, so it is assumed that the crack extension of the cold weld existed at the time the pipe was installed. The crack extension may have occurred during the mill hydrostatic test to 85 percent of SMYS.

CW Case Number 53

This case involved a hydrostatic test rupture of 20-inch-OD, 0.312-inch-wall, X42 DC-welded material. The pipe had been manufactured in 1944 by Youngstown. The API 5LX specification did not exist until 1949, but it was not unusual for materials to be designated as X grades in the period prior from about 1941 through 1948 if the purchaser and the manufacturer agreed on a minimum strength level above that of Grade B pipe. However, it would be expected that the mill test pressure would be 85 percent of the specified SMYS. The rupture in CW Case Number 53 occurred at a hoop stress level of 83.3 percent of SMYS. Dimensions of the anomaly were not available.

CW Case Number 54 and CW Case Number 55

These two cases involved two successive hydrostatic test ruptures during a test of an existing pipeline. The pipe was a 10.75-inch-OD, 0.219-inch-wall, X52 low-frequency-welded material manufactured by J&L in 1961. The first hydrostatic test rupture occurred at a hoop stress level of 83.4 percent of SMYS. The second hydrostatic test rupture occurred at a hoop stress level of 83.8 percent of SMYS. Presumably the pipe had been tested by the manufacturer to 85 percent of SMYS. These failures could easily be pressure reversals from the mill test since they occurred at stress levels just below the mill test.

Summary of Cold Weld Failures

Many of the cold welds were through-wall anomalies as manufactured. Examples were shown previously in Figure 8, Figure 9, Figure 11, and Figure 14. The fact that they did not leak until the pipes had been in service for years suggests that leakage was initially blocked by a coherent oxide. Alternatively, it is possible that the initial oxide that formed while the material was still hot after welding (probably Fe_3O_4) can be converted in the soil environment or by a chemical reaction with the product inside the pipeline to a less coherent oxide that eventually gives way and allows leakage. It seems likely that at least some of the cold weld leaks were facilitated by previous hydrostatic tests. It is speculated that a test can cause plastic deformation at the ends of the defect allowing it to open slightly, possibly dislodging or degrading the oxide thereby creating a leakage path. The anomaly in CW Case Number 9 exhibits the kind of deformation that is suspected of facilitating leakage (see Figure 16).

As can be seen in Figure 22 and Figure 23, the stress levels at which the cold weld failures occurred, many leaks and, in some cases, ruptures from cold welds occurred within the operating stress ranges of pipelines, even though such anomalies had survived a hydrostatic test by the manufacturer or an in-situ test after installation of the pipeline.

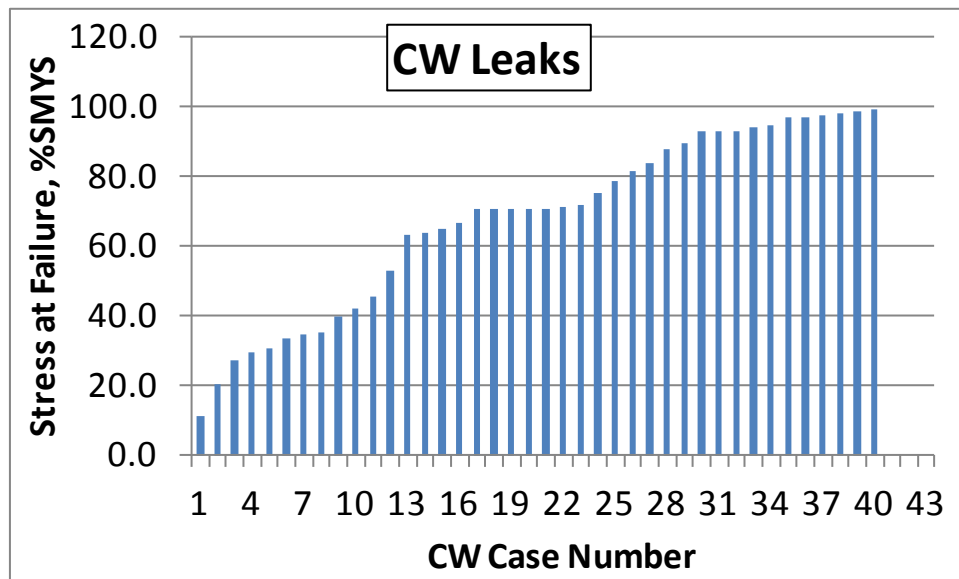


Figure 22. Stress at Failure for CW Leaks

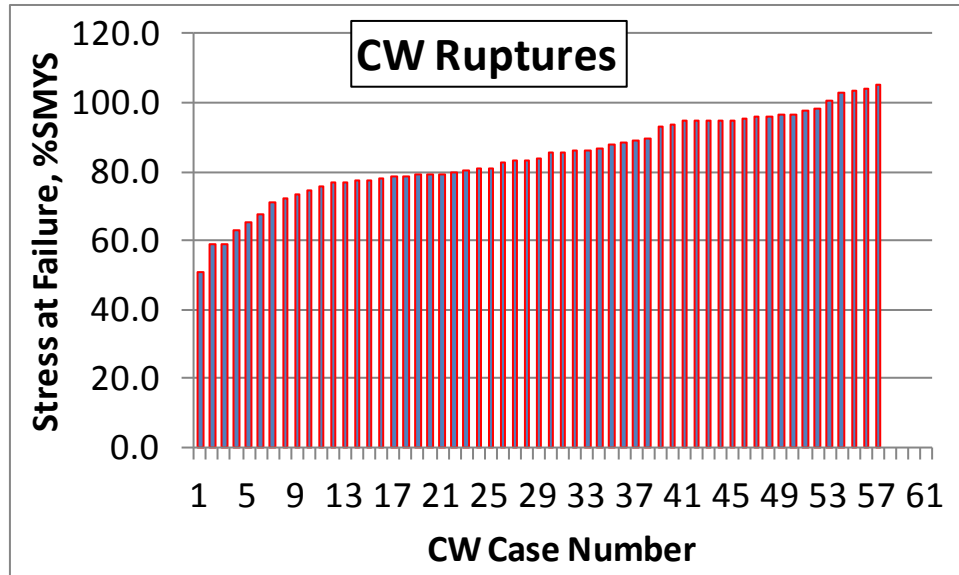


Figure 23. Stress at Failure for CW Ruptures

Twenty of the cold weld leaks occurred at stress levels ranging from 11 percent of SMYS to 72 percent of SMYS, and 7 of the cold weld ruptures occurred at stress levels ranging from 51 percent of SMYS to 71 percent of SMYS.

An important factor in the behavior of cold welds is the propensity of the bondline microstructure in low-frequency-welded, DC-welded, and flash-welded seams to behave in a brittle manner. This propensity was revealed not only by the brittle appearances of the fractures in such seams, but also by the comparisons of actual failure pressures to those that would be predicted based on the assumption that the material behaves in a ductile manner. Shown in Figure 24 are comparisons of actual failure stress levels compared to failure stress levels predicted using the Modified Ln-Sec model (elliptical c-equivalent) based on the flow stress and Charpy energy of the base metal.

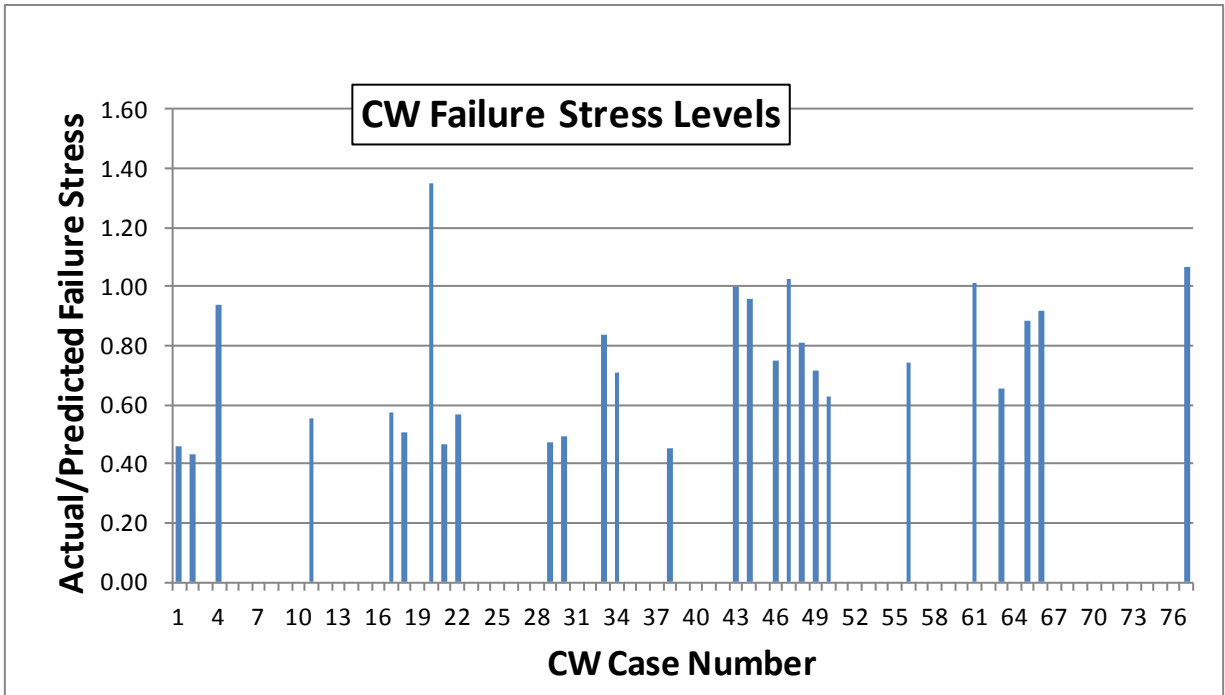


Figure 24. Actual Failure Stress Levels of Cold Welds Compared to Failure Stress Levels Predicted Using Base Metal Properties

Calculations were made only for the 27 cases where the length and depth of the cold weld could be clearly established, and no calculations were made for through-wall cold welds. The comparisons illustrated in Figure 24 show that for 22 of the 27 cases, the ratios of actual to predicted failure stress were less than 1, and for 16 of the 27 cases the ratios were less than 0.8, meaning that the actual failure stress was less, in most cases appreciably less, than the predicted failure stress. This outcome is believed to be the result of most of the cold weld failures initiating in a brittle or quasi-brittle manner. In such cases it is not surprising that a ductile crack model such as the Modified Ln-Sec model over-estimates the failure stress.

Another indication of the ability (or rather the inability) of the Modified Ln-Sec Elliptical CEQ model to predict the failure stress levels of cold welds using base metal flow stress and Charpy energy is illustrated by the lack of statistical correlation between the actual and the predicted values of failure stress for the 27 cases. Values of the ratio “actual/predicted” failure stress ranged from below 0.43 to more than 1.35. The average value is 0.74, and the standard deviation is 0.24. The R-squared coefficient is essentially zero suggesting no correlation.

The tendency of cold welds to behave in a brittle manner may help explain the fact that in many of the examples discussed above, cold weld anomalies leaked or ruptured at stress levels well below that of previous hydrostatic tests. In the domain of ductile fracture initiation, most often a defect that has survived a prior proof test stress level will not fail until stressed to level at or

above that of the prior test. That is how proof loading is supposed to work. Even for defects that behave in a ductile manner, survival upon re-stressing to the level of the proof test is not guaranteed. “Pressure reversal” is the term often used to describe cases where a defect fails at a pressure (i.e., hoop stress) level below that imposed in a prior proof test. It has been demonstrated¹ that this phenomenon results from plastic straining or ductile tearing of the defect during the proof test where the proof test pressure was released before the point of tearing instability was reached, allowing the defect to survive but leaving it in a state where it will not survive re-stressing to the level of the proof test. In most such cases the surviving defect will not fail until re-stressed to within 1 or 2 percent of the proof test stress. Larger stress reversals are possible but extremely rare.

In the case of defects that behave in a brittle manner, it may well be that pressure reversals are possible and that the propensity for large pressure reversals is greater than that for defects that behave in a ductile manner.

It is possible, but highly unlikely, that some of the pipes were not subjected to a mill test. This seems unlikely because leaks and ruptures from cold welds occurred at low stresses even in cases where the anomaly had survived a high-stress in-situ hydrostatic test.

Until an ILI crack tool evolves that can reliably find cold welds, hydrostatic testing with all the limitations discussed above is still a viable means to prevent ruptures from cold welds. These data show that many cold weld defects have been removed by hydrostatic tests to levels exceeding 90 percent of SMYS.

All findings stated herein with regard to cold welds also apply to penetrators which are discussed below.

Penetrators

“Penetrator” is another name for a through-wall cold weld. The non-bonded region where a complete bondline would be expected consists of a high-melting-temperature oxide that was not sufficiently heated and extruded out of the weld zone. Irregular skelp edges (such as attached slivers left over from poor edge machining) and/or upsets in the welding process (such as current interruptions) are believed to be factors contributing to the creation of penetrators. It will be seen that they are indistinguishable from cold welds in terms of their characteristics, aside from length. Penetrators always have very short axial extents (typically less than one wall thickness).

The cold weld anomalies that were called penetrators are summarized in Table 9 and Table 10. The penetrators are listed in order by failure stress level starting with lowest failure stress level.

Table 9. Listing of Cases Arising from Penetrators

Penertrator Case Number	Database Number	Liquid/Gas	Pipe OD, inches	Pipe WT, inch	SMYS, psi	Type of Seam	Manufacturer	Failure Pressure, %SMYS
1	247	Liquid	12.75	0.250	52,000	ERW - LF	Bethlehem	19.6
2	12	Liquid	12.75	0.250	52,000	ERW - HF	J&L	39.2
3	11	Liquid	12.75	0.250	52,000	ERW - HF	J&L	39.2
4	178	Liquid	12.75	0.250	52,000	ERW - HF	Republic	59.1
5	159	HVL	8.625	0.156	46,000	ERW - NS	NS	60.1
6	201	Liquid	20	0.219	52,000	ERW - HF	US Steel	95.7
7	200	Liquid	20	0.219	52,000	ERW - HF	US Steel	95.7
8	199	Liquid	20	0.219	52,000	ERW - HF	US Steel	95.7

Table 10. Failure Modes and Failure Stresses of Cases P1 through P8

Penertrator Case Number	Failure Mode	In-service or Hydrostatic Test	Failure Pressure, %SMYS	Pressure in last hydrostatic test, % SMYS	Pipe Vintage	Mill Test Pressure, SMYS	Failure Pressure less than Mill Test Pressure
1	Leak	In-service	19.6		1968	85	yes
2	Leak	In-service	39.2	97.6	1968	85	yes
3	Leak	In-service	39.2	97.6	1968	85	yes
4	Leak	In-service	59.1	90.0	1963	85	yes
5	Leak	In-service	60.1			75	yes
6	Leak	Hydrostatic test	95.7		1968	90	no
7	Leak	Hydrostatic test	95.7		1968	90	no
8	Leak	Hydrostatic test	95.7		1968	90	no

The picture of a penetrator, shown on a fracture surface (Figure 25) illustrates that a penetrator is a through-wall cold weld much like the one shown Figure 14. Just like short, through-wall cold welds, penetrators caused leaks at low stress levels, levels sometimes well below the level of a prior hydrostatic test.

**Figure 25. A Penetrator Shown on a Surface Created by Chilling and Breaking the Sample**

Hook Cracks

The database contains 76 incidents where the cause of failure was attributed primarily to a hook crack (HC). Hook cracks arise from laminations or layers of non-metallic inclusions. Normally, laminations or layers of non-metallic inclusions lie parallel to the surface of the hot-rolled strip steel (skelp) used to make ERW pipe. As such they usually have little or no impact on the integrity of a pipe made from the skelp because, being oriented parallel to the surfaces, they do not interfere with the stress-carrying capacity of the pipe. However, if a lamination or layers of inclusions exist at the edges of the skelp, they tend to become re-oriented at the time of seam welding to the point where they may be nearly perpendicular to the surfaces. The lamination or layer is curved toward the ID or OD surface in a “j-shaped” pattern, hence the name hook crack. In that orientation they do tend to interfere with the hoop-stress-carrying capacity of the pipe. Since the laminations or layers will upset toward the ID or OD surface depending on where in thickness they lie, it is expected they will not be deeper than half of the wall thickness. The lengths of such anomalies depend on the axial length of the initial lamination or layer, but they can be several inches in length. Some such defects will be large enough to fail in the manufacturer’s hydrostatic test, whereas others that are not large enough will survive the test.

Because the zone of upsetting of material during welding is fairly wide (one-quarter of the plate thickness on each side of the bondline is not uncommon), hook cracks often do not coincide with bondline of the weld. In cases where the hook crack is not immediately adjacent to the bondline, its behavior may be controlled more by the properties of the base metal than by the properties of the bondline. This will become apparent when the stress level range of the hook crack failures and the sizes of hook cracks are compared to those of cold welds.

Examples of hook crack characteristics are shown in Figure 26 through Figure 30.



Figure 26. Hook Crack Seen on a Fracture Surface

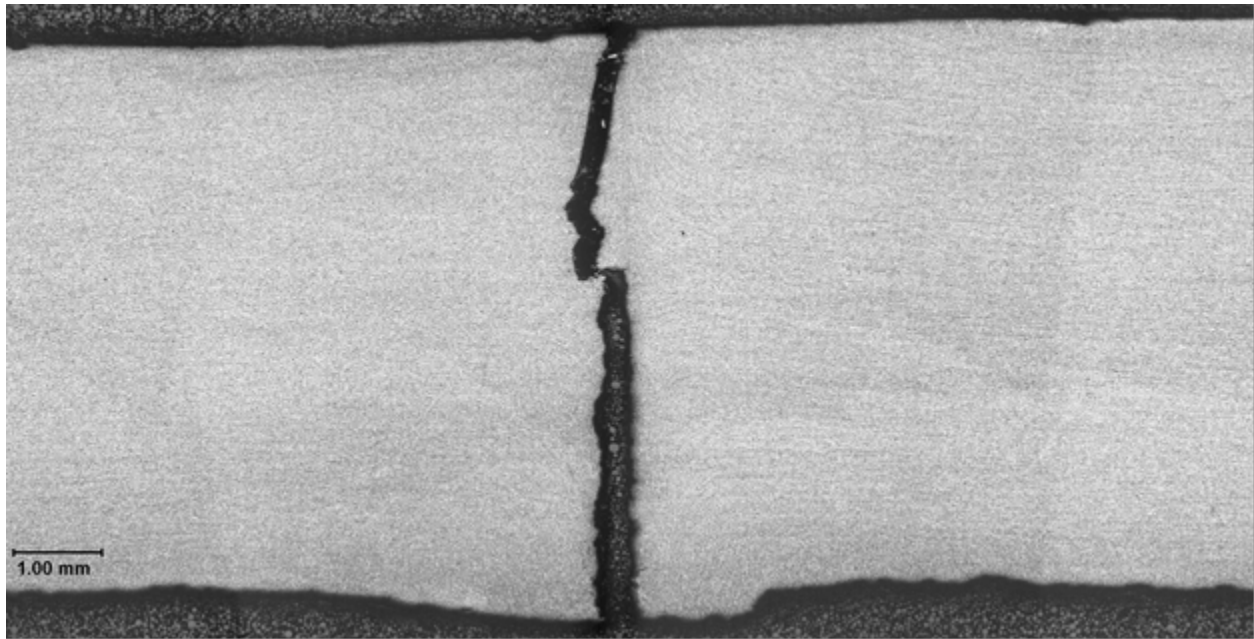


Figure 27. Cross Section of Hook Crack Shown in Figure 26 (Note that the end of the hook crack was close to the bondline and that the fracture jumped into the bondline.)

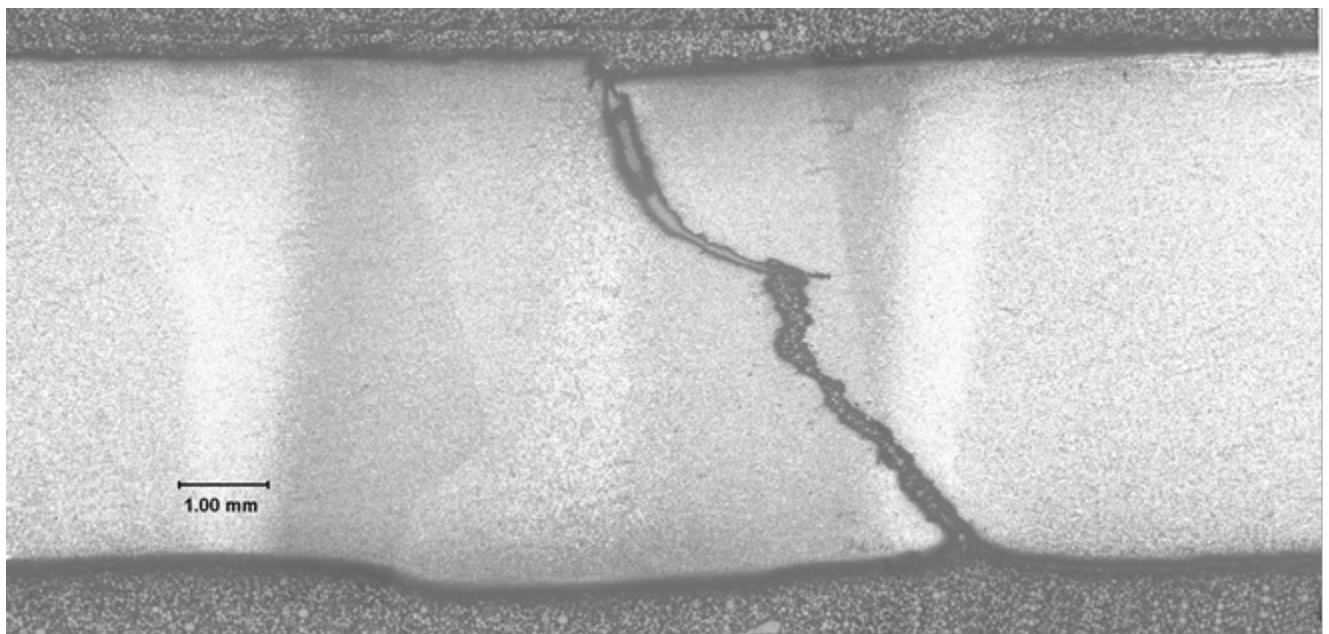


Figure 28. Cross Section of Hook Crack Where End of Hook Crack Was Not Close to the Bondline (Note that the fracture propagated in the heat-affected zone of the base metal.)

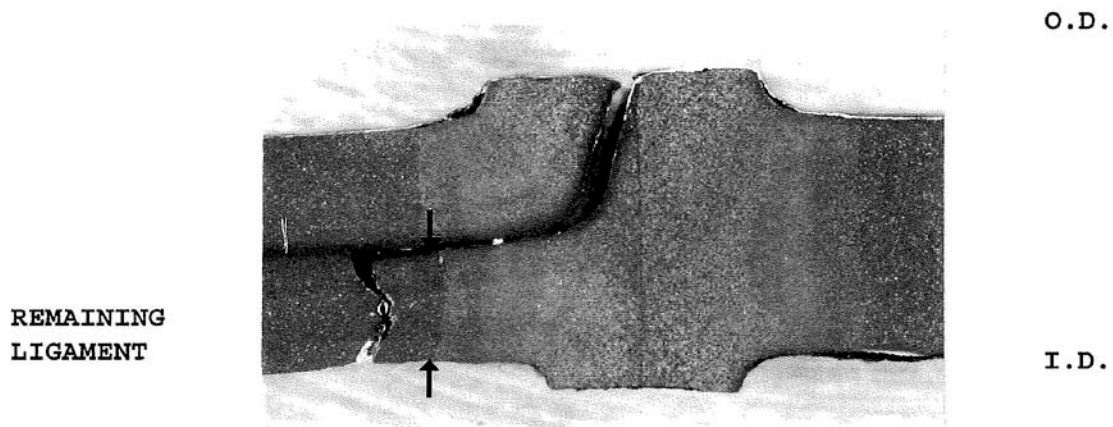


Figure 29. Cross Section of a Flash-Welded Seam Where the Hook Crack Extended Far From the Bondline (Failure is in the base metal.)

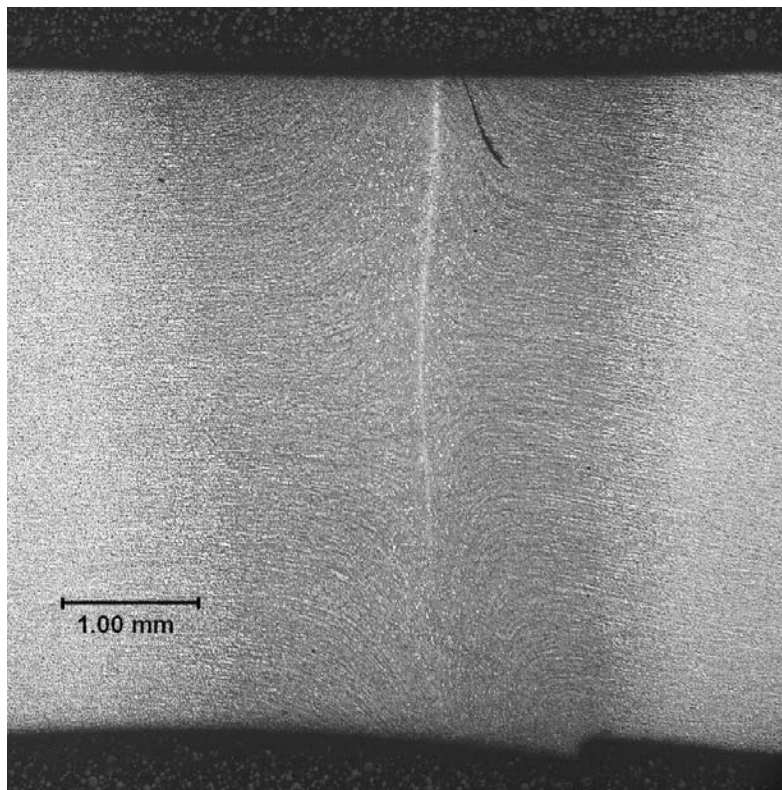


Figure 30. Cross Section of a Small Hook Crack near a Low-Frequency-Welded Seam

The pipe attributes, manufacturers, and failure stress levels are listed for the 76 hook crack failures in Table 11 (a two-page table). Note that the database number of each case is given in the second column. The failures are listed in order by failure stress level starting with lowest failure stress level. In some cases the type of fluid in the pipeline is highlighted in yellow. These highlighted cases correspond to cases involving failures that occurred in one pipeline

where the fluid was not stated. The fluid was assumed to be liquid because of the occurrence of fatigue crack growth in some cases in the same pipeline that will be discussed later.

Table 11. Listing of the Failures Caused by Hook Cracks,CasesHC1 through HC38

HC Case Number	Database Number	Liquid/Gas	Pipe OD, inches	Pipe WT, inch	SMYS, psi	Type of Seam	Manufacturer	Failure Pressure, %SMYS
1	244	Liquid	12.75	0.280	42,000	ERW - LF	Republic	56.6
2	8	Liquid	12.75	0.219	52,000	ERW - LF	J&L	68.3
3	235	Liquid	16	0.312	52,000	ERW - LF	NS	68.5
4	236	Liquid	12.75	0.281	35,000	ERW - LF	NS	78.8
5	137	Liquid	18	0.312	46,000	ERW - LF	Youngstown	80.8
6	45	HVL	10.75	0.219	52,000	ERW - LF	J&L	81.2
7	68	Liquid	20	0.312	42,000	ERW - DC	Youngstown	81.3
8	115	Liquid	22	0.312	46,000	ERW - DC	Youngstown	81.4
9	212	Liquid	16	0.25	52,000	ERW - LF	Lone Star	81.8
10	67	Liquid	20	0.312	42,000	ERW - DC	Youngstown	82.3
11	127	Liquid	8.625	0.219	52,000	ERW - LF	J&L	82.5
12	249	Gas	8.625	0.188	46,000	ERW - HF	Cal-metal pipe	82.5
13	184	Liquid	10.75	0.219	52,000	ERW - LF	J&L	83.1
14	47	HVL	10.75	0.219	52,000	ERW - LF	J&L	83.4
15	3	Liquid	16	0.308	52,000	ERW - HF	NS	83.7
16	46	HVL	10.75	0.219	52,000	ERW - LF	J&L	83.8
17	139	Liquid	18	0.312	46,000	ERW - NS	Youngstown	85.6
18	69	Liquid	20	0.312	42,000	ERW - DC	Youngstown	85.6
19	5	Liquid	10.75	0.203	52,000	ERW - HF	J&L	86.0
20	63	Liquid	20	0.312	42,000	ERW - DC	Youngstown	86.3
21	9	Liquid	12.75	0.219	52,000	ERW - LF	NS	87.4
22	182	Liquid	10.75	0.219	52,000	ERW - LF	J&L	87.6
23	183	Liquid	10.75	0.219	52,000	ERW - LF	J&L	87.6
24	237	Liquid	12.75	0.281	35,000	ERW - LF	NS	88.2
25	58	Liquid	12.75	0.25	52,000	ERW - HF	NS	88.3
26	181	Liquid	10.75	0.219	52,000	ERW - LF	J&L	88.4
27	138	Liquid	18	0.312	46,000	ERW - NS	Youngstown	88.4
28	6	Liquid	10.75	0.203	52,000	ERW - HF	J&L	89.9
29	37	HVL	12.75	0.25	52,000	ERW - LF	Lone Star	90.6
30	75	Liquid	16	0.25	52,000	ERW - DC	Youngstown	91.0
31	238	Liquid	12.75	0.281	35,000	ERW - LF	NS	91.4
32	126	Liquid	8.625	0.219	52,000	ERW - LF	J&L	91.6
33	117	Liquid	16	0.25	52,000	ERW - LF	NS	91.9
34	93	Liquid	12.75	0.25	46,000	ERW - LF	NS	92.0
35	191	Liquid	12.75	0.25	52,000	ERW - LF	Lone Star	92.3
36	40	HVL	12.75	0.25	52,000	ERW - LF	Lone Star	92.7
37	187	Liquid	12.75	0.25	52,000	ERW - LF	Lone Star	93.5
38	36	HVL	12.75	0.25	52,000	ERW - LF	Lone Star	94.0

Table 11. (continued) Listing of the Failures Caused by Hook Cracks, Cases HC39 through HC76 (the highlighted cells correspond to cases where the type of fluid was assumed to be liquid)

HC Case Number	Database Number	Liquid/Gas	Pipe OD, inches	Pipe WT, inch	SMYS, psi	Type of Seam	Manufacturer	Failure Pressure, %SMYS
39	173	Liquid	12.75	0.25	46,000	ERW - LF	Republic	94.1
40	104	Liquid	12.75	0.25	46,000	ERW - LF	Republic	94.3
41	198	Liquid	12.75	0.25	52,000	ERW - LF	Lone Star	94.3
42	143	Liquid	10.75	0.25	42,000	ERW - LF	Republic	94.9
43	145	Liquid	10.75	0.25	42,000	ERW - LF	Republic	94.9
44	193	Liquid	12.75	0.25	52,000	ERW - LF	Lone Star	94.9
45	144	Liquid	10.75	0.25	42,000	ERW - LF	Republic	95.0
46	192	Liquid	12.75	0.25	52,000	ERW - LF	Lone Star	95.8
47	88	Liquid	12.75	0.25	46,000	ERW - LF	NS	95.9
48	188	Liquid	12.75	0.25	52,000	ERW - LF	Lone Star	96.1
49	216	Liquid	6.625	0.125	60,000	ERW - HF	TexTube Pipe C	97.3
50	174	Liquid	20	0.312	46,000	ERW - DC	Youngstown	98.0
51	208	Liquid	26	0.281	52,000	Flash-weld	A.O. Smith	100.0
52	234	HVL	8.625	0.156	46,000	ERW - LF	Lone Star	100.7
53	175	Gas	16	0.25	46,000	ERW - HF	US Steel	100.9
54	161	Liquid	10.75	0.188	52,000	ERW - HF	NS	101.7
55	160	Liquid	10.75	0.188	52,000	ERW - HF	NS	102.2
56	267	Liquid	20	0.312	52,000	Flash-weld	A.O. Smith	103.2
57	253	Liquid	20	0.312	52,000	Flash-weld	A.O. Smith	112.5
58	254	Liquid	20	0.312	52,000	Flash-weld	A.O. Smith	112.5
59	255	Liquid	20	0.312	52,000	Flash-weld	A.O. Smith	112.6
60	256	Liquid	20	0.312	52,000	Flash-weld	A.O. Smith	112.7
61	116	Liquid	16	0.25	42,000	ERW - LF	NS	113.5
62	258	Liquid	20	0.312	52,000	Flash-weld	A.O. Smith	115.6
63	277	Liquid	12.75	0.209	52,000	ERW - LF	Page Hersey	116.1
64	273	Liquid	20	0.312	52,000	Flash-weld	A.O. Smith	117.1
65	271	Liquid	20	0.312	52,000	Flash-weld	A.O. Smith	118.7
66	271	Liquid	20	0.312	52,000	Flash-weld	A.O. Smith	120.2
67	259	Liquid	20	0.312	52,000	Flash-weld	A.O. Smith	126.4
68	260	Liquid	20	0.312	52,000	Flash-weld	A.O. Smith	126.4
69	261	Liquid	20	0.312	52,000	Flash-weld	A.O. Smith	126.4
70	278	Liquid	12.75	0.228	52,000	ERW - LF	Page Hersey	127.1
71	269	Liquid	20	0.312	52,000	Flash-weld	A.O. Smith	132.5
72	250		20	0.312	52,000	ERW - DC	Youngstown	135.6
73	251		20	0.312	52,000	ERW - DC	Youngstown	135.6
74	252		20	0.312	52,000	ERW - DC	Youngstown	135.6
75	273	Liquid	20	0.312	52,000	Flash-weld	A.O. Smith	138.7
76	265	Liquid	20	0.312	52,000	Flash-weld	A.O. Smith	140.2

As seen in Table 11, hook cracks have occurred across large ranges of pipe sizes, material grades, and manufacturers. They have caused failures in both gas and liquid pipelines, and they have appeared in all types of non-filler-metal seams (i.e., LF-ERW, DC-ERW, HF-ERW, and EFW).

Along with the failure stress levels of the 76 hook crack failures, Table 12 (also given in two parts) presents the mode of failure (leak or rupture), whether the event occurred in-service or during a hydrostatic test, and the stress levels reached in the most recent hydrostatic test and the mill hydrostatic test. The vintage of the pipe is included, and whether or not the failure occurred below the mill test pressure is noted.

Note that HC Case Numbers 57 through 76 have failure stress levels ranging from 112.5 to 140.2 percent of SMYS. These cases represent burst tests of pipes that had been removed from service because of anomalies found by an ILI crack tool. They were subsequently burst tested to determine the failure stress levels of the anomalies.

Table 12. Failure Modes and Failure Stresses of Cases HC1 through HC38

HC Case Number	Failure Mode	In-service or Hydrostatic Test	Failure Pressure, %SMYS	Pressure in last hydrostatic test, % SMYS	Pipe Vintage	Mill Test Pressure, SMYS	Failure Pressure less than Mill Test Pressure
1	Rupture		56.6	74.8	1949	85	yes
2	Rupture	Hydrostatic test	68.3		1962	85	yes
3	Rupture	Hydrostatic test	68.5	86.8	1965	85	yes
4	Rupture	Hydrostatic test	78.8	77.8	1948	60	no
5	Rupture	Hydrostatic test	80.8		1950	85	yes
6	Rupture	Hydrostatic test	81.2		1961	85	yes
7	Rupture	Hydrostatic test	81.3	85.2	1944	85	yes
8	Rupture	Hydrostatic test	81.4	81.2	1949	85	yes
9	Rupture	Hydrostatic test	81.8		1961	85	yes
10	Rupture	Hydrostatic test	82.3	81.8	1944	85	yes
11	Rupture	Hydrostatic test	82.5		1960	75	no
12	Rupture	Hydrostatic test	82.5		1963	75	no
13	Rupture	Hydrostatic test	83.1	83.7	1961	85	yes
14	Rupture	Hydrostatic test	83.4		1961	85	yes
15	Rupture	Hydrostatic test	83.7	88.3	1967	85	yes
16	Rupture	Hydrostatic test	83.8		1961	85	yes
17	Rupture	Hydrostatic test	85.6		1950	85	no
18	Rupture	Hydrostatic test	85.6	86.2	1944	60	no
19	Rupture	Hydrostatic test	86.0		1962	85	no
20	Rupture	Hydrostatic test	86.3	75.9	1944	60	no
21	Rupture	Hydrostatic test	87.4		1962	85	no
22	Rupture	Hydrostatic test	87.6	82.0	1961	85	no
23	Rupture	Hydrostatic test	87.6	82.0	1961	85	no
24	Rupture	Hydrostatic test	88.2	77.8	1948	60	no
25	Rupture	Hydrostatic test	88.3	89.3	1971	85	no
26	Rupture	Hydrostatic test	88.4	82.7	1961	85	no
27	Rupture	Hydrostatic test	88.4		1950	85	no
28	Rupture	Hydrostatic test	89.9		1962	85	no
29	Rupture	Hydrostatic test	90.6		1961	85	no
30	Rupture	Hydrostatic test	91.0	87.0	1954	85	no
31	Rupture	Hydrostatic test	91.4	77.8	1948	60	no
32	Rupture	Hydrostatic test	91.6		1960	75	no
33	Rupture	Hydrostatic test	91.9		1960	85	no
34	Rupture	Hydrostatic test	92.0	93.0	1964	85	no
35	Rupture	Hydrostatic test	92.3	89.1	1961	85	no
36	Rupture	Hydrostatic test	92.7		1961	85	no
37	Rupture	Hydrostatic test	93.5	87.7	1961	85	no
38	Rupture	Hydrostatic test	94.0		1961	85	no

Table 12. (continued) Failure Modes and Failure Stresses of Cases HC39 through HC76

HC Case Number	Failure Mode	In-service or Hydrostatic Test	Failure Pressure, %SMYS	Pressure in last hydrostatic test, % SMYS	Pipe Vintage	Mill Test Pressure, SMYS	Failure Pressure less than Mill Test Pressure
39	Rupture	Hydrostatic test	94.1	95.9	1964	85	no
40	Rupture	Hydrostatic test	94.3	94.2	1958	85	no
41	Rupture	Hydrostatic test	94.3	88.4	1961	85	no
42	Rupture	Hydrostatic test	94.9		1954	85	no
43	Rupture	Hydrostatic test	94.9		1954	85	no
44	Rupture	Hydrostatic test	94.9	88.3	1961	85	no
45	Rupture	Hydrostatic test	95.0		1954	85	no
46	Rupture	Hydrostatic test	95.8	87.7	1961	85	no
47	Rupture	Hydrostatic test	95.9	93.0	1964	85	no
48	Rupture	Hydrostatic test	96.1	90.7	1961	85	no
49	Rupture	Hydrostatic test	97.3	100.1	1982	75	no
50	Rupture	Hydrostatic test	98.0		1950	85	no
51	Leak	Hydrostatic test	100.0		1956	90	no
52	Rupture	Hydrostatic test	100.7		1968	75	no
53	Rupture	Hydrostatic test	100.9	84.5	1964	85	no
54	Rupture	Hydrostatic test	101.7		1970	85	no
55	Rupture	Hydrostatic test	102.2		1970	85	no
56	Rupture	Hydrostatic test	103.2		1950s	90	no
57	Rupture	Hydrostatic test	112.5		1950s	90	no
58	Rupture	Hydrostatic test	112.5		1950s	90	no
59	Rupture	Hydrostatic test	112.6		1950s	90	no
60	Rupture	Hydrostatic test	112.7		1950s	90	no
61	Rupture	Hydrostatic test	113.5		1960	85	no
62	Rupture	Hydrostatic test	115.6		1950s	90	no
63	Rupture	Hydrostatic test	116.1	88.9	1961	85	no
64	Rupture	Hydrostatic test	117.1		1950s	90	no
65	Rupture	Hydrostatic test	118.7		1950s	90	no
66	Rupture	Hydrostatic test	120.2		1950s	90	no
67	Rupture	Hydrostatic test	126.4		1950s	90	no
68	Rupture	Hydrostatic test	126.4		1950s	90	no
69	Rupture	Hydrostatic test	126.4		1950s	90	no
70	Rupture	Hydrostatic test	127.1	88.9	1961	85	no
71	Rupture	Hydrostatic test	132.5		1950s	90	no
72	Rupture	Hydrostatic test	135.6		1950s	90	no
73	Rupture	Hydrostatic test	135.6		1950s	90	no
74	Rupture	Hydrostatic test	135.6		1950s	90	no
75	Rupture	Hydrostatic test	138.7		1950s	90	no
76	Rupture	Hydrostatic test	140.2		1950s	90	no

All but one of the hook crack failures occurred as ruptures; only one failed as a leak. This probably reflects the tendency of hook cracks to be long in the axial direction unlike cold welds which are often quite short. All except one of the hook crack failures occurred during hydrostatic tests. In the other case whether the failure occurred in-service, information regarding a hydrostatic test was not provided. Thirteen of the 76 hook crack failures occurred at stress levels below that of the manufacturer's hydrostatic test. The rest occurred at levels above the manufacturer's hydrostatic test. These results tend to suggest that hook cracks are less a threat to pipeline integrity provided that they do not grow in service from pressure-cycle-induced fatigue than cold welds. However, it is necessary to look at a few individual cases to see if such general conclusions are warranted.

HC Case Number 1

HC Case Number 1 involved a rupture in the seam of a 12.75-inch-OD, 0.280-inch-wall, X42 low-frequency-welded ERW material manufactured by Republic in 1949. The rupture initiated at an OD-surface-connected hook crack at a hoop stress level of 56.6 percent of SMYS. This stress level is well below the 85-percent-of-SMYS mill test pressure. It was concluded that this anomaly failed as the result of "stable crack growth from a few large pressure cycles leading to a pressure reversal". Whether this failure occurred in service or in a hydrostatic test was not revealed. The pipeline was a liquid pipeline. Dimensions of the hook crack were not provided.

HC Case Number 2

HC Case Number 2 involved a hydrostatic test rupture in the seam of a 12.75-inch-OD, 0.219-inch-wall, X52 low-frequency-welded ERW material manufactured by J&L in 1962. The rupture initiated at an OD-surface-connected hook crack at a hoop stress level of 68.3 percent of SMYS. This stress level is well below the 85-percent-of-SMYS mill test pressure.

The length of the hook crack was 7.5 inches, and it penetrated 30 percent of the wall thickness. The predicted failure stress level based on these dimensions and a full-size-equivalent Charpy upper shelf energy of 26 ft lb was calculated to be 100.9 percent of SMYS via the Modified Ln-Sec Elliptical-C-equivalent method. Thus, this hook crack failed at a stress level only 68 percent of the predicted level. No evidence of crack growth from fatigue was observed, however, there was evidence of ductile tearing at the base of the hook crack and that the fracture then jumped into the bondline.

A photograph of a metallographic section across this anomaly is shown in Figure 31 where the almost-detached piece of material and the transition from a hook crack to a bondline failure can be seen.

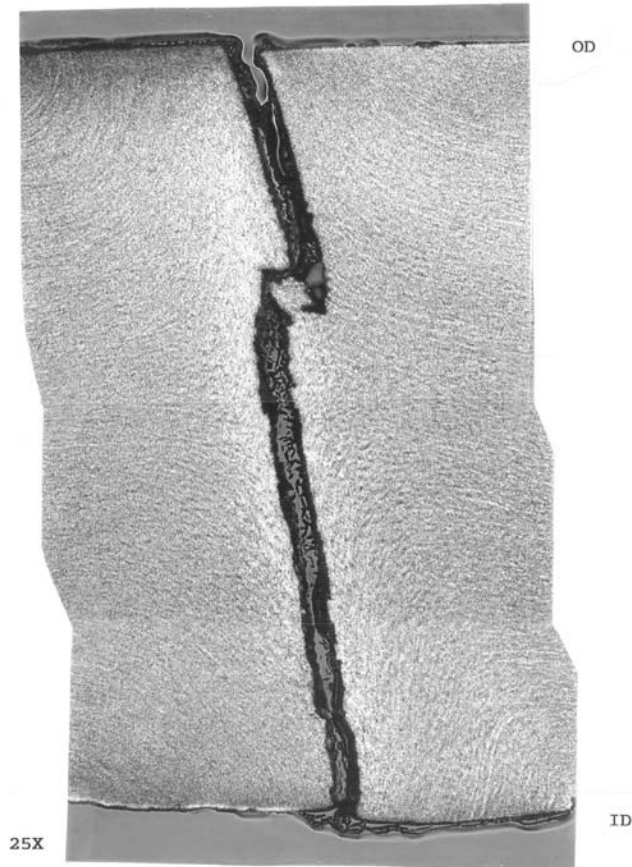


Figure 31. Cross Section across HC Case Number 2 Defect

The end of the crack is close to the bondline in the manner shown in Figure 27. Moreover, the appearance of the fracture shown in Figure 31 is similar to the appearance of the metallographic section of the likely origin of the Carmichael service failure (see Figure 32). Both appeared to have been extended by some amount of ductile crack extension followed by an abrupt transition step from the hook crack to a bondline failure. Both had survived previous tests to stress levels considerably above the observed failure stress of the anomaly. The anomaly in HC Case Number 2 failed at a hoop stress level of about 80 percent of the hoop stress level in the manufacturer's hydrostatic test conducted 32 years earlier. The anomaly that likely initiated the Carmichael failure, failed at a hoop stress level of about 80 percent of the hoop stress level in a previous hydrostatic test conducted 23 years earlier. The implication is that something changed in both situations over the period between the tests and the subsequent failures at much lower stress levels. Growth of the defects either by ductile tearing or pressure-cycle-induced fatigue is assumed to have occurred, and that growth may have facilitated the abrupt failure of the bondline in a brittle manner in both cases.



Figure 32. Metallographic Section across Likely Origin of the Carmichael failure.

HC Case Number 3

HC Case Number 3 involved a hydrostatic test rupture in the seam of a 16-inch-OD, 0.312-inch-wall, X52 low-frequency-welded ERW material manufactured in 1965. The manufacturer was not stated. The rupture initiated at a hook crack at a hoop stress level of 68.5 percent of SMYS. This stress level was well below that 85-percent-of-SMYS mill test pressure and also well below a prior field hydrostatic test to a level of 86.8 percent of SMYS. The pipeline was a liquid pipeline. The hook crack had a length of 44 inches and a maximum depth-to-thickness ratio of 0.4. The base material had a full-size-equivalent Charpy upper shelf energy of 29 ft lb. Using the defect dimensions and the shelf energy, one can predict a failure stress level of 58.1 percent of SMYS via the Modified Ln-Sec Elliptical-C-equivalent method for the hook crack.

HC Case Number 4

HC Case Number 4 involved a hydrostatic test rupture in the seam of a 12.75-inch-OD, 0.281-inch-wall, Grade B low-frequency-welded ERW material manufactured in 1948. The manufacturer was not stated. The rupture initiated at a hook crack at a hoop stress level of 78.8 percent of SMYS. This stress level exceeded both the 60-percent-of-SMYS mill test pressure and a prior field hydrostatic test to a level of 77.8 percent of SMYS. The pipeline was a liquid pipeline. The hook crack had a length of 22 inches and a maximum depth-to-thickness ratio of 0.5. Although no Charpy data were provided for this material, a reasonable assumption for the base material would be a full-size-equivalent Charpy upper shelf energy of 25 ft lb. Using the

defect dimensions and the assumed shelf energy and an assumed flow stress of 50,000 psi, one can predict a failure stress level of 61.9 percent of SMYS via the Modified Ln-Sec Elliptical-C-equivalent method. Because this rupture occurred at the highest stress level the pipe had ever experienced, its occurrence is not surprising.

HC Case Numbers 11 and 12

Similar to Case Number 4, the hook cracks in Case Numbers 11 and 12 failed at stress levels above the levels of their mill hydrostatic tests. Hence, these occurrences are not surprising.

HC Case Number 5

HC Case Number 5 involved a hydrostatic test rupture in the seam of an 18-inch-OD, 0.312-inch-wall, X46 DC -welded ERW material manufactured by Youngstown in 1950. The rupture initiated at a hook crack at a hoop stress level of 80.8 percent of SMYS. While no evidence of crack growth by fatigue was mentioned, this rupture occurred at a stress level below that of the 85-percent-of-SMYS mill test.

The length of the OD-connected hook crack was 6 inches, and it penetrated 50 percent of the wall thickness. The predicted failure stress based on these dimensions and a full-size-equivalent Charpy upper shelf energy of 25 ft lb was calculated to be 82.3 percent of SMYS via the Modified Ln-Sec Elliptical-C-equivalent method.

HC Case Numbers 6, 14, and 16

HC Case Numbers 6, 14, and 16 involved successive hydrostatic test ruptures in the seams of three pieces of 10.75-inch-OD, 0.219-inch-wall, X52 low-frequency-welded ERW material manufactured by J&L in 1961. The rupture in HC Case Number 6 initiated at a hook crack at a hoop stress level of 81.2 percent of SMYS. The rupture in HC Case Number 14 initiated at a hook crack at a hoop stress level of 83.4 percent of SMYS. The rupture in HC Case Number 16 initiated at a hook crack at a hoop stress level of 83.8 percent of SMYS. While no evidence of crack growth by fatigue was mentioned in these cases, all three ruptures occurred at stress levels below that of the 85-percent-of-SMYS mill test.

The length of the OD-connected hook crack in Case Number 6 was 9 inches, and it penetrated 38 percent of the wall thickness. The predicted failure stress based on these dimensions and a full-size-equivalent Charpy upper shelf energy of 42 ft lb was calculated to be 91.0 percent of SMYS via the Modified Ln-Sec Elliptical-C-equivalent method.

The length of the OD-connected hook crack in Case Number 14 was 3 inches, and it penetrated 39 percent of the wall thickness. The predicted failure stress based on these dimensions and a

full-size-equivalent Charpy upper shelf energy of 44 ft lb was calculated to be 113.7 percent of SMYS via the Modified Ln-Sec Elliptical-C-equivalent method.

The length of the OD-connected hook crack in Case Number 16 was 8.5 inches, and it penetrated 40 percent of the wall thickness. The predicted failure stress based on these dimensions and a full-size-equivalent Charpy upper shelf energy of 29 ft lb was calculated to be 90.3 percent of SMYS via the Modified Ln-Sec Elliptical-C-equivalent method.

HC Case Numbers 7 and 10

These two failures occurred as successive ruptures in a hydrostatic test of an existing pipeline. The pipe was 20-inch-OD, 0.312-inch-wall, X42, DC-welded material. The pipe had been manufactured in 1944 by Youngstown. The API 5LX specification did not exist until 1949, but it is not unusual for materials to be designated as X grades in the period prior from about 1941 through 1948 if the purchaser and the manufacturer agreed on a minimum strength level above that of Grade B pipe. However, it would be expected that the mill test pressure would be 85 percent of the specified SMYS. The rupture in HC Case Number 7 occurred at a hoop stress level of 81.3 percent of SMYS, and the rupture of HC Case Number 10 occurred at a hoop stress level of 82.3 percent of SMYS. Dimensions of the anomalies were not available.

HC Case Numbers 8

HC Case Number 8 involved a hydrostatic test rupture in the seam of a 22-inch-OD, 0.312-inch-wall, X46, DC-welded ERW material manufactured by Youngstown in 1949. The rupture initiated at a hook crack at a hoop stress level of 81.4 percent of SMYS. While no evidence of crack growth by fatigue was mentioned, this rupture occurred at a stress level below that of the 85-percent-of-SMYS mill test.

The length of the OD-connected hook crack was 1.6 inches, and penetrated 30 percent of the wall thickness. The predicted failure stress base on these dimensions and a full-size-equivalent Charpy upper shelf energy of 16 ft lb was calculated to be 138.4 percent of SMYS via the Modified Ln-Sec Elliptical-C-equivalent method. Because the hook crack failed at a much lower stress level, it appears that the effective toughness of the material near the bondline was much less than that of the base metal. One possible reason for this is that the weld heat-affected zone was excessively hard (21 to 36 Rockwell C), something not unexpected for Youngstown pipe of this vintage.

HC Case Number 9

HC Case Number 9 involved a hydrostatic test rupture in the seam of a 16-inch-OD, 0.250-inch-wall, X52, low-frequency-welded ERW material manufactured by Lone Star in 1961. The

rupture initiated at an embedded hook crack at a hoop stress level of 81.9 percent of SMYS. While no evidence of crack growth by fatigue was mentioned, this rupture occurred at a stress level below that of the 85-percent-of-SMYS mill test.

Because the hook crack was imbedded, no attempt was made to calculate a predicted failure stress level.

HC Case Number 13

HC Case Number 13 involved a hydrostatic test rupture in the seam of a 10.75-inch-OD, 0.219-inch-wall, X52, low-frequency-welded ERW material manufactured by J&L in 1961. The rupture initiated at a hook crack at a hoop stress level of 81.2 percent of SMYS. While no evidence of crack growth by fatigue was mentioned, the rupture occurred at a stress level below that of the 85-percent-of-SMYS mill test.

The length of the OD-connected hook crack in Case Number 13 was 10.75 inches, and it penetrated 35 percent of the wall thickness. The predicted failure stress base on these dimensions and a full-size-equivalent Charpy upper shelf energy of 43 ft lb was calculated to be 91.7 percent of SMYS via the Modified Ln-Sec Elliptical-C-equivalent method.

HC Case Number 15

HC Case Number 15 involved a hydrostatic test rupture in the seam of a 16-inch-OD, 0.308-inch-wall, X52, high-frequency-welded ERW material manufactured in 1967. The manufacturer of the pipe is unknown. The rupture initiated at a hook crack at a hoop stress level of 83.7 percent of SMYS. While no evidence of crack growth by fatigue was mentioned, this rupture occurred at a stress level below that of the 85-percent-of-SMYS mill test.

The length of the OD-connected hook crack was 6.5 inches, and it penetrated 39 percent of the wall thickness. The predicted failure stress base on these dimensions and a full-size-equivalent Charpy upper shelf energy of 38 ft lb was calculated to be 95.7 percent of SMYS via the Modified Ln-Sec Elliptical-C-equivalent method.

Summary of Hook Crack Failures

Seventy-five of the 76 hook crack failures were ruptures; only one failed as a leak. The failure stress levels of the hook cracks as a percent of SMYS are shown in Figure 33. Thirteen of these 76 hook cracks failed at stress levels either below that of the mill test or a previous field hydrostatic test. It is seen that four of the hook crack failures occurred at stress levels less than 80 percent of SMYS.

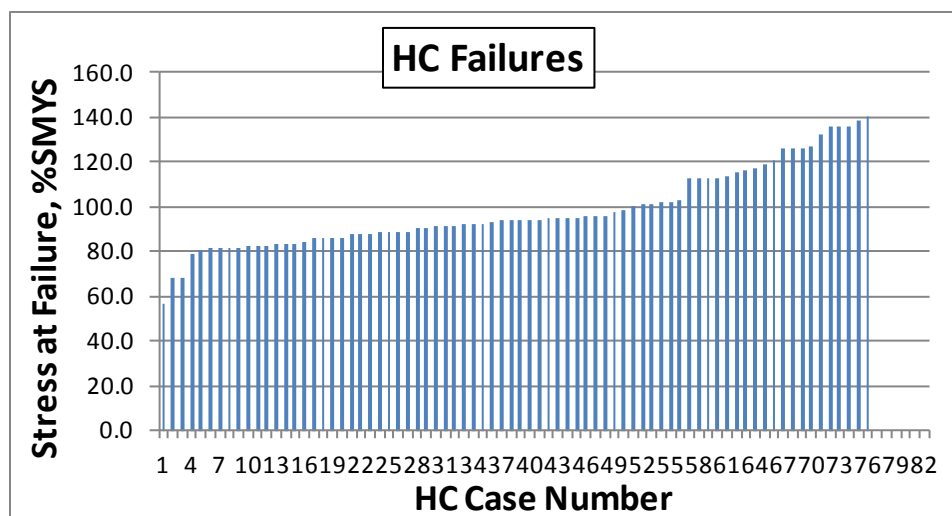


Figure 33. Stress Levels of Hook Crack Failures

As discussed above, whether the rupture with the lowest failure stress level failed in-service or in a hydrostatic test is not known. The other three ruptures that occurred at stress levels below 80 percent of SMYS occurred during hydrostatic tests. The failure investigations of two of the four cases with failure stress levels below 80 percent of SMYS (Case Numbers 1 and 2) indicate that some sort of crack growth (ductile tearing in prior pressurizations or possibly fatigue) is believed to have occurred leading to reduced failure pressures. It is believed that some amount of crack growth must have occurred in Case Number 3 as well, but no information was available to that effect. In Case Number 4, the mill test pressure is believed to have been only to the 60-percent-of-SMYS level, so the fact that the failure occurred at a pressure level of 78.8 percent of SMYS is not surprising.

The remaining hook cracks which failed at hoop stress levels below 85 percent of SMYS (the level of their mill hydrostatic tests) failed at stress levels ranging from 80.8 to 83.8 percent of SMYS. It is conceivable that the mill test with its 5 or 10 second hold time does not allow sufficient time for defects with failure pressures near the mill test pressure to grow to failure. Instead what growth may occur in the process would tend to lead to pressure reversals the next time those pieces are subjected to pressurization to near-mill-test levels. So, it is likely that most if not all of the failures that occurred at stress levels within 95 percent of the mill test pressure can be attributed to pressure reversals. In effect a mill test only assures integrity to about 95 percent of the mill test stress level.

Throughout the rest of the database of 76 hook cracks, it is seen in Table 12 that some of the hook cracks failed at stress levels below that of a previous hydrostatic test. These cases likely involved pressure reversals from the previous tests. The worst case was HC Case Number 49

where a pressure reversal of 2.8 percent would explain the failure. Pressure reversals of this size are not all that unusual.

The ability of a ductile fracture model (the Modified Ln-Sec Elliptical CEQ model) to predict the failure stress levels of hook cracks using base metal flow stress and Charpy energy is illustrated in Figure 34. Values of the ratio “actual/predicted” failure stress ranged from below 0.6 to more than 1.8. The average value is 1.06, but the standard deviation is 0.35 and the R-squared coefficient is only 0.07 suggesting a poor correlation.

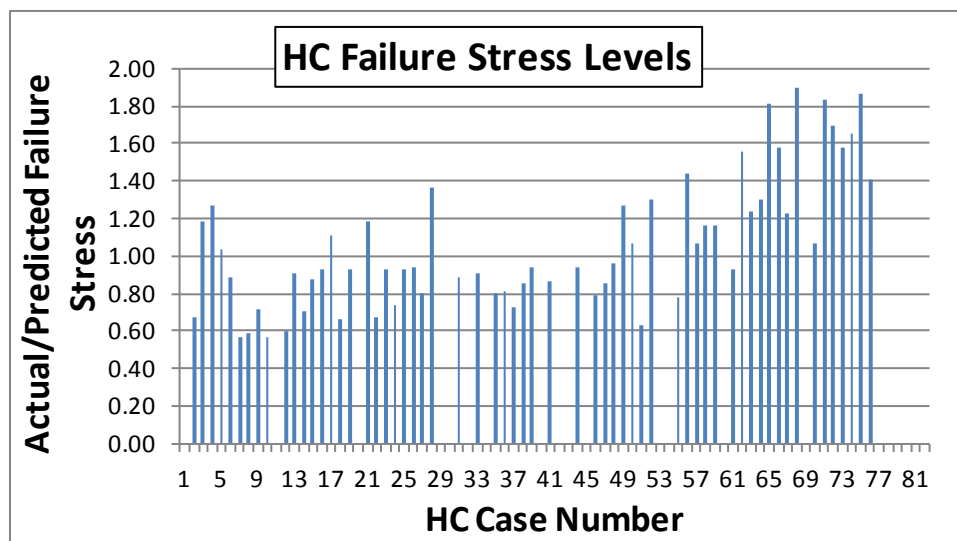


Figure 34. Ratio of Actual Failure Stress to Predicted Failure Stress

The depths of the hook cracks in the database varied from 14 percent to 60 percent of the wall thickness as shown in Figure 35. In view of the way hook cracks are formed, it is surprising to see depths greater than 50 percent of the wall thickness. Pictures of the deepest cracks were not available. However, one explanation could be that some of the depths given included apparent crack extension. Without seeing the pictures, one can only speculate as to the reasons for some hook cracks being deeper than 50 percent of the wall thickness. In some rare cases, none of which appeared in the database, hook cracks have been known to reverse curvature upon some type of erratic upsetting. In those cases the effective depth of a hook crack could exceed 50 percent of the wall thickness.

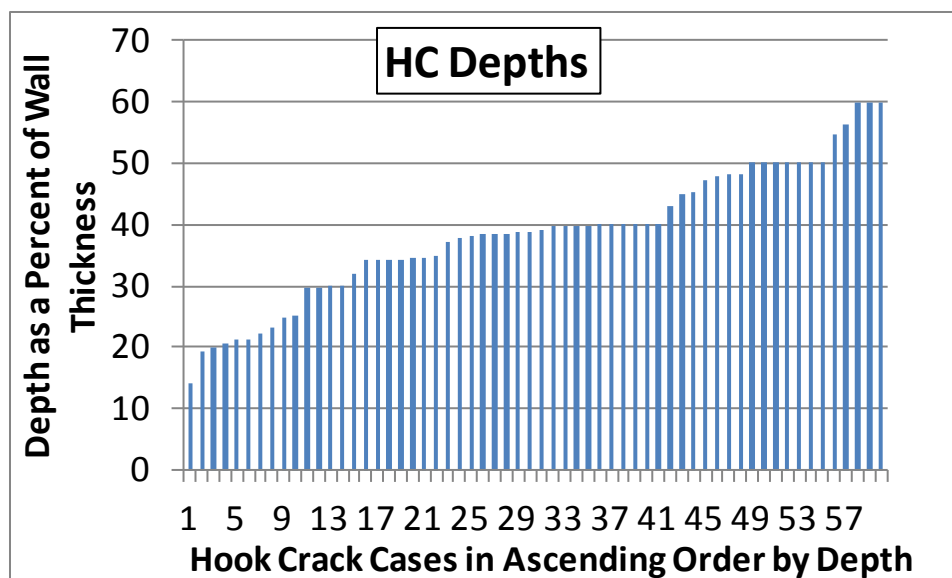


Figure 35. Depths of Hook Cracks

As with any anomaly that is on the verge of failure but does not fail in a hydrostatic test, hook cracks can be adversely affected by a hydrostatic test opening up the possibility of a pressure reversal. However, the fact that most, if not all of these hook crack failures occurred during hydrostatic tests and not in-service, suggests that hydrostatic testing is an effective way of eliminating the threat posed by a hook crack.

Cold Weld + Hook Crack

Occasionally, ERW seam failures have been observed to initiate from a combination of a cold weld and a hook crack. Five such failures are summarized in Table 13 and Table 14.

Table 13. Listing of Cases Arising from Combinations of a Cold Weld and a Hook Crack (the highlighted cell indicates a case where the fluid type was assumed to be a liquid)

CW+HC Case Number	Database Number	Liquid/Gas	Pipe OD, inches	Pipe WT, inch	SMYS, psi	Type of Seam	Manufacturer	In-service or Hydrostatic Test
1	77	Liquid	12.75	0.25	42,000	ERW - LF	Kaiser Steel	In-service
2	91	Liquid	12.75	0.25	46,000	ERW - LF	NS	Hydrostatic test
3	96	Liquid	12.75	0.25	46,000	ERW - LF	Republic	Hydrostatic test
4	105	Liquid	12.75	0.25	46,000	ERW - LF	Republic	Hydrostatic test
5	276	Liquid	20	0.312	52,000	Flash-weld	A.O. Smith	Hydrostatic test

Table 14. Failure Modes and Failure Stresses of Cases Arising from Combinations of a Cold Weld and a Hook Crack

CW+HC Case Number	Failure Mode	In-service or Hydrostatic Test	Failure Pressure, %SMYS	Pressure in last hydrostatic test, % SMYS	Pipe Vintage	Mill Test Pressure, SMYS	Failure Pressure less than Mill Test Pressure
1	Leak	In-service	27.3	92.2		85	yes
2	Rupture	Hydrostatic test	97.0	93.0	1964	85	no
3	Leak	Hydrostatic test	95.5	93.0	1958	85	no
4	Rupture	Hydrostatic test	90.8	94.2	1958	85	no
5	Rupture	Hydrostatic test	126.4		1950s	90	no

CW+HC Case Number 1

CW+HC Case Number 1 involved a 12.75-inch-OD, 0.250-inch-wall, X42, low-frequency-welded pipe manufactured by Kaiser. The year of manufacturing was unknown, but the metallography clearly showed that the weld had been made by low-frequency welding. The failure mode was a leak in service discovered while the pipeline was being operated at a hoop stress level of 27.3 percent of SMYS. The most recent hydrostatic test conducted 11 years prior to the discovery of the leak was carried out at a hoop stress level of 92.2 percent of SMYS. The anomaly had survived not only this latter test but a mill test to a stress level of 85 percent of SMYS.

The nature of the combined cold weld and hook crack is shown in Figure 36 and Figure 37. The cold weld in this case was less than ½ inch long, and it was ID-surface connected and extended about 60 percent through the wall. Opposite the cold weld at the OD surface was a long hook crack that had a depth of about 30 percent of the wall thickness. It appears that the leak was caused by tearing of the remaining ligament between the cold weld and the hook crack. Perhaps this tearing was caused by the hydrostatic test 11 years prior to the discovery of the leak.



Figure 36. Leak Associated with an OD-connected Hook Crack and ID-connected Cold Weld

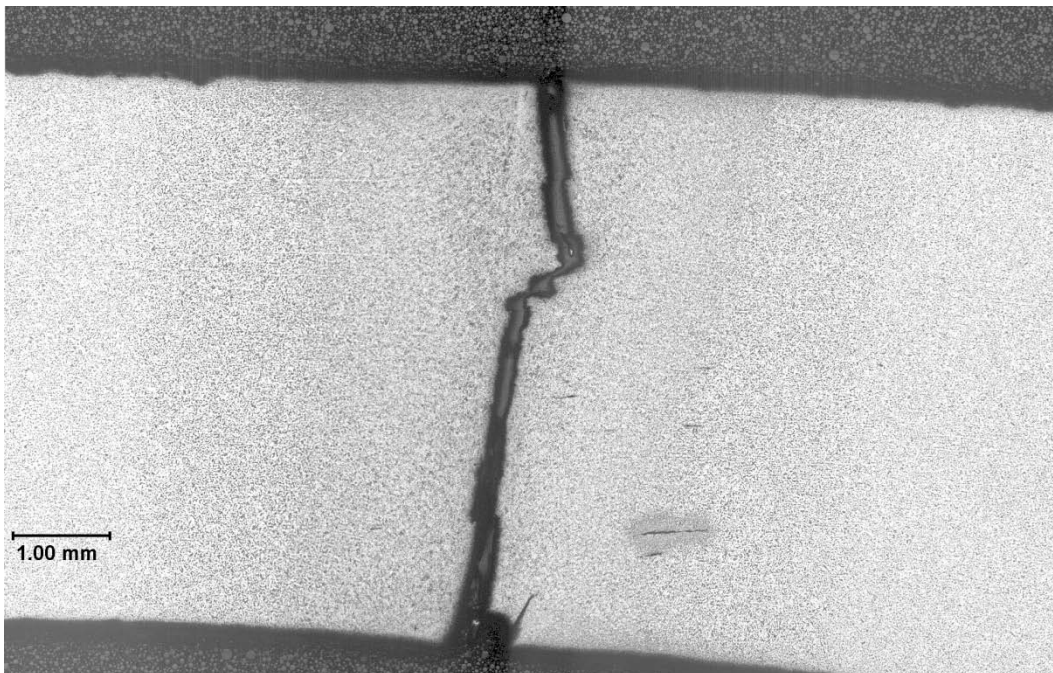


Figure 37. Metallographic Section across Leak Associated with a Cold Weld and a Hook Crack Showing that the Leak Path was the Result of Ductile Tearing Between the Two Anomalies

The other four combinations of cold welds and hook cracks failed at stress levels well above the level of the mill test. It is seen that in one case, Case Number 4, the failure took place at a stress level 3.4 percent below that of a previous hydrostatic test. It is reasonable to believe that combinations of cold welds and hook cracks such as these will behave in much the same manner as cold welds and hook cracks separately. As the Case Number 1 and Case Number 4 examples show, hydrostatic testing does not provide a guarantee that such anomalies will not fail at lower stress levels if such testing causes growth but not failure of the anomaly.

Stitching

The term “stitching” refers to a repetitive pattern that appears on the surfaces of a fracture along the bondline of a low-frequency-welded ERW seam. Such an appearance was seen previously in Figure 8 and Figure 12 in conjunction with cold welds, but the phenomenon can be seen on fracture surfaces where no cold weld exists as shown in Figure 38 below. The stitching phenomenon is attributed to variations in the strength of the bond resulting from variable heat input either from power fluctuations or too high a travel speed during welding. The power delivered by alternating current fluctuates because the voltage and current vary and are out of phase with one another. The phenomenon of stitching is associated only with low-frequency current because the rate of power variation is in the range where it can affect the bonding strength as the pipe moves through the welding stand. The power fluctuations of a high-frequency welder are much too fast to cause periodic variations in bonding, and the absence of power fluctuations associated with DC welding and flash welding eliminate the possibility of stitching in DC-welded or flash-welded pipe.

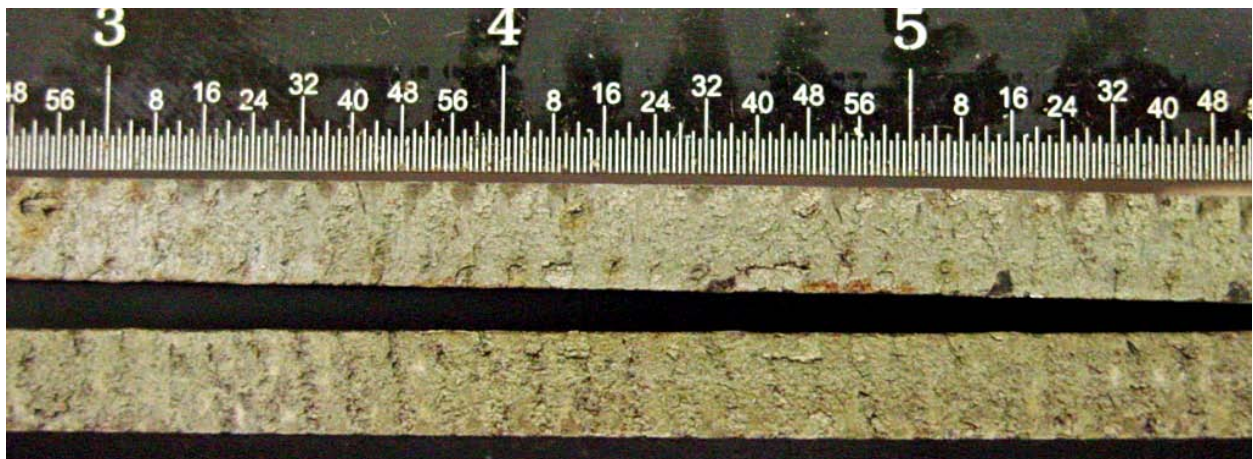


Figure 38. Stitch Pattern on a Fracture of the Bondline of a LF- ERW Seam

Seven failures in the database were associated with bondline fractures that exhibited stitching but no other recognizable defect. These are summarized in Table 15 and Table 16.

Table 15. Listing of Cases Arising from Stitching

Stitching Case Number	Database Number	Liquid/Gas	Pipe OD, inches	Pipe WT, inch	Pipe Grade	SMYS, psi	Type of Seam	Manufacturer
1	35	HVL	12.75	0.25	X52	52,000	ERW - LF	Lone Star
2	38	HVL	12.75	0.25	X52	52,000	ERW - LF	Lone Star
3	141	Gas	6.625	0.188	Grade B	35,000	ERW - LF	NS
4	142	Gas	6.625	0.188	Grade B	35,000	ERW - LF	NS
5	189	Liquid	12.75	0.25	X52	52,000	ERW - LF	Lone Star
6	190	Liquid	12.75	0.25	X52	52,000	ERW - LF	Lone Star
7	197	Liquid	12.75	0.25	X52	52,000	ERW - LF	Lone Star

Table 16. Failure Modes and Failure Stresses of Failures Attributed to Stitching

Stitching Case Number	Failure Mode	In-service or Hydrostatic Test	Failure Pressure, %SMYS	Pipe Vintage	Mill Test Pressure, SMYS	Failure Pressure less than Mill Test Pressure
1	Rupture	Hydrostatic test	91.2	1961	85	no
2	Rupture	Hydrostatic test	89.5	1961	85	no
3	Rupture	Hydrostatic test	91.7	1973	75	no
4	Rupture	Hydrostatic test	95.0	1973	75	no
5	Rupture	Hydrostatic test	96.4	1961	85	no
6	Rupture	Hydrostatic test	96.1	1961	85	no
7	Rupture	Hydrostatic test	94.2	1961	85	no

As seen in the tables, all seven cases occurred in low-frequency-welded pipe, all were ruptures and all occurred during hydrostatic tests at stress levels above the mill test stress levels. It is believed that these stitched welds failed in the absence of any actual anomaly because the stitched bondline was weaker than the surrounding base material. It was not uncommon for stitching to appear on the surface of the required weld tensile test for each heat. As long as the failure took place at a stress level above the specified minimum ultimate tensile strength of the base metal, the heat of pipe was considered acceptable. Stitching is a phenomenon that can be expected to appear on fracture surfaces of some low-frequency-welded bondlines. It means that the bondline has less-than-optimum fracture resistance. Stitching often appears on a fracture surface created by the failure of a defect. It may appear on a fracture surface in the absence of an initiating defect but usually when that fracture is created at a stress level well above the mill test pressure.

Woody Fracture

Woody Fracture is a term applied to the fracture surface of a failed ERW seam where the fracture has followed a highly irregular pattern usually because the fracture has included numerous planes of weakness caused by non-metallic inclusions near but not necessarily on the bondline. The appearances associated with two different “woody fractures” are shown in Figure 39 through Figure 42.

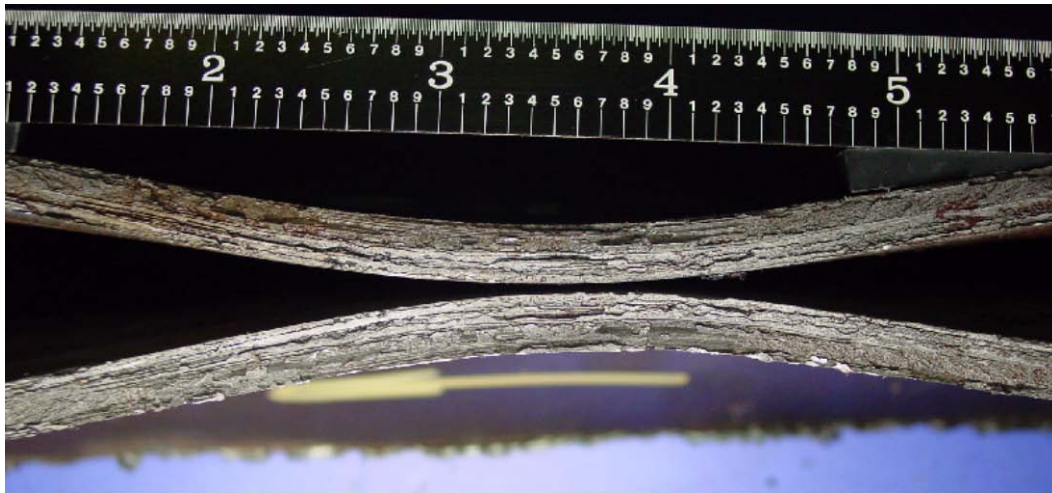


Figure 39. Fracture Surface of a Woody Fracture – Case Number W2

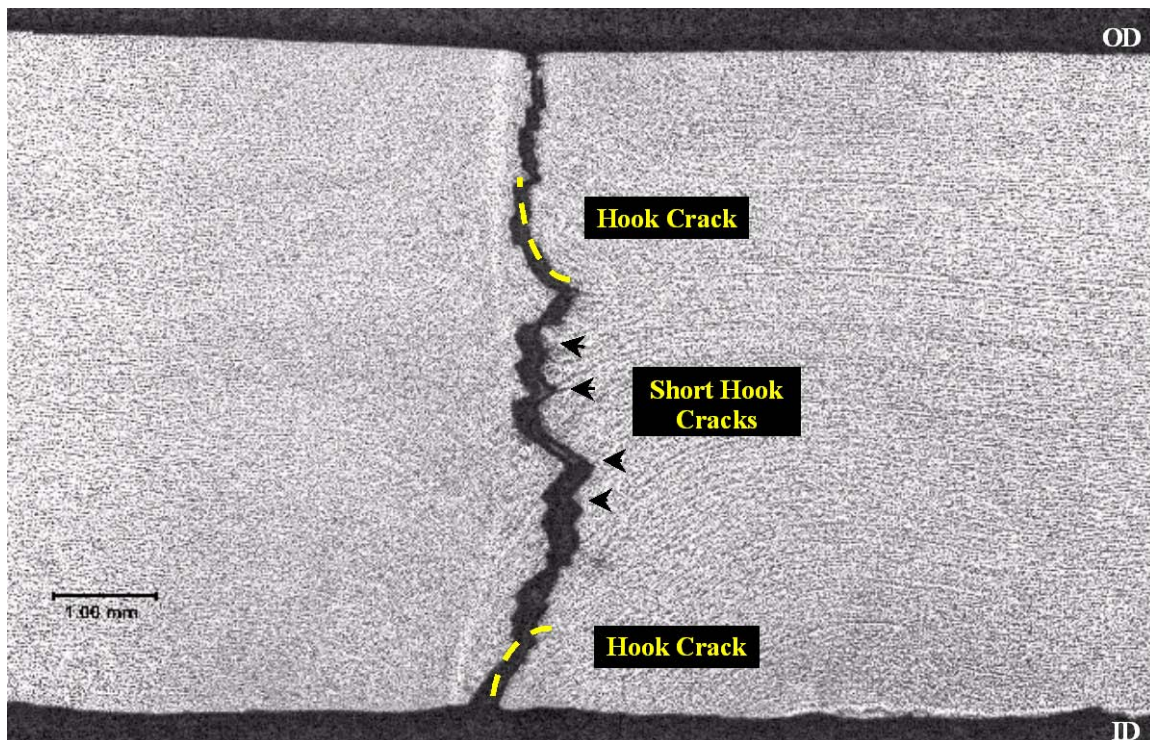


Figure 40. Metallographic Section across Woody Fracture – Case Number W2



Figure 41. Fracture Surface of a Woody Fracture – Case Number W3



Figure 42. Metallographic Section across Woody Fracture – Case Number W3

Six examples of ERW seam failures involving woody fractures are contained in the database, and they are listed in Table 17 and Table 18 below.

Table 17. Listing of Cases Involving Woody Fracture

Woody Fracture Case Number	Database Number	Liquid/Gas	Pipe OD, inches	Pipe WT, inch	Pipe Grade	SMYS, psi	Type of Seam	Manufacturer
1	34	HVL	12.75	0.25	X52	52,000	ERW - LF	Lone Star
2	102	Liquid	12.75	0.25	X46	46,000	ERW - LF	Republic
3	162	Liquid	10.75	0.188	X52	52,000	ERW - HF	NS
4	165	Liquid	10.75	0.188	X52	52,000	ERW - HF	NS
5	167	Liquid	10.75	0.188	X52	52,000	ERW - HF	NS
6	168	Liquid	10.75	0.188	X52	52,000	ERW - HF	NS

Table 18. Failure Modes and Failure Stresses of Cases of Woody Fractures

Woody Fracture Case Number	Failure Mode	In-service or Hydrostatic Test	Failure Pressure, %SMYS	Pressure in last hydrostatic test, % SMYS	Pipe Vintage	Mill Test Pressure, SMYS	Failure Pressure less than Mill Test Pressure
1	Rupture	Hydrostatic test	94.7		1961	85	no
2	Rupture	Hydrostatic test	95.6	94.2	1958	85	no
3	Rupture	Hydrostatic test	99.9		1970	85	no
4	Rupture	Hydrostatic test	105.0		1970	85	no
5	Rupture	Hydrostatic test	103.8		1970	85	no
6	Rupture	Hydrostatic test	104.6		1970	85	no

All six occurred as ruptures during hydrostatic tests at stress levels ranging from 94.7 to 104.6 percent of SMYS. It is believed that a woody fracture is the result of the interaction of many small non-metallic inclusions, small hook cracks, and/or small cold welds that, in combination, create a path of weakness. A woody fracture surface may accompany the failure of a defect, but the high failure stress levels associated with these woody fractures when no defect was present suggest that the welds, while not perfect, were not a significant threat to pipeline integrity.

Selective Seam Weld Corrosion

Overview

The database contains 24 incidents where the cause of failure was attributed primarily to selective seam weld corrosion (SSWC). All 24 cases involved external corrosion of the seam although selective seam weld corrosion can take place at either the OD or the ID surface if an

environment conducive to corrosion is present. Selective seam weld corrosion refers to the phenomenon where corrosion-caused metal loss occurs at a higher rate at the bondline and the surrounding heat-affected zone of an ERW or flash-welded seam than in the adjacent base metal. Research has shown that not all ERW materials are equally susceptible to selective seam weld corrosion².

Selective seam weld corrosion is of more concern for pipeline integrity assessment purposes than corrosion-caused metal loss in the base metal for a number of reasons:

- It progresses at a higher rate than corrosion in the pipe body.
- It is harder to detect with ILI than pipe body metal loss.
- The currently available ILI tools for assessing long axial flaws and crack-like flaws cannot accurately characterize the size of a selective seam weld corrosion anomaly.
- It tends to create narrow grooves, sometimes with almost crack-like sharpness in a material that usually has less fracture resistance than the pipe body.
- The narrowness of the groove created by selective seam weld corrosion makes it hard to determine the depth of the grooving when it is examined in the field.
- Methods for predicting remaining strength in the case of corrosion-caused pipe body metal loss should not be applied to selective seam weld corrosion because of its crack-like nature and its typically being located in a material with significantly less fracture resistance than the pipe body.

Selective seam weld corrosion as it appears at the surface of a pipeline is illustrated in Figure 43. It tends to appear as a straight groove within an area of corrosion-caused metal loss.

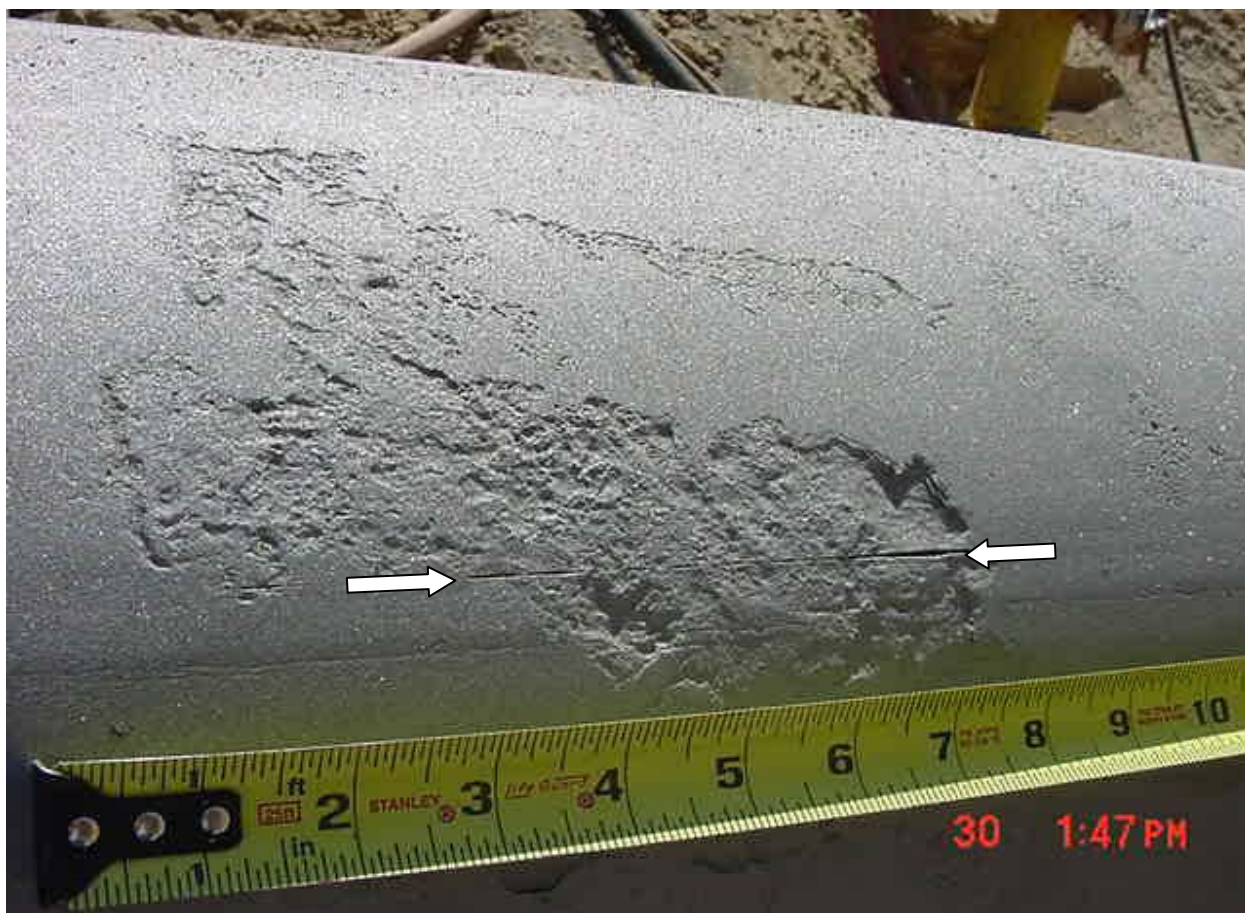


Figure 43. Selective Seam Weld Corrosion

Selective seam weld corrosion typically advances at a rate of 2 to 4 times that of the corrosion in the surrounding base metal. Consequently, selective seam weld corrosion will tend to appear as a deeper groove at the bondline within the adjacent, shallower pipe body metal loss. The ratio of depth of corrosion at the bondline to the depth of corrosion in the adjacent pipe body is sometimes referred to as the “grooving” ratio. An example of the grooving is shown in a cross-section of the wall thickness in Figure 44.

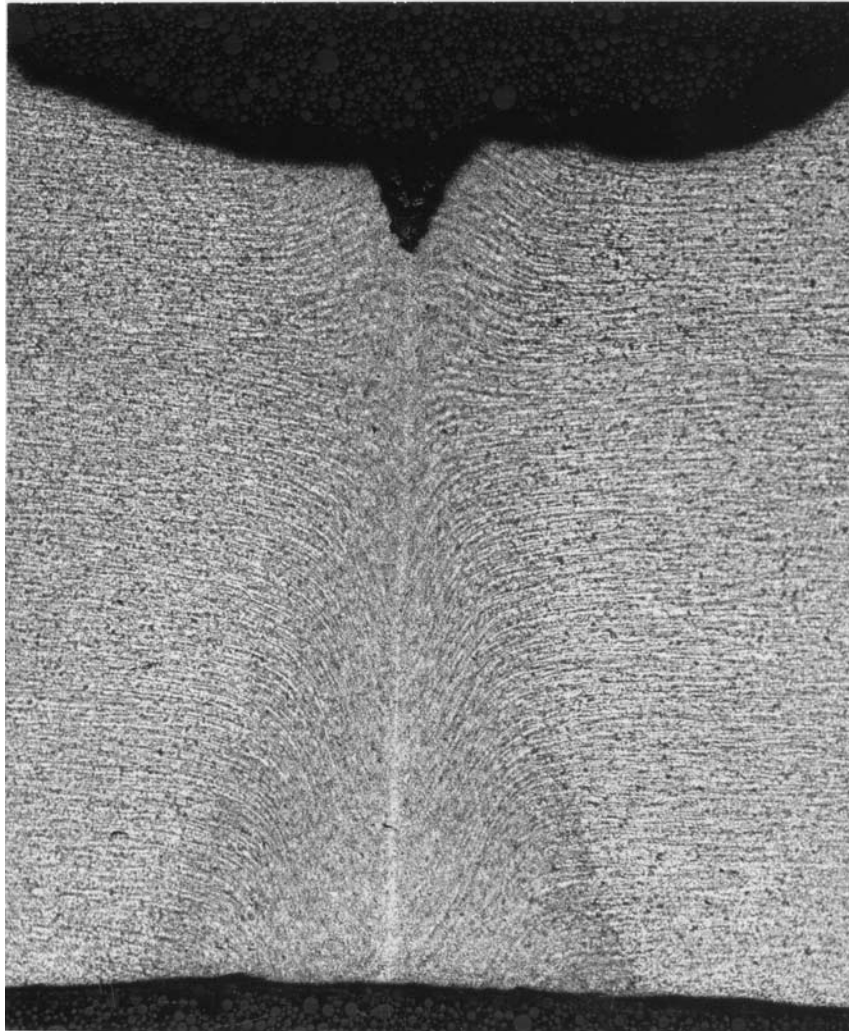


Figure 44. Selective Seam Corrosion with a Grooving Ratio of About 2 in a High-Frequency-Welded Seam

Selective Seam Weld Corrosion Incidents in the Database

The pipe attributes, failure mode, and whether the incident occurred in service or in a hydrostatic test are listed in Table 19.

Table 19. Pipe Attributes, Failure Mode, and Type of Incident (in-service or test) for Incidents that were Attributed to SSWC (highlighted cells indicate where a reasonable guess was made where data were not available)

SSWC Case Number	Database Number	Liquid/Gas	Pipe OD, inches	Pipe WT, inch	SMYS, psi	Type of Seam	Manufacturer	Failure Mode	In-service or Hydrostatic Test
1	13	Liquid	10.75	0.279	46,000	ERW - LF	Unknown	Rupture	In-service
2	15	Gas	8.625	0.277	35,000	ERW - LF	Kaiser Steel	Leak	In-service
3	16	Gas	20	0.312	42,000	ERW - DC	Youngstown	Rupture	In-service
4	29	Liquid	12.75	0.25	52,000	ERW - LF	Unknown	Rupture	In-service
5	70	Liquid	12.75	0.25	52,000	ERW - HF	Republic	Rupture	In-service
6	71	Liquid	12.75	0.25	52,000	ERW - HF	Republic	Rupture	In-service
7	86	Liquid	8.625	0.277	35,000	ERW - LF	Republic	Leak	In-service
8	129	HVL	8.625	0.156	46,000	ERW - LF	Lone Star	Leak	In-service
9	132	Liquid	8.625	0.25	42,000	ERW - LF	Unknown	Rupture	In-service
10	134	Liquid	12.75	0.203	42,000	ERW - HF	Unknown	Leak	In-service
11	135	Liquid	6.625	0.188	42,000	ERW - LF	Unknown	Leak	In-service
12	140	Gas	18	0.25	42,000	ERW - DC	Youngstown	Rupture	In-service
13	148	Liquid	16	0.25	35,000	ERW - LF	Unknown	Rupture	In-service
14	171	Liquid	12.75	0.25	46,000	ERW - LF	Republic	Rupture	Hydrostatic test
15	177	Gas	16	0.375	35,000	ERW - LF	Unknown	Rupture	In-service
16	203	Liquid	12.75	0.25	35,000	ERW - LF	Unknown	Rupture	Hydrostatic test
17	204	Liquid	8.625	0.203	42,000	ERW - LF	Bethlehem	Leak	Hydrostatic test
18	205	Liquid	8.625	0.203	42,000	ERW - LF	Bethlehem	Rupture	Hydrostatic test
19	217	Gas	10.75	0.219	46,000	ERW - LF	Unknown	Rupture	Hydrostatic test
20	224	Liquid	8.625	0.203	42,000	ERW - LF	Bethlehem	Rupture	In-service
21	231	Gas	12.75	0.312	42,000	ERW - LF	Unknown	Rupture	In-service
22	240		8.625	0.219	46,000	ERW - LF	Unknown	Rupture	In-service
23	241	Liquid	8.625	0.300	40,000	ERW - DC	Youngstown	Rupture	In-service
24	243	Liquid	10.75	0.280	35,000	ERW - DC	Youngstown	Rupture	In-service

With regard to seam type, 17 of the 24 incidents were associated with low-frequency-welded ERW pipe, 4 were associated with DC-welded ERW pipe, and 3 were associated with high-frequency-welded ERW pipe. No incident in the database was associated with flash-welded pipe, but incidents arising from selective seam weld corrosion in flash-welded pipes are known to have occurred.

Manufacturers of pipe that exhibited SSWC included Youngstown (4), Republic (4), Bethlehem (3), Kaiser (1), and Lone Star (1). In 11 of the incidents the manufacturers are unknown.

As shown in Table 20, fourteen of the 24 SSWC incidents involved in-service ruptures. Five involved in-service leaks. Four of the 5 hydrostatic test incidents were ruptures; one was a leak.

Table 20. Date of Failure, Failure Mode, Failure Stress Level, and Time-Relevant Information for Incidents That Were Attributed to SSWC (highlighted cells indicate where a reasonable guess was made where data were not available)

SSWC Case Number	Date of Failure	Failure Mode	In-service or Hydrostatic Test	Failure Pressure, psig	Failure Pressure, %SMYS	Pressure in last hydrostatic test, % SMYS	Time to Failure after Test, years	Pipe Vintage	Time to Failure after Installation, years
1	1997	Rupture	In-service	680	28.5	62.9	22	1955	42
2	1995	Leak	In-service	800	35.6			1959	36
3	1992	Rupture	In-service	860	65.6		23	1947	45
4	2003	Rupture	In-service	1257	61.6	91.7	20	1958	45
5	2003	Rupture	In-service	1100	53.9	73.6	8	1964	39
6	2005	Rupture	In-service	1150	56.4	73.6	10	1964	41
7	2007	Leak	In-service	365	16.2	38.7	24	1933	74
8	1996	Leak	In-service	780	46.9			1968	28
9	1999	Rupture	In-service	1000	41.1	67.2	2	1956	43
10	2003	Leak	In-service	600	44.9			1965	38
11	2008	Leak	In-service	970	40.7			1965	43
12	2001	Rupture	In-service	364	31.2	64.3		1952	49
13	2005	Rupture	In-service	50	4.6			1957	48
14	2008	Rupture	Hydrostatic test	1567	86.9	95.9	3	1964	44
15	2009	Rupture	In-service	120	7.3			1946	63
16	2010	Rupture	Hydrostatic test	1114	81.2	83.1	18	1941	69
17	2010	Leak	Hydrostatic test	1824	92.3			1963	47
18	2010	Rupture	Hydrostatic test	1576	79.7			1963	47
19	2008	Rupture	Hydrostatic test	1400	74.7			1957	51
20	1980	Rupture	In-service	1235	62.5			1963	17
21	2009	Rupture	In-service	650	31.6			1948	61
22	2002	Rupture	In-service	1117	47.8			1958	44
23	2002	Rupture	In-service	617	22.2	48.2	14	1936	66
24	2004	Rupture	In-service	1032	56.6			1948	56

The significance of the data can be understood in terms of Figure 45 through Figure 47. First, consider Figure 45. Selective seam corrosion failures in the database occurred at failure stresses ranging from 7.3 to 92.3 percent of SMYS, and the one that occurred a 7.3 percent of SMYS occurred as a rupture in a gas pipeline in service. What that suggests is that selective seam weld corrosion, if not arrested and/or remediated, will eventually lead to a leak or a rupture regardless of the hoop stress level in the pipe. Because of the likelihood of low fracture resistance of the low-frequency-welded, DC-welded, and flash-welded seams, such failures are prone to occur as ruptures.

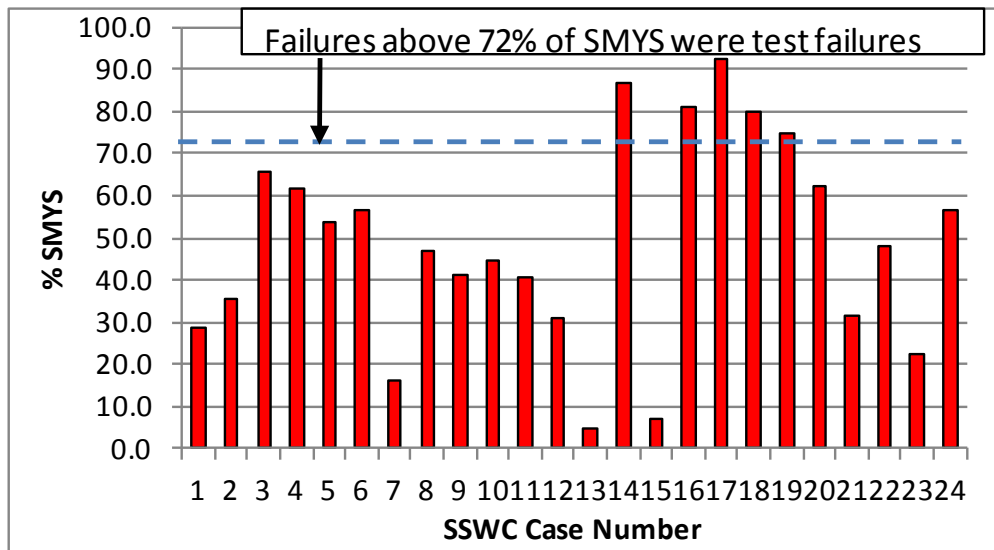


Figure 45. Failure Stress Levels of Selective Seam Weld Corrosion Failures

The times to failure after the pipelines were installed for selective seam weld corrosion anomalies in the database are shown in Figure 46. They range from 17 to 74 years. The mean value is 47 years. The standard deviation is 13 years. The median value is 45 years.

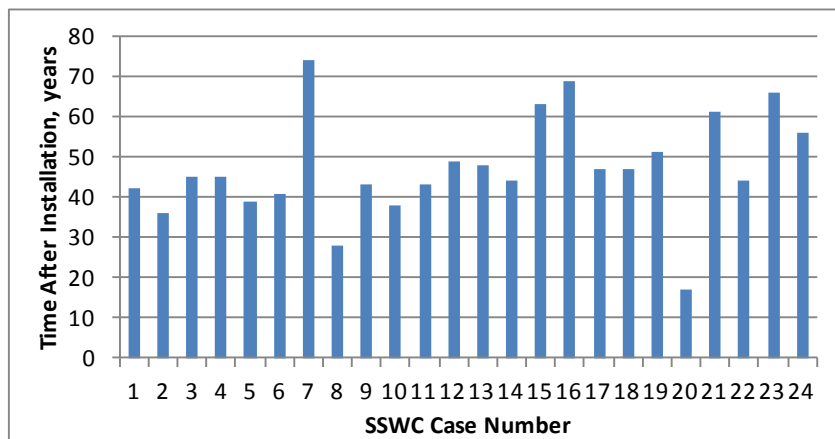


Figure 46. Times to Failure after Pipeline Installation for Selective Seam Corrosion Anomalies

To see if there was any relationship between time to failure and coating type or cathodic protection, the coating types were examined. Recall that all 24 cases in the database are believed to have involved external corrosion. Nine of the failures occurred in pipelines that were coated with coal tar, at least 7 of which were under cathodic protection. The times to failure for these cases ranged from 38 to 69 years. Four cases were associated with bare pipelines, at least 3 of which were under cathodic protection. The times for these cases ranged from 45 to 74 years. Four cases involved pipelines coated with tape coating (believed to be single layer polyethylene) which were assumed to be under cathodic protection. The times for these cases ranged from 17 to 47 years. The SSWC failure in the only asphalt-coated line (status of cathodic protection not

known) failed after 36 years. The type of coating and status of cathodic protection was not available for 6 of the cases.

The findings with regard to coating and cathodic protection cannot be easily interpreted without knowing the mileages of pipelines with each type of coating. Nevertheless, it may be important that the shortest time to failure (17 years) was associated with a tape coating. Such coatings tend to shield the pipe from cathodic protection if they become disbonded.

Another significant time factor in selective seam weld corrosion failures relates to the time to failure after the most recent hydrostatic test. For 10 of the cases information on a prior hydrostatic test after the original pre-service test was available. The times are shown in Figure 47. These times varied over a wide range (2 years to 24 years). The most likely explanation for this is that the corrosion rates varied widely.

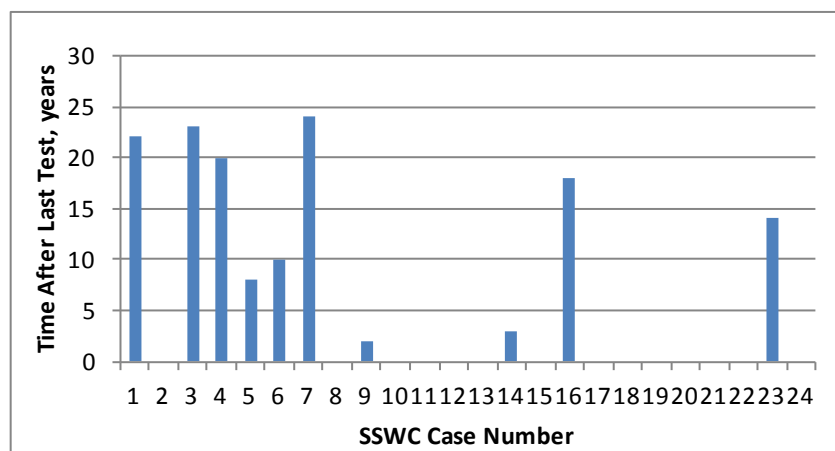


Figure 47. Times to Failure after the Most Recent Hydrostatic Test for Selective Seam Corrosion Anomalies

The ability (or lack thereof) to predict the failure stress levels of selective seam weld corrosion anomalies on the basis of their dimensions using base metal properties and a ductile fracture initiation model such as the Modified Ln-Secant Elliptical CEQ model is illustrated in Figure 48. Failure stress levels were predicted for ten incidents where the dimensions were reasonably easily to ascertain. All ten incidents involved either low-frequency-welded or DC-welded seams. As seen in Figure 48, the actual failure stresses in most cases were considerably less than the predicted levels. The fact that most of the predicted failure stresses are much higher than the actual failure stresses probably has a lot to do with the propensity of flaws in low-frequency-welded ERW bondlines to fracture in a brittle manner.

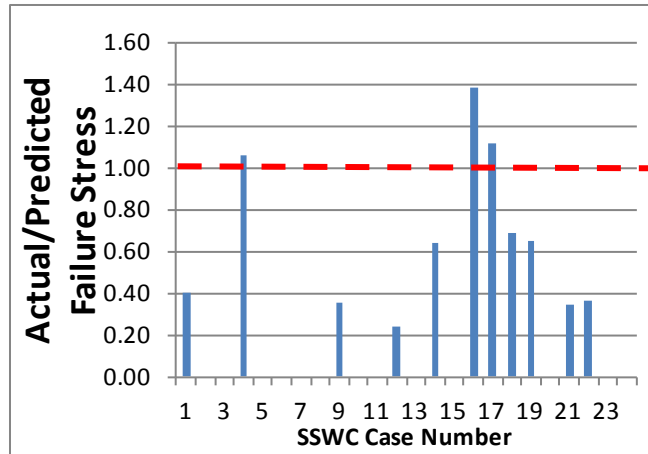


Figure 48. Actual Failure Stress Levels of Selective Seam Weld Corrosion Anomalies Compared to Failure Stress Levels Predicted Using Base Metal Properties

Details of Selected Individual Failures

The following cases are reviewed in detail to examine the nature of the corrosion, the effects of the test-to-operating-pressure ratio and the ability (or lack thereof) to predict the actual failure stress using a ductile fracture model and base metal properties. Cases 5 and 6 below involved high-frequency-welded pipe. The rest involved low-frequency-welded or DC-welded pipe.

SSWC Case Number 1

In this case the 10.75-inch-OD, 0.279-inch-wall X46 low-frequency-welded pipe ruptured in-service at a stress level of 28.5 percent of SMYS 22 years after a test to a stress level of 62.9 percent of SMYS. The test-pressure-to-failure-pressure-ratio was 2.21. A metallographic section across the rupture is shown in Figure 49 and at a higher magnification in Figure 50.

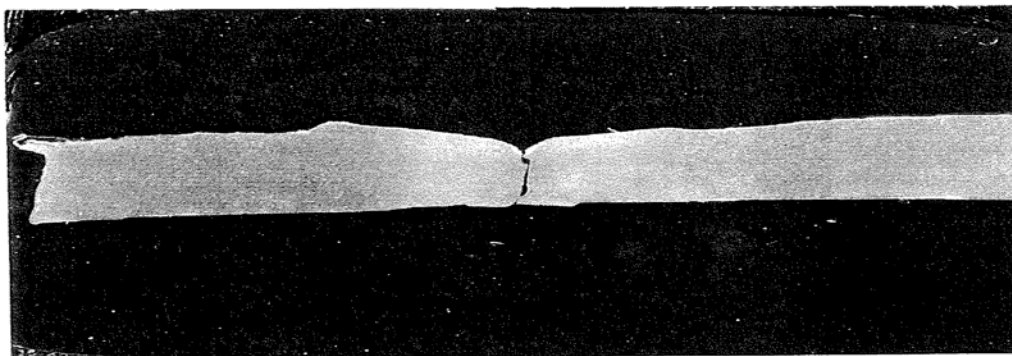


Figure 49. Selective Seam Weld Corrosion Case Number 1

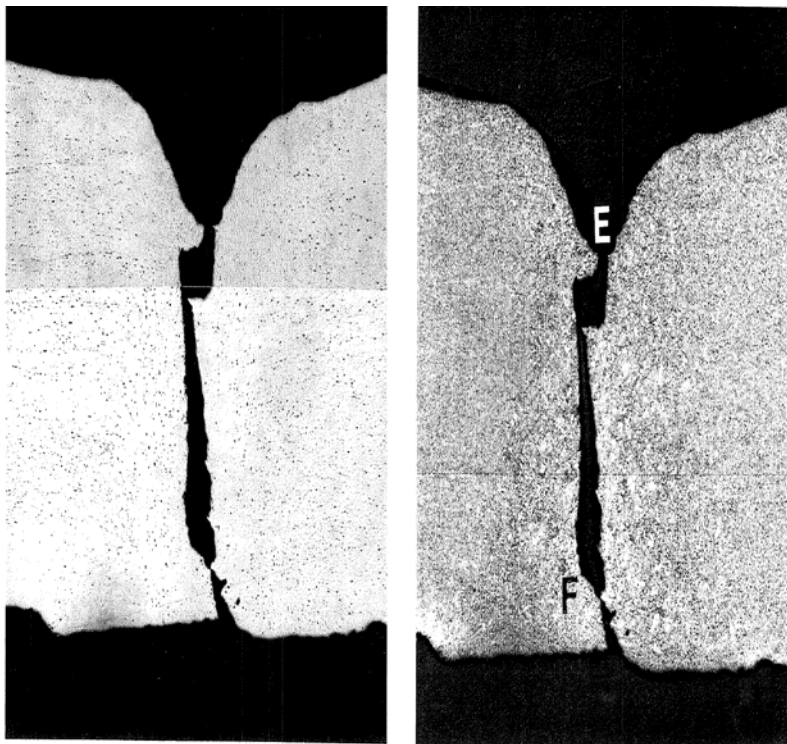


Figure 50. Close-up of the Selective Seam Corrosion in Case Number 1 Showing that it Was Not Centered on the Bondline

The v-shaped groove is not centered on the bondline. However, the failure involves the bondline through a shearing path from the tip of the corrosion anomaly into the bondline.

The initiating defect was 5 inches long, and it had penetrated to a maximum depth of 59 percent of the wall thickness. Using the Modified Ln-Sec EllipticalCEQ model, with the base metal flow stress of 67,000 and the full-size-equivalent Charpy upper shelf energy of 21 ft lb, one calculates a hoop stress at failure of 75.2 percent of SMYS. The actual failure stress, 28.5 percent of SMYS, is only 40 percent of the predicted value. The bondline properties determined where the failure would occur, and those properties clearly corresponded to less fracture resistance than that of the base metal.

SSWC Case Number 4

In this case the 12.75-inch-OD, 0.250-inch-wall, X52, low-frequency-welded pipe ruptured in service at a stress level of 61.6 percent of SMYS 20 years after a test to a stress level of 91.7 percent of SMYS. The test-pressure-to-failure-pressure-ratio was 1.49. A metallographic section across the rupture is shown in Figure 51. Although the seam area is selectively corroded, the tip of the corrosion is relatively blunt.

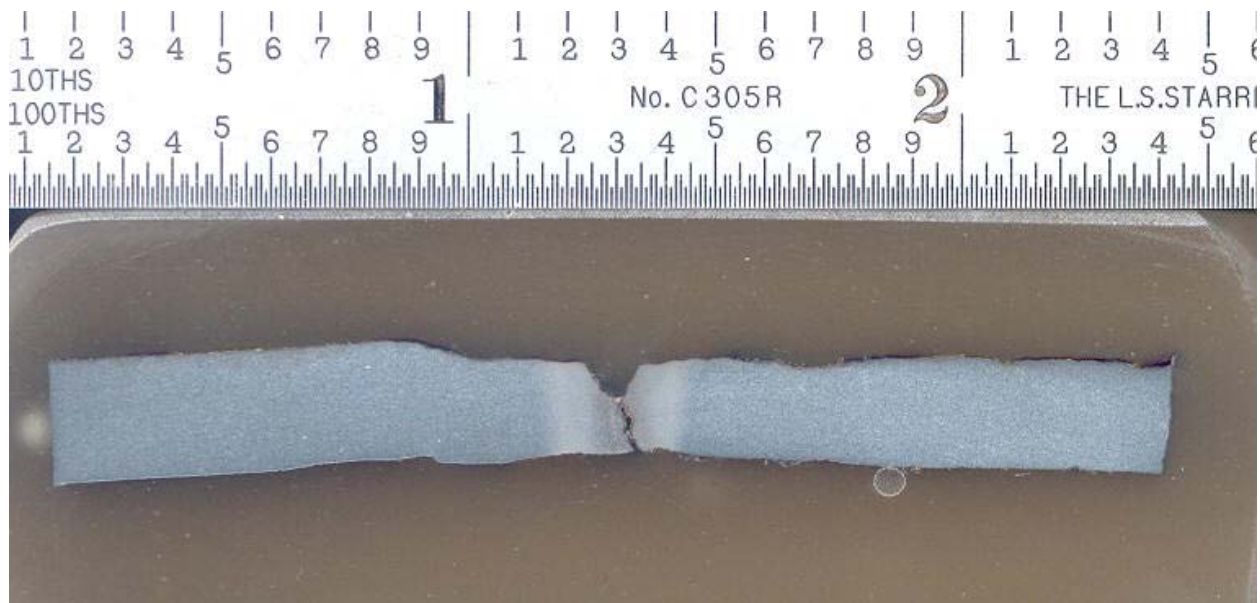


Figure 51. Selective Seam Weld Corrosion in Case Number 2 showing a Relatively Blunt Corrosion Tip

The initiating defect was 6.5 inches long, and it had penetrated to a maximum depth of 66 percent of the wall thickness. The grooving ratio associated with this case was about 2. The failure of the remaining ligament beneath the corrosion was ductile and did not coincide with the bondline. Using the Modified Ln-Sec EllipticalCEQ model, with the base metal flow stress of 70,000 and the full-size-equivalent Charpy upper shelf energy of 23 ft lb, one calculates a predicted hoop stress at failure of 58.0 percent of SMYS. The actual failure stress, 61.6 percent of SMYS, was in reasonable agreement with the predicted failure stress.

SSWC Case Number 5

In SSWC Case Number 5 the pipe was a 12.75-inch-OD, 0.250-inch-wall, X52 material with a high-frequency-welded seam. The pipe ruptured in-service at a stress level of 53.9 percent of SMYS 8 years after a test to a stress level of 73.6 percent of SMYS. The test-pressure-to-operating pressure-ratio was 1.37. Dimensions of the anomaly were not available.

SSWC Case Number 6

In this case the pipe was a 12.75-inch-OD, 0.250-inch-wall, X52 material with a high-frequency-welded seam. The pipe ruptured in-service at a stress level of 56.4 percent of SMYS 10 years after a test to a stress level of 73.6 percent of SMYS. The test-pressure-to-failure-pressure-ratio was 1.30. Dimensions of the anomaly were not available.

SSWC Case Number 7

In this case the pipe was an 8.625-inch-OD, 0.277-inch-wall, Grade B pipe with a low-frequency-welded seam. The operating stress level at the time the leaks were discovered was 16.3 percent of SMYS. A single pipe was found to be leaking at two areas of selective seam corrosion. The shapes and size of the two anomalies on the chilled and broken-open surfaces were about the same. Both anomalies were about 4 inches long, and both penetrated the wall thickness, but only at one point. Aside from the point of the leak the defects were fairly elliptical and had peak depths other than at the leak of about 80 percent of the wall thickness. The pipe had been subjected to a hydrostatic test 24 years earlier to a stress level of 38.7 percent of SMYS. The test-pressure-to-failure-pressure-ratio was 2.37.

SSWC Case Number 9

The pipe in SSWC Case Number 9 was an 8.625-inch-OD, 0.250-inch-wall, X42 material with a low-frequency-welded ERW seam. It ruptured in-service at a stress level of 41.1 percent of SMYS two years after a test to a stress level of 67.2 percent of SMYS. The test-pressure-to-failure-pressure-ratio was 1.64. The anomaly that initiated the rupture as it appeared on the fracture surfaces is shown in Figure 52 and a metallographic section through it is shown in Figure 53. A metallographic section through a nearby intact anomaly is shown in Figure 54.



Figure 52. SSWC Case Number 9 Anomaly as It Appeared on the Fracture Surfaces

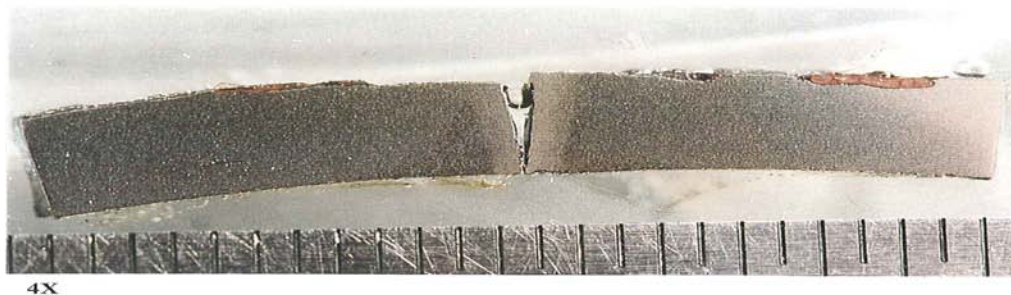


Figure 53. Cross Section of SSWC Case Number 9 Anomaly



Figure 54. Cross Section of a Nearby Intact SSWC Anomaly

The selective seam weld corrosion in this case appears to have an exceptionally high grooving ratio. An intact anomaly shown in Figure 54 exhibits a similarly deep, narrow groove, but also has cracking at its tip. The cause of the cracking is unknown, but the fact that was associated with a corrosive environment suggests that SCC may have been occurring as well as corrosion-caused metal loss. In any case the anomaly that initiated the failure was about 1 inch long and had penetrated 70 percent of the wall thickness.

Using the Modified Ln-Sec EllipticalCEQ model, with the base metal flow stress of 67,000 and an assumed full-size-equivalent Charpy upper shelf energy of 25 ft lb, one calculates a hoop stress at failure of 115.6 percent of SMYS. The actual failure stress, 41.1 percent of SMYS, is only 36 percent of the predicted value.

SSWC Case Number 12

In this case the pipe was an 18-inch-OD, 0.250-inch-wall, X42 material with a DC-welded ERW seam. The pipe ruptured in service at a stress level of 31.2 percent of SMYS 49 years after a test to a stress level of 64.3 percent of SMYS. The test-pressure-to-prior-test-pressure-ratio was 2.06. The nature of the anomaly is shown in Figure 55 and Figure 56.

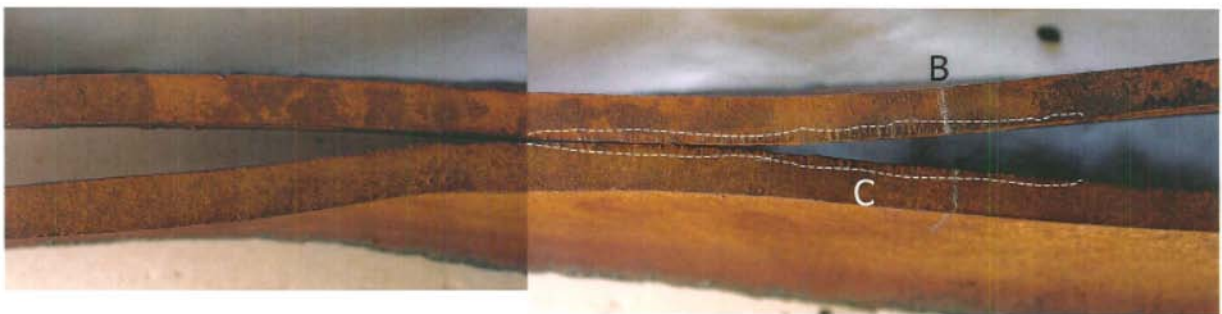


Figure 55. SSWC Case Number 12 Anomaly as it Appeared on the Fracture Surfaces

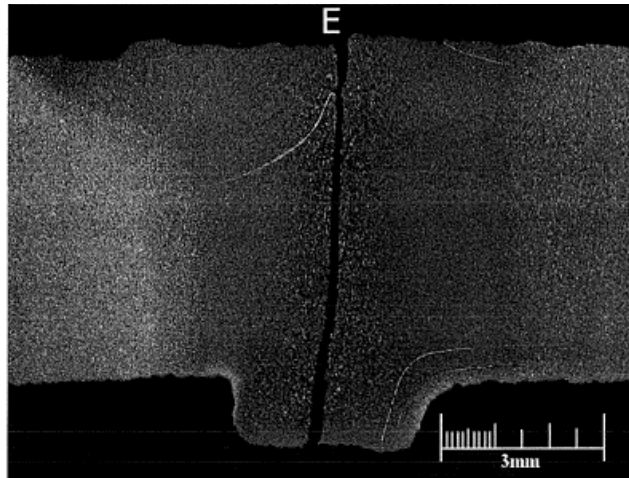


Figure 56. Cross Section of SSWC Case Number 12 Anomaly

The anomaly is relatively shallow and sharp, but it was apparently created by selective seam corrosion. It is speculated that the narrowness and deepness may indicate that a cold weld was present initially and that the corrosion enlarged it and removed the evidence of its existence. It was 3.3 inches in length and had penetrated 30 percent of the wall thickness.

Using the Modified Ln-Sec EllipticalCEQ model, with the base metal flow stress of 67,000 and an assumed full-size-equivalent Charpy upper shelf energy of 25 ft lb, one calculates a hoop stress at failure of 132.6 percent of SMYS. The actual failure stress, 31.2 percent of SMYS, is only 24 percent of the predicted value. The pipe in which this anomaly existed was of the vintage of Youngstown pipe that often possessed excessively hard heat affected zones. Although hardness was not measured in this instance, it is possible the weld zone possessed high hardness, and therefore, it may have been especially susceptible to failure in the presence of a sharp notch.

SSWC Case Number 14

In this case the pipe was a 12.75-inch-OD, 0.250-inch-wall, X46 material with a low-frequency-welded seam. The pipe ruptured in a hydrostatic test at a stress level of 86.9 percent of SMYS three years after a test to a stress level of 95.9 percent of SMYS. The test-pressure-to-prior-test-pressure-ratio was 1.10. The selective seam corrosion anomaly that initiated the failure was 2 inches long and had penetrated 24 percent of the wall thickness. A cross section of the anomaly is shown in Figure 57. A small ID-surface-connected hook crack may have contributed to this failure.

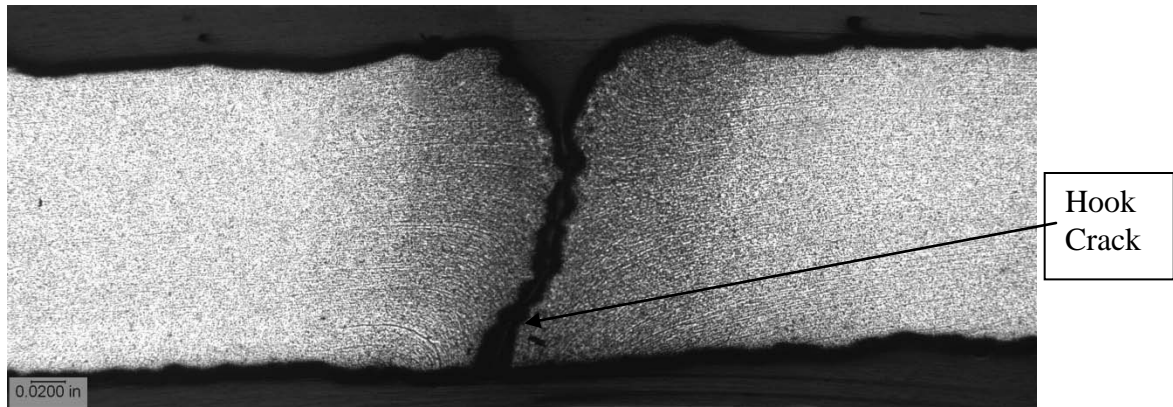


Figure 57. Cross Section of SSWC Case Number 14 Anomaly

Using the Modified Ln-Sec EllipticalCEQ model, with the base metal flow stress of 66,000 and an assumed full-size-equivalent Charpy upper shelf energy of 37 ft lb, and ignoring the contribution of the hook crack, one calculates a hoop stress at failure of 135.8 percent of SMYS. The actual failure stress, 86.9 percent of SMYS, is only 64 percent of the predicted value.

SSWC Case Number 15

In this case the pipe was a 16-inch-OD, 0.375-inch-wall, Grade B material with a low-frequency-welded seam. The pipe ruptured in-service at a stress level of 7.3 percent of SMYS. No prior hydrostatic test had been conducted as this pipe was part of a natural gas distribution system with an MAOP of less than 20 percent of SMYS. The selective seam weld corrosion was narrow and deep with a grooving ratio in excess of 4. The cross section of the corrosion is shown in Figure 58.

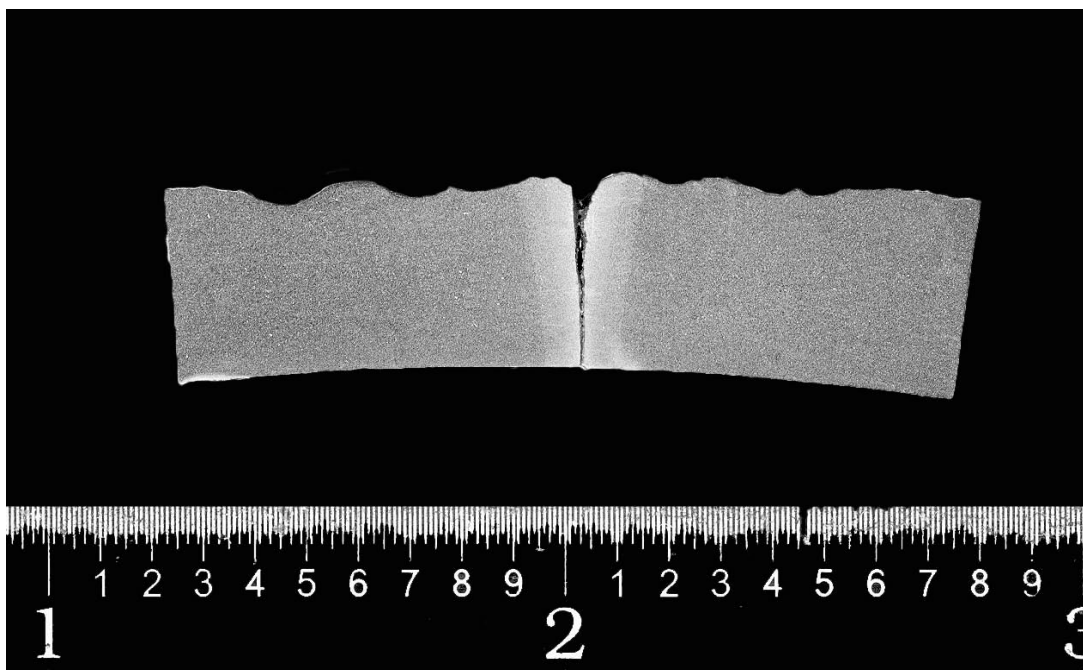


Figure 58. Cross Section of SSWC Case Number 15 Anomaly

The selective seam corrosion anomaly in this case was believed to have occurred at a location of a poorly bonded seam leading to the observed, very low failure stress level. A piece of the same pipe that remained intact contained an even larger selective seam weld corrosion anomaly. When the latter pipe was subjected to a burst test, the failure stress was 21 percent of SMYS, 2.9 times the failure stress of the in-service rupture.

A Method for Determining Re-Assessment Intervals for Selective Seam Weld Corrosion if Hydrostatic Testing is the Method of Re-Assessment

It seems that a method for scheduling retests of pipelines affected by stress corrosion cracking such as the “Fessler-Rapp” method³ or the “modified Fessler-Rapp” method⁴ could be applied as well to the scheduling of retests of pipelines affected by selective seam weld corrosion. Essentially, those methods rely on certain assumptions about defect growth and the results of two successive hydrostatic tests to determine when future tests are needed to prevent in-service failure from stress corrosion cracking. The one important assumption that applies to the use of these methods for stress corrosion cracking is that the rate of crack growth is constant. In other words, the depths of cracks increase linearly with time. It is reasonable to make that assumption for selective seam weld corrosion as well.

Summary of the Findings on Selective Seam Weld Corrosion

Selective seam weld corrosion is a significant pipeline integrity concern. The main issues of concern are that it is hard to detect and characterize using ILI, that it occurs in materials that may have much less resistance to defects than the base metal, that neither the models used to predict failure stress levels for corrosion-caused metal loss nor ductile fracture initiation models can be expected to give reliable estimates of its effect on remaining strength, and that hydrostatic testing, if used to control it, would have to be applied periodically, possibly at intervals as short as two years. Once it has been identified as a threat to the integrity of a particular pipeline, periodic assessment using ILI or hydrostatic testing is necessary. If ILI is used to detect and control selective seam weld corrosion, an adequate number of excavations should be used to examine seam weld anomalies in order to develop confidence in the ILI tool used. Reassessment intervals for an ILI program should be based on worst-case estimates of a corrosion rate. If hydrostatic testing is used to control selective seam weld corrosion, retest intervals could be based on the Fessler-Rapp method that is sometimes applied to schedule retests for SCC.

Pressure-Cycle-Induced-Fatigue

The database contains 37 incidents where the cause of failure was attributed to fatigue crack growth initiating at a pre-existing ERW or flash-weld manufacturing defect. Twenty-five such failures initiated at hook cracks. Two other hook cracks were placed in this category as well because fatigue was suspected to have contributed to the failures. For six of the fatigue failures, the initiator of fatigue cracking was a mismatched edge. One failure on the list appeared to have initiated at a cold weld (called LOF by the contributor), one failure was said to have initiated at a damaged edge, and one failure was said to have initiated at an ID feature. All of the fatigue failures occurred in liquid or HVL service; none occurred in a natural gas pipeline.

The pipe attributes, manufacturers, and initiators of fatigue crack growth are listed in Table 21. As before, items highlighted in yellow are best estimates of data that were not available.

**Table 21. List of Fatigue Failures, Pipe Attributes and Type of Initiating Anomaly
(highlighted cells indicate where a reasonable guess was made where data were not available)**

Fatigue Case Number	Database Number	Pipe OD, inches	Pipe WT, inch	SMYS, psi	Type of Seam	Manufacturer	Fatigue Initiator	Pipe Vintage
1	4	16	0.218	60,000	ERW - HF		Hook Crack	1969
2	7	12.75	0.219	52,000	ERW - LF	J&L	Hook Crack	1962
3	10	10.75	0.203	52,000	ERW - HF	J&L	Hook Crack	1967
4	24	10.75	0.25	46,000	Flash-weld	A.O. Smith	Hook Crack	1954
5	25	10.75	0.25	46,000	Flash-weld	A.O. Smith	Mismatched edge	1953
6	26	10.75	0.307	46,000	ERW - LF	Republic	Hook Crack	1953
7	30	12.75	0.25	45,000	Flash-weld	A.O. Smith	Mismatched edge	1948
8	31	8.625	0.188	52,000	ERW - LF	Bethlehem	Mismatched edge	1962
9	41	10.75	0.219	52,000	ERW - LF	J&L	Hook Crack	1961
10	57	6.625	0.125	60,000	ERW - HF	TexTube Pipe Corp.	Hook Crack	1983
11	72	12.75	0.203	52,000	ERW - LF	Bethlehem	Hook Crack	1964
12	73	16	0.25	52,000	ERW - DC	Youngstown	Hook Crack	1954
13	76	16	0.25	52,000	ERW - DC	Youngstown	Hook Crack	1954
14	87	20	0.312	52,000	Flash-weld	A.O. Smith	Hook Crack	1952
15	90	12.75	0.25	46,000	ERW - LF		Hook Crack	1964
16	95	12.75	0.25	46,000	ERW - LF	Republic	Hook Crack	1958
17	103	12.75	0.25	46,000	ERW - LF	Republic	Hook Crack	1958
18	113	22	0.344	46,000	ERW - DC	Youngstown	Hook Crack	1949
19	114	22	0.312	46,000	ERW - DC	Youngstown	Hook Crack	1949
20	158	8.625	0.203	35,000	Flash-weld	A.O. Smith	Mismatched edge	1946
21	180	10.75	0.219	52,000	ERW - LF	J&L	Hook Crack	1961
22	186	10.75	0.219	52,000	ERW - LF	J&L	Hook Crack	1961
23	209	26	0.281	52,000	Flash-weld	A.O. Smith	Hook Crack	1957
24	210	26	0.281	52,000	Flash-weld	A.O. Smith	Hook Crack	1954
25	213	34	0.281	52,000	Flash-weld	A.O. Smith	Hook Crack	1967
26	215	20	0.219	52,000	ERW - HF	US Steel	Hook Crack	1968
27	225	18	0.219	52,000	ERW - DC	Youngstown	Damaged edge	1962
28	227	26	0.281	52,000	Flash-weld	A.O. Smith	Mismatched edge	1956
29	230	8.625	0.188	46,000	ERW - LF	Lone Star	ID feature	1973
30	239	24	0.328	70,000	ERW - HF	Stupp	LOF defect	1998
31	257	20	0.312	52,000	Flash-weld	A.O. Smith	Hook Crack	1955
32	263	20	0.312	52,000	Flash-weld	A.O. Smith	Hook Crack	1955
33	264	20	0.312	52,000	Flash-weld	A.O. Smith	Hook Crack	1955
34	267	20	0.312	52,000	Flash-weld	A.O. Smith	Hook Crack	1955
35	269	20	0.312	52,000	Flash-weld	A.O. Smith	Hook Crack	1955
36	279	26	0.281	52,000	Flash-weld	A.O. Smith	Hook Crack	1956
37	280	20	0.230	52,000	ERW - DC	Youngstown	Mismatched edge	1968

The failure modes, failure stresses, prior test data, times to failure, and whether the failure occurred in service or during a hydrostatic test are shown in Table 22.

Table 22. Failure Modes, Failure Stresses and Times to Failure for Fatigue Failure (highlighted cells indicate where a reasonable guess was made where data were not available)

Fatigue Case Number	Failure Mode	In-service or Hydrostatic Test	Failure Pressure, %SMYS	Pressure in last hydrostatic test, % SMYS	Test-Pressure-to-Operating-Pressure Ratio	Time To Failure After Test, years	Time To Failure After Installation, years
1	Leak	Hydrostatic test	85.6	90.2		34	34
2	Rupture	Hydrostatic test	66.9				32
3	Leak	Hydrostatic test	82.2				30
4	Rupture	Hydrostatic test	95.8	93.9		4	49
5	Rupture	Hydrostatic test	79.8				46
6	Rupture	Hydrostatic test	81.2				46
7	Rupture	In-service	61.7	90.8	1.5	3	60
8	Rupture	In-service	69.7				38
9	Rupture	Hydrostatic test	81.8	89.7		21	43
10	Rupture	Hydrostatic test	93.7	99.8		23	23
11	Rupture	In-service	59.8	82.1	1.4	9	42
12	Rupture	Hydrostatic test	81.6	84.4		8	45
13	Rupture	Hydrostatic test	81.8	93.7		9	54
14	Rupture	In-service	55.3	90.0	1.6	22	45
15	Rupture	Hydrostatic test	97.0	93.0		4	35
16	Rupture	Hydrostatic test	96.5	93.0		4	41
17	Rupture	Hydrostatic test	94.7	94.2		5	46
18	Rupture	Hydrostatic test	85.9	0.0			55
19	Rupture	Hydrostatic test	78.0	81.2		13	55
20	Leak	In-service	69.8	94.8	1.4	12	56
21	Rupture	Hydrostatic test	81.6	81.5		5	48
22	Rupture	Hydrostatic test	87.2	84.4		5	48
23	Rupture	Hydrostatic test	87.8				38
24	Leak	In-service	55.7	87.6	1.6	5	46
25	Leak	In-service	12.8	94.0	7.3	27	28
26	Rupture	In-service	54.3	91.1	1.7	34	40
27	Rupture	In-service	60.6	90.1	1.5	21	49
28	Rupture	In-service	64.5	100.3	1.6	16	54
29	Rupture	Hydrostatic test	67.8	95.1		37	37
30	Rupture	In-service	69.6	96.0	1.4	9	9
31	Rupture	Hydrostatic test	115.6	90.0		32	53
32	Rupture	Hydrostatic test	95.5	90.0		32	53
33	Rupture	Hydrostatic test	107.9	90.0		32	53
34	Rupture	Hydrostatic test	120.2	90.0		32	53
35	NS	In-service	55.3	90.0	1.6	32	53
36	Leak	Hydrostatic test	100.0	89.9		19	38
37	Rupture	In-service	70.8	92.8	1.3	25	25

As can be seen in Table 21, fatigue failures have occurred in a wide range of line pipe materials and vintages. Pipes from most of the manufacturers have been involved. As can be seen in Table 22, 24 of the failures occurred during hydrostatic tests; 13 occurred in service. The failure stress levels of fatigue-enlarged anomalies that failed during hydrostatic tests are illustrated in Figure 59. The levels ranged from 66.9 percent of SMYS to 120.2 percent of SMYS. Those that occurred at stress levels above 100 percent of SMYS are believed to have been associated with burst tests of samples removed from pipelines after ILI crack-tool runs.

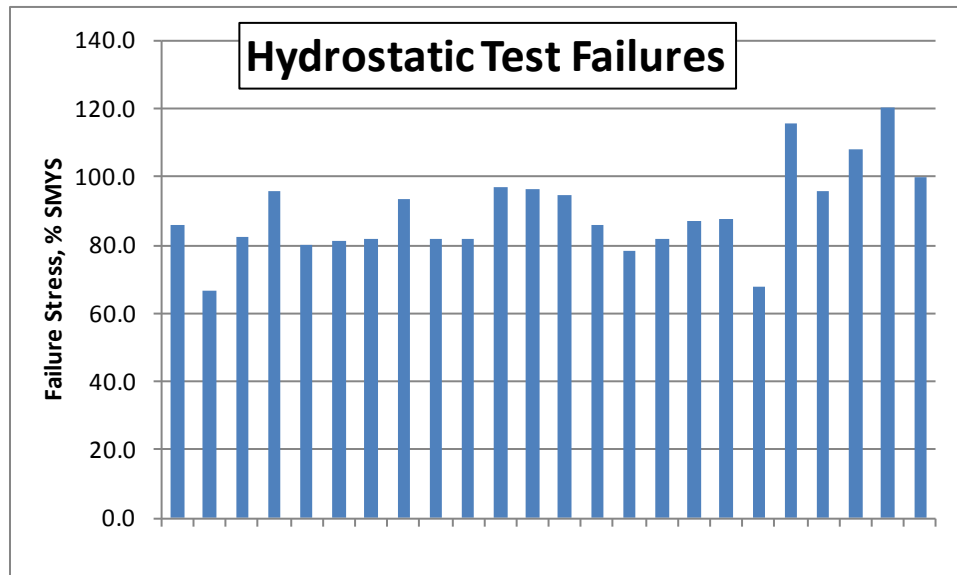


Figure 59. Failure Stress Levels for Fatigue-Enlarged Anomalies that Failed in Hydrostatic Tests

The failure stress levels of fatigue-enlarged anomalies that failed in service are illustrated in Figure 60. The levels ranged from 12.8 percent of SMYS to 70.8 percent of SMYS.

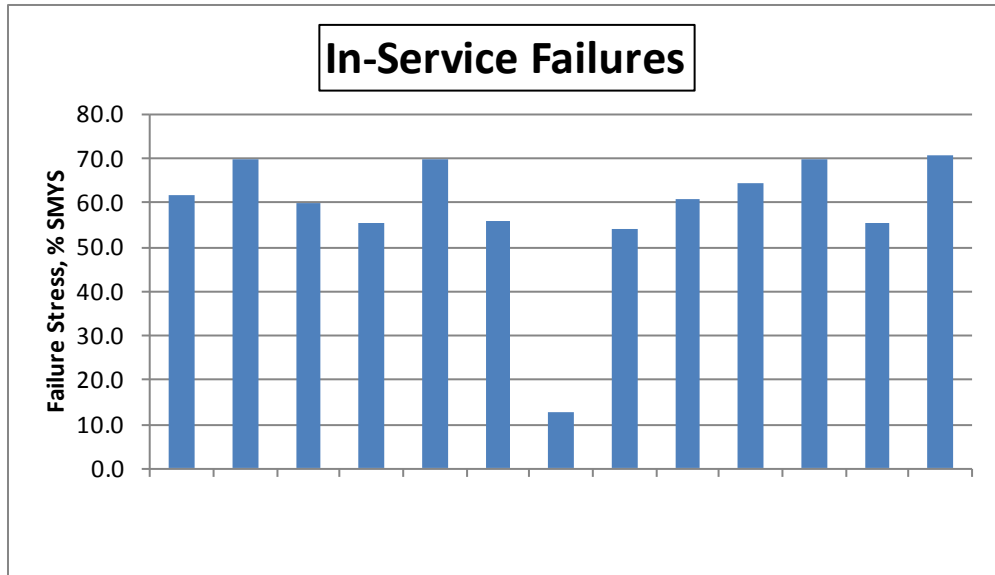


Figure 60. Failure Stress Levels for Fatigue-Enlarged Anomalies that Failed In-Service

The times to failure after pipeline installation for fatigue-enlarged anomalies are given in Figure 61. The times ranged from 9 to 60 years. The mean time was 43 years with a standard deviation of 11 years. The median time was 46 years.

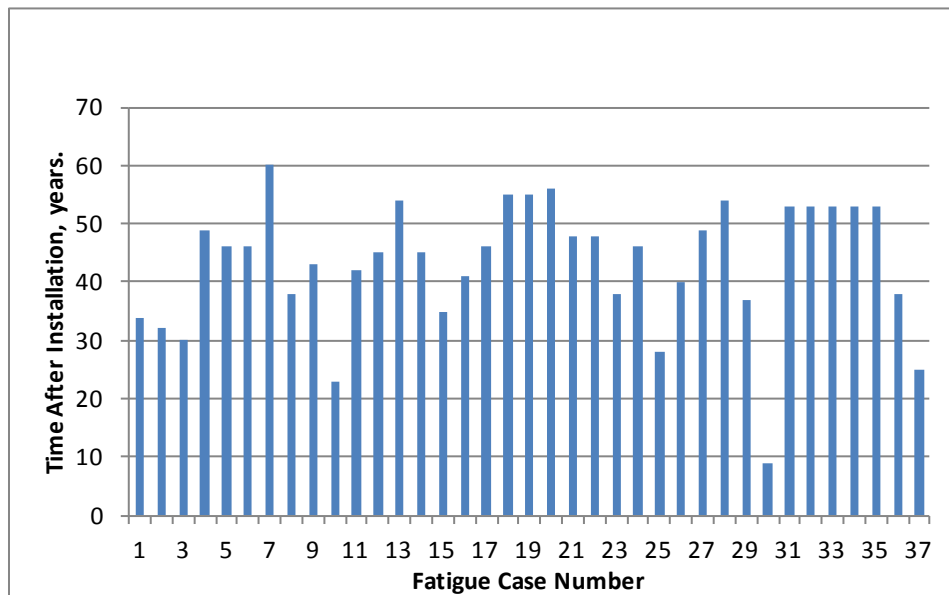


Figure 61. Times to Failure After Pipeline Installation for Fatigue-Enlarged Anomalies

The times to failure for fatigue-enlarged anomalies after a hydrostatic test are portrayed in Figure 62 where they are plotted as a function of the test-pressure-to-failure-pressure ratio. The times vary widely and do not seem to be affected significantly by the test-pressure-to-failure-pressure

ratio. The most likely explanation is that either pressure-cycle-aggressiveness or crack-growth rate or both are the main drivers. Neither of these parameters has been incorporated into the database. If a family of cases could be assembled where pressure-cycle aggressiveness and crack growth rate are held constant, one would expect to see the test-pressure-to-failure-pressure ratio having a significant effect. The higher the ratio, the longer the time to failure one would expect.

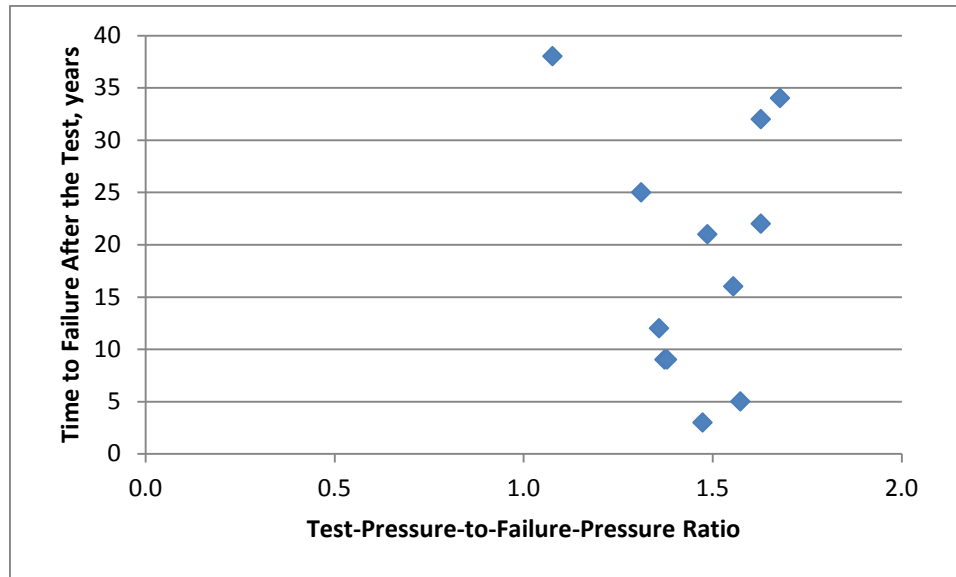


Figure 62. Times to Failure In Service after a Hydrostatic Test for Fatigue-Enlarged Anomalies

The failure stress levels for fatigue-enlarged defects were calculated based on stated dimensions using the Modified Ln-Sec EllipticalCEQ model with material strength represented by the flow stress of the base metal and toughness corresponding to the full-size-equivalent Charpy upper shelf energy of the base metal. The actual/predicted failure stress ratios are shown in Figure 63. Note that the figure is cut off at a ratio of 1.5 and that several of the ratios were significantly above 1.5. The minimum ratio is 0.81 and the maximum is 3.51. While the predictions are not all that good, they do suggest that the failures of fatigue-enlarged anomalies tend to be ductile more often than not.

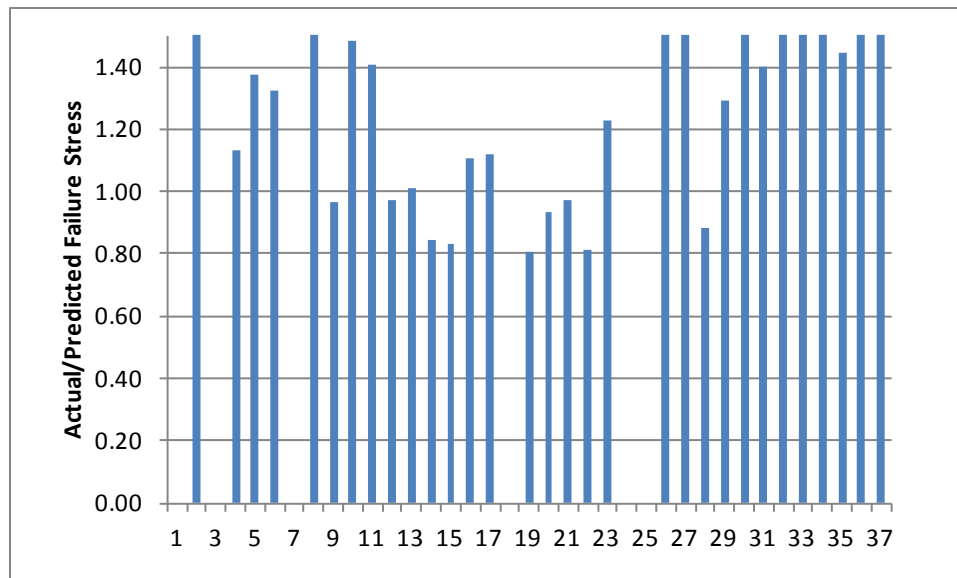


Figure 63. Ratios of Actual to Predicted Failure Stresses for Fatigue-Enlarged Anomalies

Details of Selected Individual Failures

It is worth reviewing certain cases individually to examine the nature of the initiating anomaly, the fatigue crack growth, and the ability or lack thereof of a ductile fracture initiation model to predict the failure stress.

Fatigue Case Number 1

Fatigue Case Number 1 involved a leak in a 16-inch-OD, 0.218-inch-wall, X60 pipe with a high-frequency-welded ERW seam. Fracture surfaces exposed by breaking open the defect show an ID thumbnail comprised of woody fracture. The appearance of the rest of the fracture suggests a region of probable crack growth near mid-wall, then more woody fracture. This leak occurred during a hydrostatic test at a hoop stress level of 85.6 percent of SMYS. The anomaly had survived a hydrostatic test to 90.2 percent of SMYS 34 years prior to the time of the leak. One scenario is that the ID woody fracture arose during the first test and that crack growth occurred over 34 years, followed by the final failure. Uncertainty as to the nature and the boundaries of the initial defect and the crack growth, plus the fact that this defect failed as a leak, prevent any meaningful comparison of actual to predicted failure stress level. A metallographic section across the leak illustrates the three regions of fracture (see Figure 64).

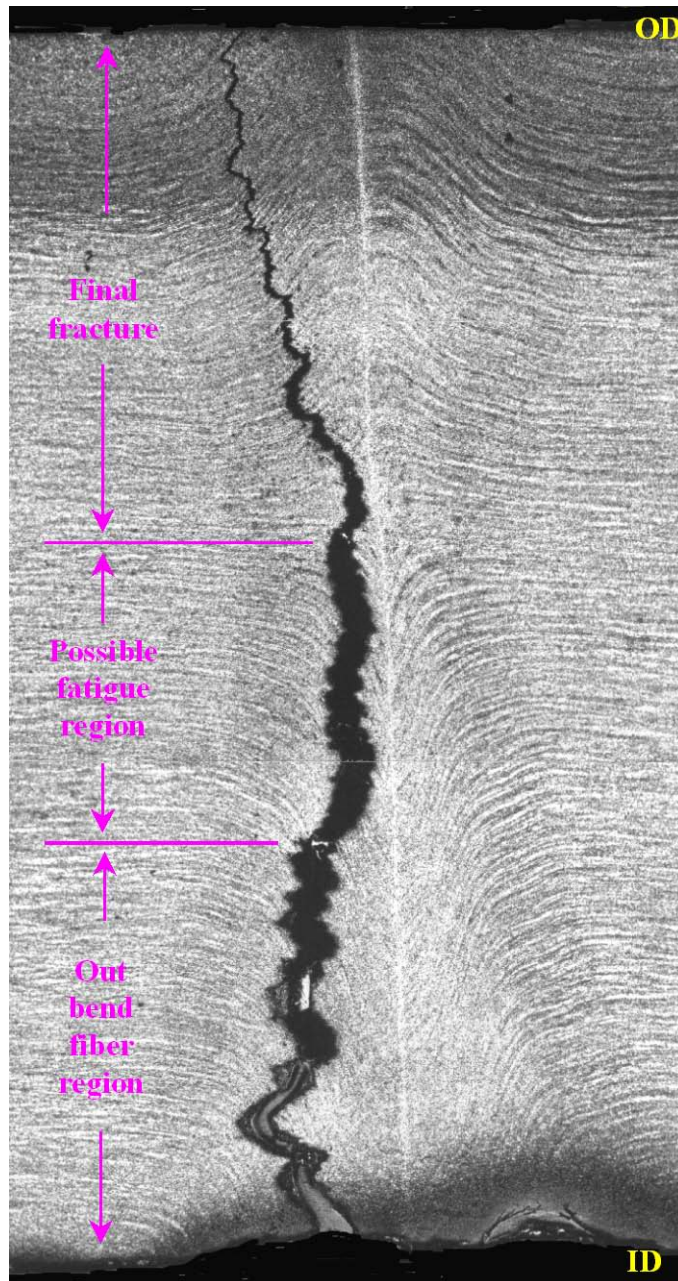


Figure 64. Cross Section of Fatigue Case Number 1 Anomaly

Fatigue Case Number 2

Fatigue Case Number 2 involved a leak in a 12.75-inch-OD, 0.219-inch-wall, X52 pipe with a low-frequency-welded ERW seam. The rupture of this defect occurred during a hydrostatic test at a hoop stress level of 66.9 percent of SMYS. No information on a prior hydrostatic test was available, but the anomaly failed 32 years after installation. Therefore, the initiating anomaly had at least survived the mill hydrostatic test to 85 percent of SMYS.

The initiating anomaly was a 7.5-inch-long, 45-percent-through-wall, semi-elliptically-shaped hook crack. The predicted failure stress level of this defect by itself based on the Modified Ln-Sec Elliptical C-equivalent model with a flow stress of 77,000 psi and the base metal full-size Charpy upper shelf energy of 26 ft lb is 88.4 percent of SMYS. That is consistent with its having survived the mill hydrostatic test to 85 percent of SMYS. The maximum depth of this defect plus the subsequent fatigue crack growth is 90 percent of the wall thickness. Using the Modified Ln-Sec Elliptical C-equivalent model with a flow stress of 77,000 psi and the base metal full-size Charpy upper shelf energy of 26 ft lb, one would predict the failure stress of the anomaly to be 19.1 percent of SMYS. Hence, the actual failure stress was larger than the predicted failure stress by a factor of 3.51.

The hook crack and fatigue crack growth as they appeared on the fracture surfaces are shown in Figure 65. A metallographic section across the hook crack and fatigue crack growth is shown in Figure 66. Note that the tip of the hoop crack and the fatigue crack growth lie in the heat-affected zone of the seam and not on the bondline line.

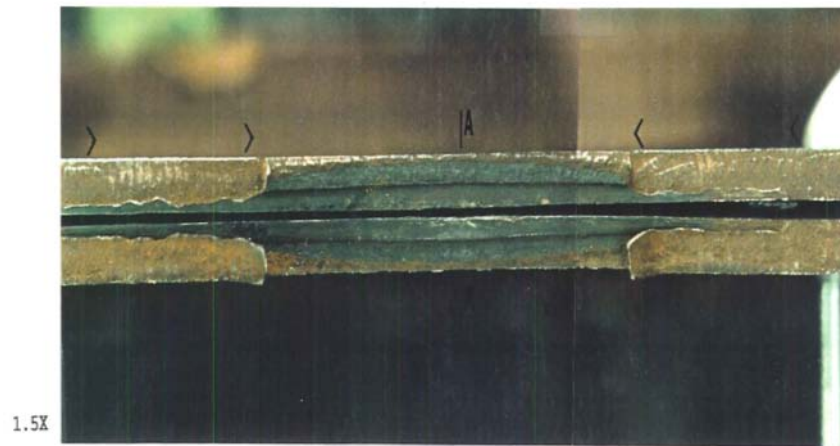


Figure 65. Fracture Surfaces of Fatigue Case Number 2 Anomaly

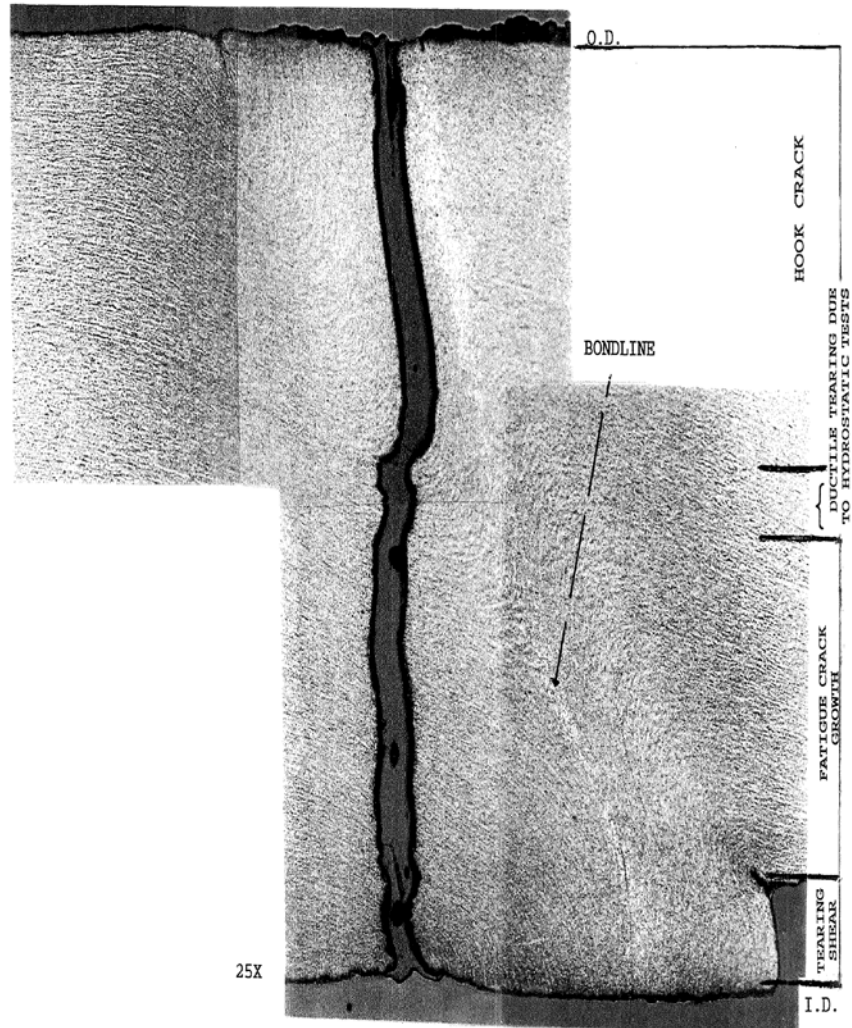


Figure 66. Cross Section of Fatigue Case Number 2 Anomaly

Fatigue Case Number 3

This leak occurred during a hydrostatic test of a piece of 10.75-inch-OD, 0.203-inch-wall, X52 high-frequency-welded ERW pipe. The sample was broken open after it had been chilled in liquid nitrogen to expose the fractures. The metallographic section across the anomaly, *not at the actual leak*, is shown in Figure 67. Figure 67 shows that the leakage path consists of three separate crack growth stages, the first stage, having started at an external hook crack, was likely fatigue crack propagation. The second stage which is offset from the first stage because the first stage apparently ends at another inclusion is probably fatigue cracking as well. The final fracture shown in this section was along the bondline, and it was created when the specimen was broken open. The leak itself appears to have involved the fatigue crack linking to an ID-connected bondline anomaly. Note that the crack propagation occurred in base metal.

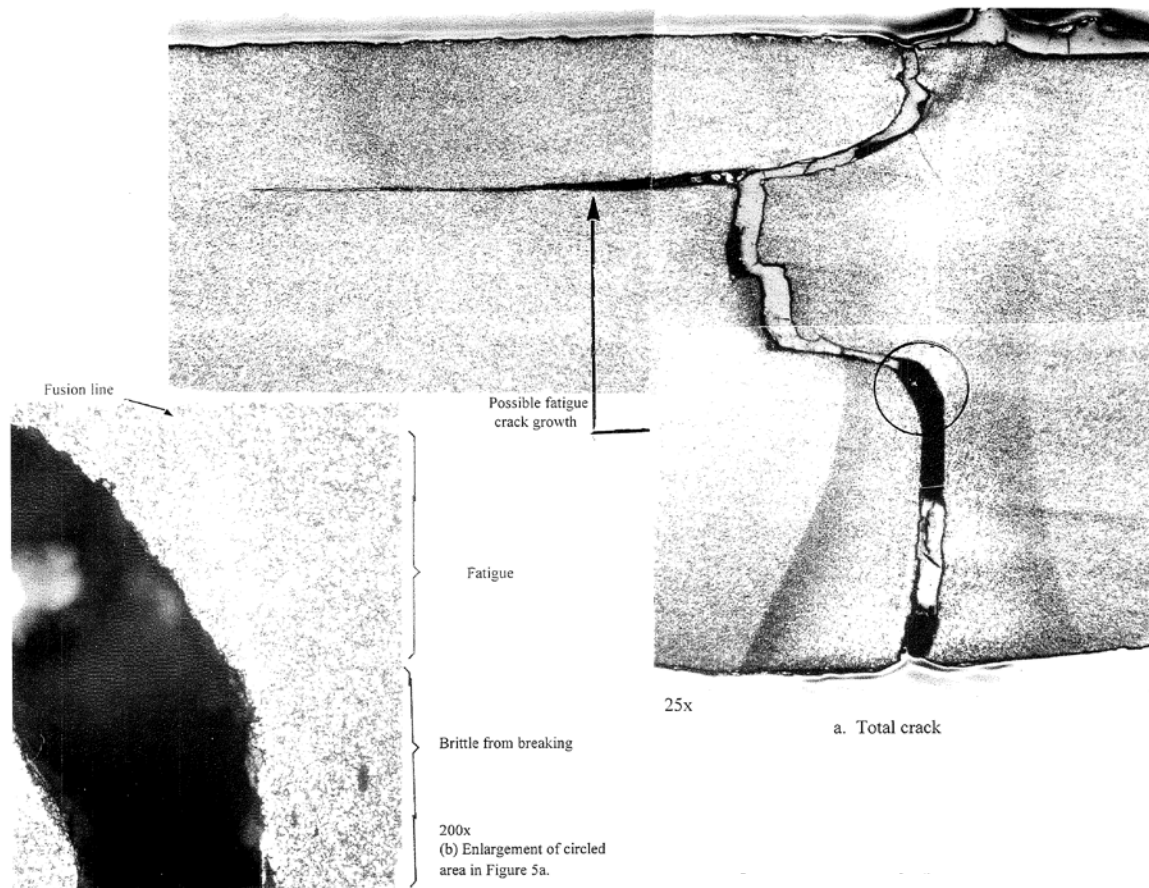


Figure 67. Cross Section of Fatigue Case Number 3 Anomaly

Fatigue Case Number 4

Fatigue Case Number 4 involved a rupture in a 10.75-inch-OD, 0.250-inch-wall, X46 pipe with a flash-welded seam. The rupture of this defect occurred during a hydrostatic test at a hoop stress level of 95.8 percent of SMYS. This was apparently the highest pressure level the pipe had ever experienced. Nevertheless, there was evidence of fatigue crack growth on the fracture surfaces. The probable initiating anomaly is the ID-connected hook crack shown on the fracture surface in Figure 68 and in the metallographic section shown in Figure 69. Note that the tip of the hook crack and the fatigue crack growth lie in the base metal of the pipe. What may be evidence of fatigue crack growth is shown in Figure 70, a 6,500X scanning electron microscope view of a part of the dark, semi-elliptically-shaped region on the fracture surface.

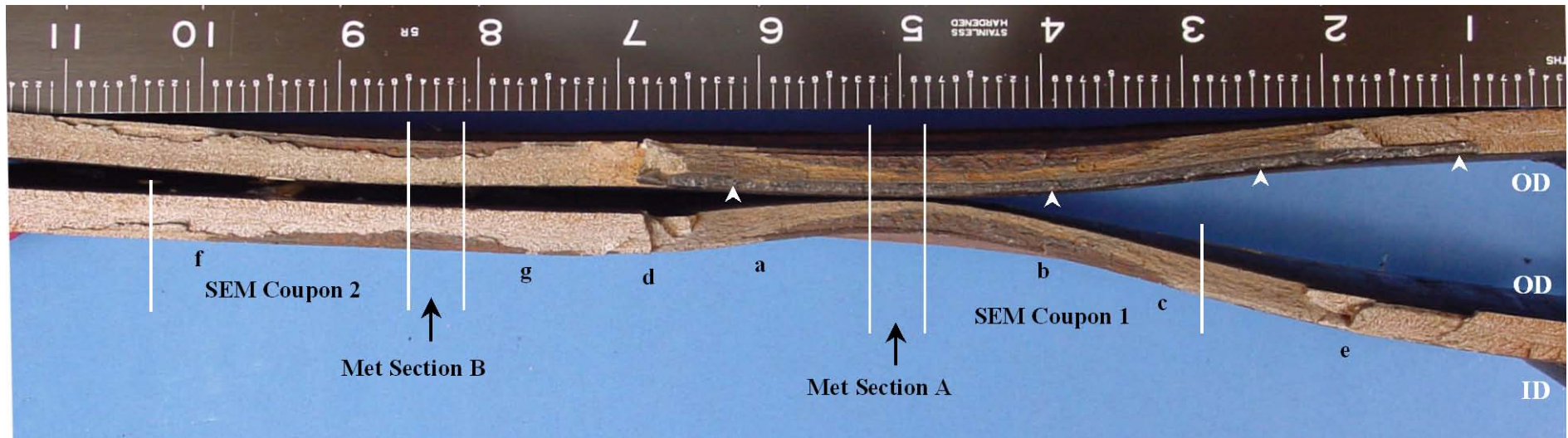


Figure 68. Fracture Surfaces of Fatigue Case Number 4 Anomaly

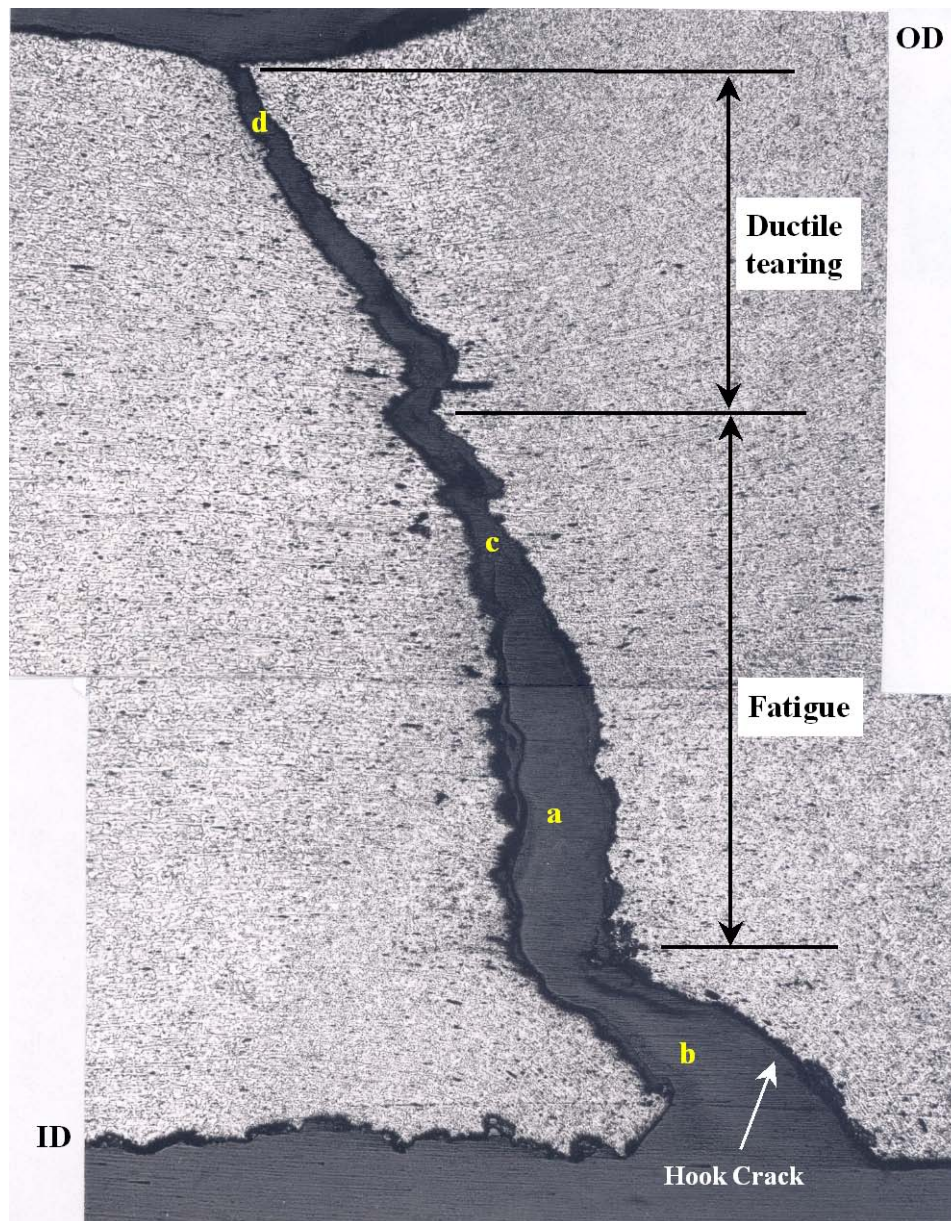


Figure 69. Cross Section of Fatigue Case Number 4 Anomaly

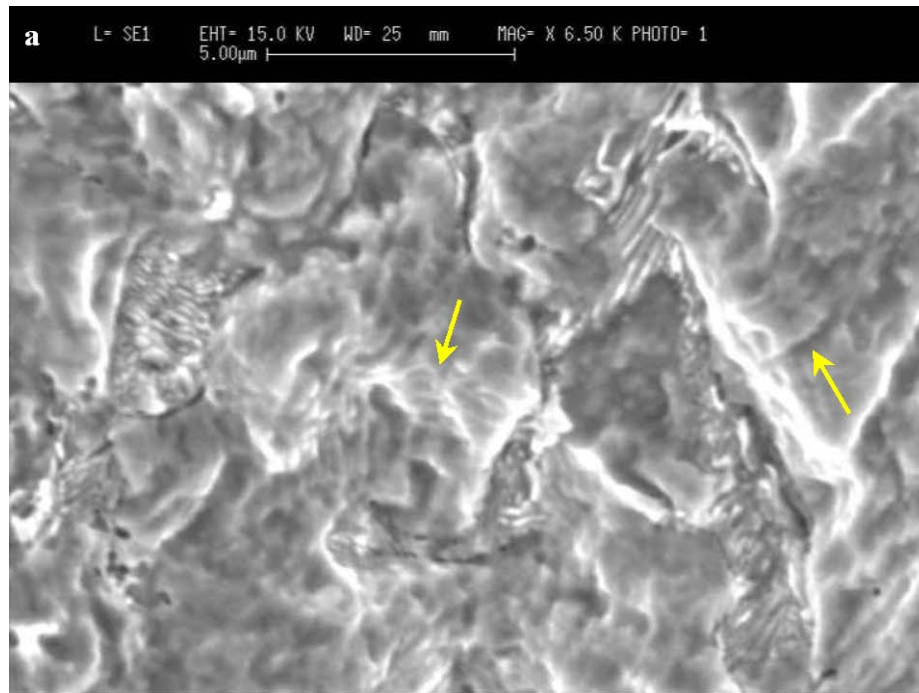


Figure 70. SEM Image of Possible Fatigue Crack Area, 6500X

The anomaly including the initiating hook crack and the dark elliptically-shaped area has an overall length of 2.33 inches and penetrates 70 percent of the wall thickness at the deepest point. Using the Modified Ln-Sec Elliptical C-equivalent model with a flow stress of 64,000 psi and the base metal full-size Charpy upper shelf energy of 22 ft lb, one would predict the failure stress of the anomaly to be 84.7 percent of SMYS. Hence, the actual failure stress was larger than the predicted failure stress by a factor of 1.13.

Fatigue Case Number 5

Fatigue Case Number 5 involved a rupture in a 10.75-inch-OD, 0.250-inch-wall, X46 pipe with a flash-welded seam. The rupture of this defect occurred during a hydrostatic test at a hoop stress level of 79.8 percent of SMYS. No information on a prior hydrostatic test was available, but the anomaly failed 46 years after installation. Therefore, the initiating anomaly had at least survived the mill hydrostatic test to 85 percent of SMYS.

There was evidence of fatigue crack growth on the fracture surfaces of the pipe as shown in Figure 71. The apparent crack is visible as the dark elliptically-shaped area between the two arrows in the photograph. Note that the thicknesses of the two pieces in the photograph are obviously not the same. That is because the initiating anomaly was a mismatched plate edge at the ID surface. The mismatch is clearly shown on the metallographic section in Figure 72. Note that the fatigue crack growth lies in the base metal of the pipe.



Figure 71. Fracture Surfaces of Fatigue Case Number 5 Anomaly

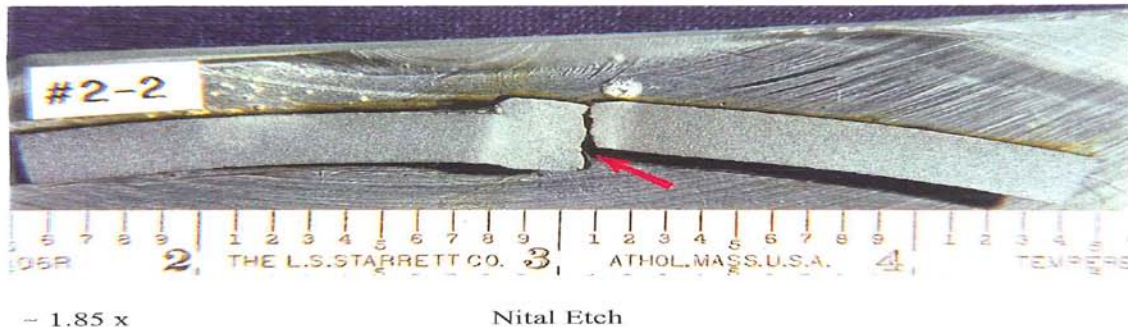


Figure 72. Cross Section of Fatigue Case Number 5 Anomaly

The anomaly including the initiating mismatch and the dark elliptically-shaped area has an overall length of 7 inches and penetrates 70 percent of the wall thickness at the deepest point. Using the Modified Ln-Sec Elliptical C-equivalent model with a flow stress of 72,000 psi and the base metal full-size Charpy upper shelf energy of 29 ft lb, one would predict the failure of the final anomaly to be 58.1 percent of SMYS. Hence, the actual failure stress was larger than the predicted failure stress by a factor of 1.37.

Fatigue Case Number 6

Fatigue Case Number 6 involved a rupture in a 10.75-inch-OD, 0.307-inch-wall, X46 pipe with a low-frequency-welded seam. The rupture of this defect occurred during a hydrostatic test at a hoop stress level of 81.2 percent of SMYS. No information on a prior hydrostatic test was available, but the anomaly failed 46 years after installation. Therefore, the initiating anomaly had at least survived the mill hydrostatic test to 85 percent of SMYS.

There was evidence of fatigue crack growth on the fracture surfaces of the pipe as shown in Figure 73. The apparent crack is visible as the dark, semi-elliptically-shaped area between the two arrows in the photograph. The initiating anomaly was an ID-surface-connected hook crack that penetrated only about 10 to 15 percent of the wall thickness along its length. The hook crack is visible as the dark, smooth area in Figure 73. The hook crack and the fatigue crack

growth are shown on the metallographic section in Figure 74. The fatigue crack growth lies near to but not on the bondline of the ERW seam.

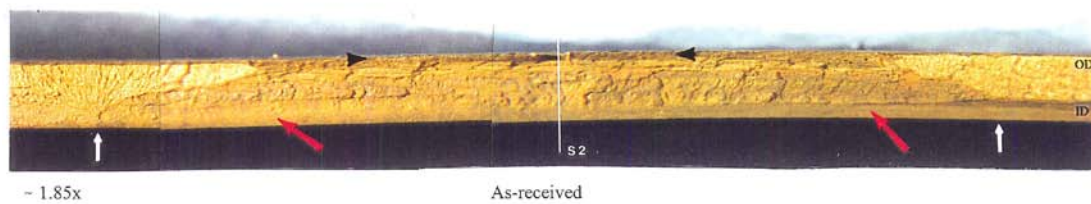


Figure 73. Fracture Surfaces of Fatigue Case Number 6 Anomaly

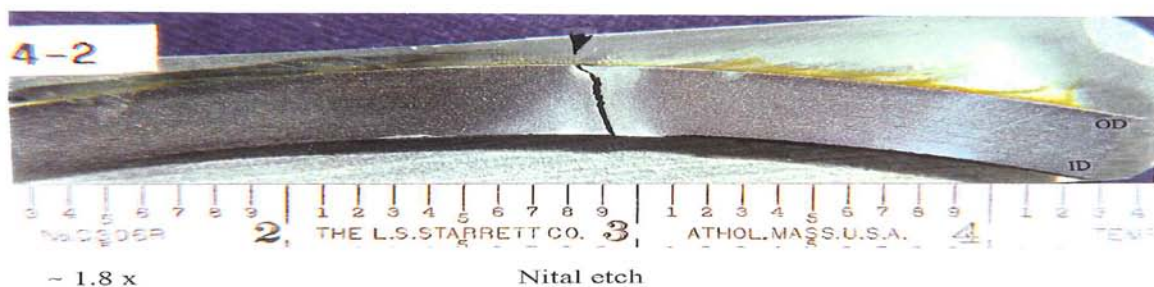


Figure 74. Cross Section of Fatigue Case Number 6 Anomaly

The anomaly including the initiating hook crack and the dark elliptically-shaped area has an overall length of 4.2 inches and penetrates 75 percent of the wall thickness at the deepest point. Using the Modified Ln-Sec Elliptical C-equivalent model with a flow stress of 64,500 psi and the base metal full-size Charpy upper shelf energy of 27 ft lb, one would predict the failure stress of the anomaly to be 61.3 percent of SMYS. Hence, the actual failure stress was larger than the predicted failure stress by a factor of 1.33.

Fatigue Case Number 7

Fatigue Case Number 7 involved a rupture in a 12.75-inch-OD, 0.250-inch-wall, X45 pipe with a flash-welded seam. The rupture of this defect occurred in service at a hoop stress level of 61.7 percent of SMYS, but the operator believes that it was probably leaking up to 36 hours before the rupture occurred. This failure occurred within 3 years of a hydrostatic test to a stress level of 90.8 percent of SMYS, 1.5 times the stress level at failure. The fracture surfaces of this rupture, shown in Figure 75, reveal two halves of apparently different thickness (as is typical with mismatched edges), clear evidence that crack growth has taken place, and an unusual appearance in the central portion that was caused by erosion during the period when a high-pressure leak

existed. The mismatch is clearly shown on the metallographic section in Figure 76. Note that the fatigue crack growth lies in the base metal of the pipe.

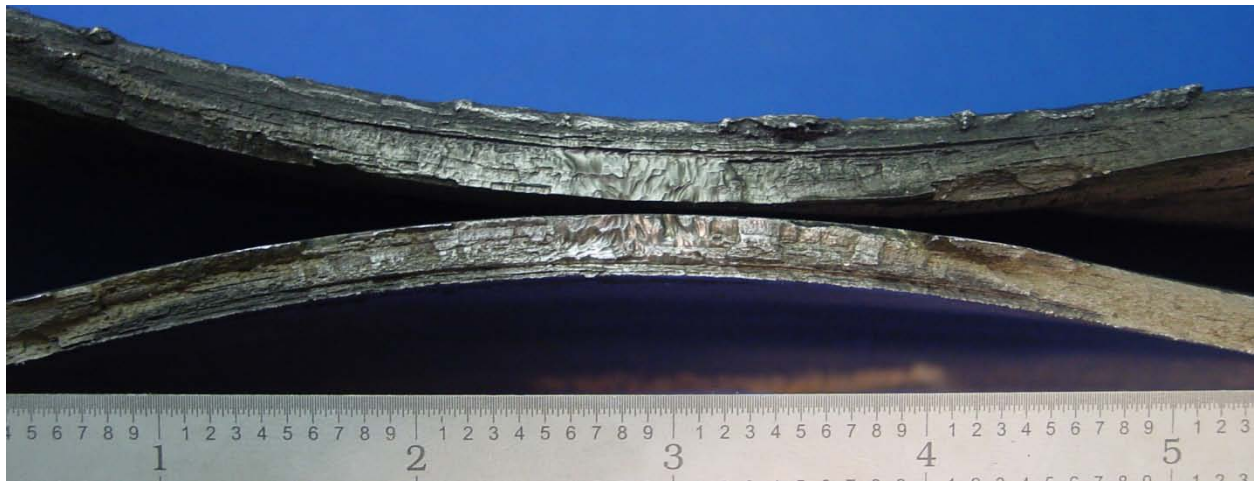


Figure 75. Fracture Surfaces of Fatigue Case Number 7 Anomaly

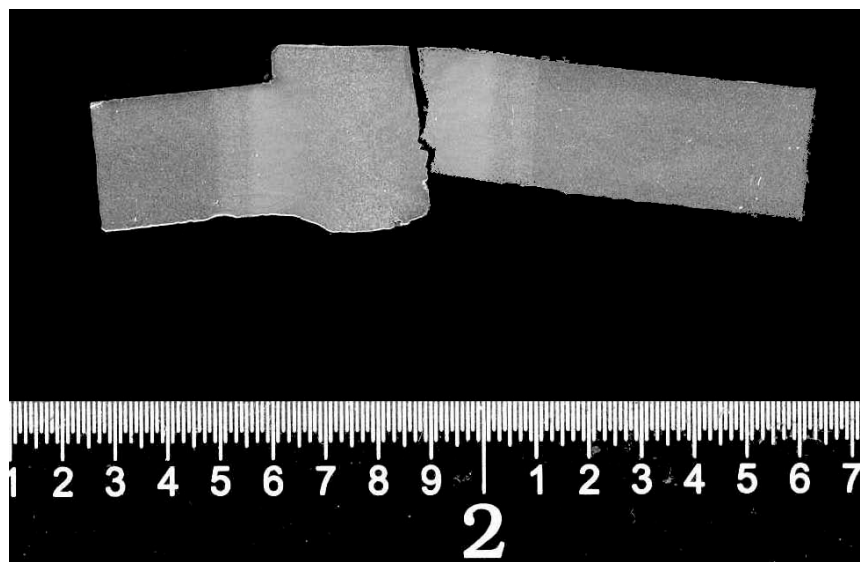


Figure 76. Cross Section of Fatigue Case Number 7 Anomaly

The length of the fatigue growth area is about 4 inches, but the erosion has obliterated the area where one might have seen the maximum depth of the crack. One benchmark on the depth is provided by the fact that this defect had survived a hydrostatic test to 90.8 percent of SMYS three years prior to its failing in service. Using the Modified Ln-Sec Elliptical C-equivalent model with a flow stress of 70,500 psi and the base metal full-size Charpy upper shelf energy of 36 ft lb, one would predict that for the defect to have survived the previous test, it could have been no deeper than about 63 percent of the wall thickness. Using the same type of calculation one would predict that the defect should have failed at a stress level of 61.7 percent of SMYS if it were to have grown to a depth of 79 percent of the wall thickness. It can be shown that the

model predicts a leak as the mode of failure for this defect at the stress level of 61.7 percent of SMYS. Apparently, the erosion enlarged the length of the leak to the point where the pipe ruptured.

Fatigue Case Number 8

Fatigue Case Number 8 involved a rupture in an 8.625-inch-OD, 0.188-inch-wall, X52 pipe with a low-frequency welded ERW seam. The seam failed in service at a hoop stress level of 69.7 percent of SMYS. As seen in Figure 77 and Figure 78 the cause was fatigue crack growth from a mismatched plate edge. Note that in Figure 77 the fracture edges are obviously different as expected with mismatched edges. The crack growth occurred in the heat-affected base metal adjacent to the bondline.

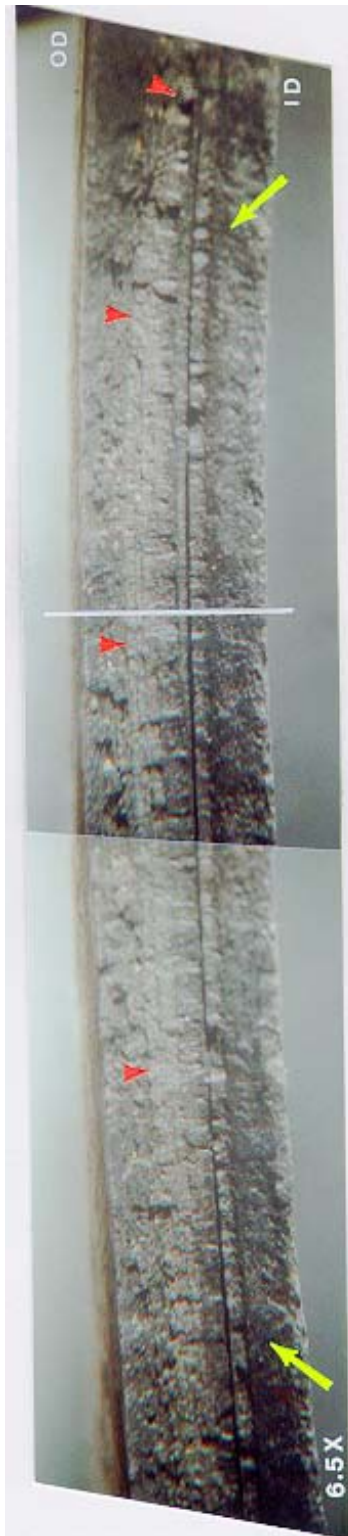


Figure 77. Fracture Surfaces of Fatigue Case Number 8 Anomaly

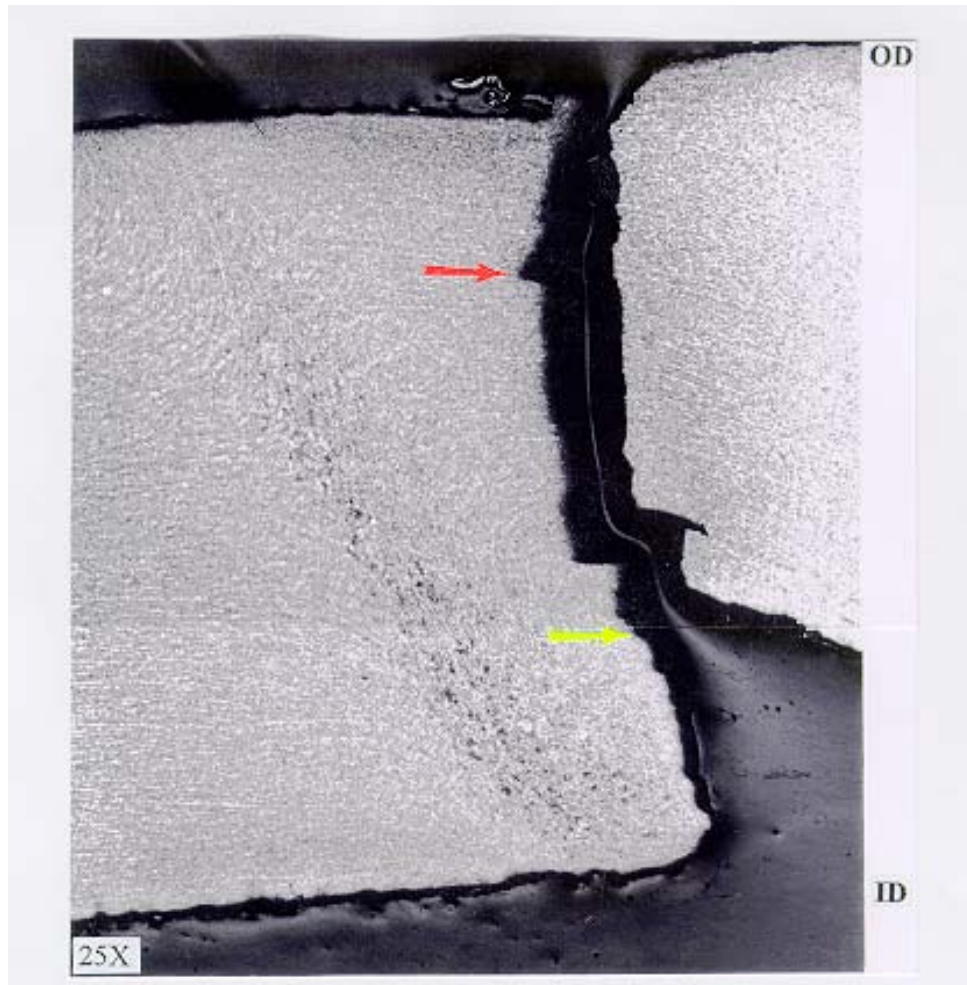


Figure 78. Cross Section of Fatigue Case Number 8 Anomaly

The area of fatigue crack growth has an overall length of 6.75 inches. Together with the mismatch, the anomaly penetrates 69 percent of the wall thickness at the deepest point. Using the Modified Ln-Sec Elliptical C-equivalent model with a flow stress of 60,000 psi and the base metal full-size Charpy upper shelf energy of 18 ft lb, one would predict the failure stress of the anomaly to be 41 percent of SMYS. The actual failure stress was larger than the predicted failure stress by a factor of 1.70.

Fatigue Case Number 9

Fatigue Case Number 9 involved a rupture in a 10.75-inch-OD, 0.219-inch-wall, X52 pipe with a low-frequency-welded seam. The rupture of this defect occurred during a hydrostatic test at a hoop stress level of 81.8 percent of SMYS. The analysis of this failure was made difficult because the sample was allowed to sit outdoors for months after it had been removed from the pipeline. The investigators picked two possible origins, but in retrospect, the origin is most likely the hook crack shown in Figure 79. This hook crack was 5 inches long and penetrated 40

percent of the wall thickness. Note that the fracture extends approximately in the radial direction from the bottom of the hook crack to a depth of about 57 percent of the wall thickness. Ductile tearing during the test makes up the remainder of the fracture. Although the fracture surface characteristics had been obliterated by corrosion, it is reasonable to believe based on other similar hook crack/fatigue crack failures that fatigue was the cause of this failure.

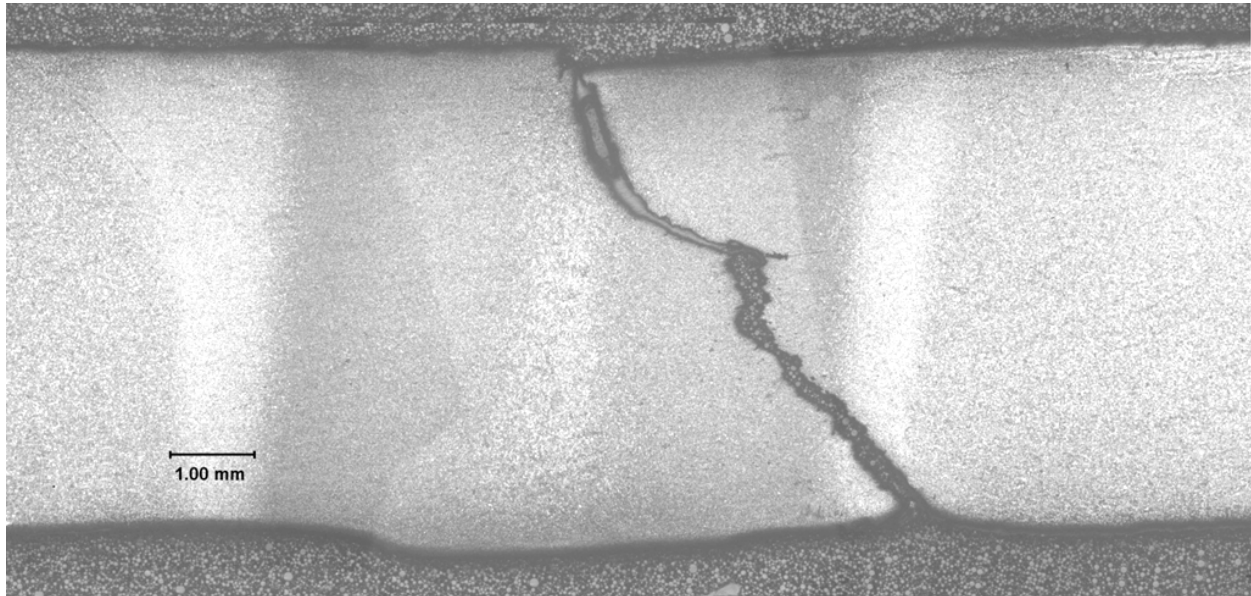


Figure 79. Cross Section of Fatigue Case Number 9 Anomaly

Using the Modified Ln-Sec Elliptical C-equivalent model with a flow stress of 76,500 psi and the base metal full-size Charpy upper shelf energy of 57 ft lb, one would predict the failure stress of the anomaly to be 84.7 percent of SMYS. Hence, the actual failure stress was 97 percent of this predicted failure stress.

Fatigue Case Number 10

Fatigue Case Number 10 involved a rupture in a 6.625-inch-OD, 0.125-inch-wall, X60 pipe with a high-frequency-welded seam. The rupture of this defect occurred during a hydrostatic test at a hoop stress level of 93.7 percent of SMYS. A 6-inch-long, 25-percent-through hook crack was found to be the initiator of fatigue crack growth. The hook crack is visible in Figure 80 and the possible fatigue crack extension of it is shown in Figure 81. The total defect depth (hook crack plus fatigue) was 56 percent of the wall thickness. The anomaly failed as a 3.1 percent pressure reversal from a previous high pressure test cycle just prior to the failure.

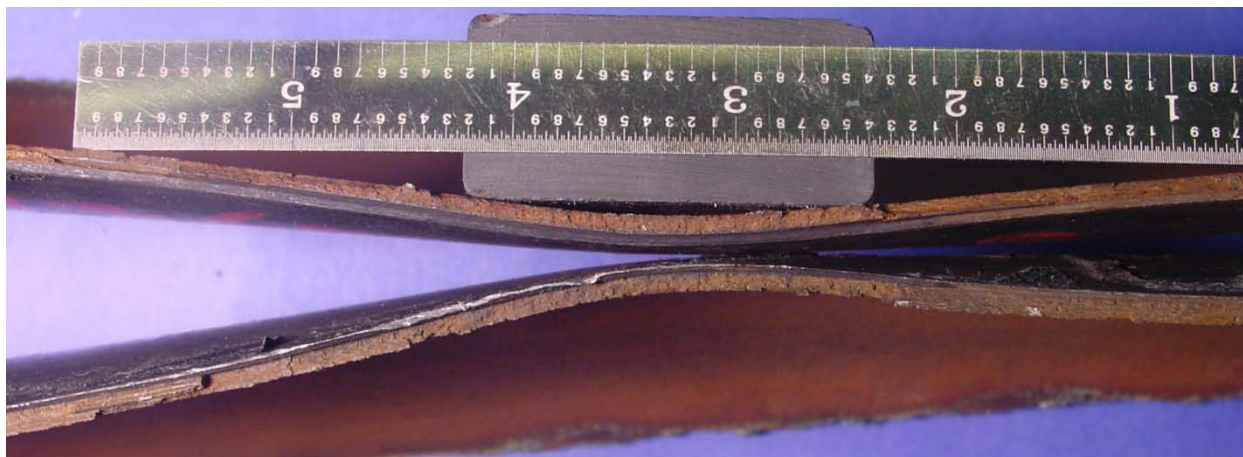


Figure 80. Fracture Surfaces of Fatigue Case Number 10 Anomaly

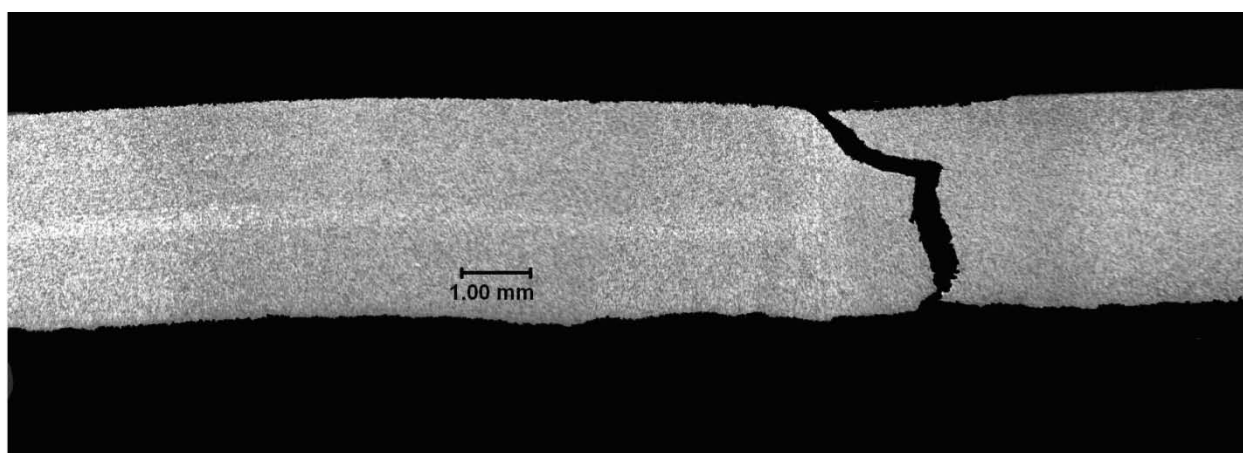


Figure 81. Cross Section of Fatigue Case Number 10 Anomaly

Using the Modified Ln-Sec Elliptical C-equivalent model with the flaw length of 6 inches and depth of 56 percent of the wall, a flow stress of 78,500 psi, and the base metal full-size Charpy upper shelf energy of 30 ft lb, one would predict the failure stress of the anomaly to be 63.1 percent of SMYS. The actual failure stress was 97 percent of this predicted failure stress. Hence, the actual failure stress was larger than the predicted failure stress by a factor of 1.48.

Fatigue Case Number 11

Fatigue Case Number 11 involved an in-service rupture in a 12.75-inch-OD, 0.203-inch-wall X52 pipe with a low-frequency-welded seam. The failure occurred at a hoop stress level of 59.8 percent of SMYS. The initial defect was a 9.5-inch-long, rectangular-shaped, ID-surface-connected hook crack that penetrated 45 percent of the wall thickness (see Figure 82 and Figure 83). Fatigue cracking occurred in two stages. Stage 1, which had probably occurred prior to a hydrostatic test to 82.1 percent of SMYS 9 years prior to the failure, took the depth to 60 percent of the wall thickness. The second stage took the total crack depth to 80 percent of the wall

thickness. It appeared that the fatigue cracking did not propagate along the entire tip of the hook crack. Visual inspection of the photographs of the fracture surfaces suggest the Stage 1 cracking did not extend more than about 6 inches and that Stage 2 cracking did not extend more than about 4 inches. This anomaly apparently was not identified as a serious anomaly during a circumferential MFL tool run a year before the failure, and it was also not identified as a serious anomaly during an ultrasonic crack-detection tool run a few months before the failure.



Figure 82. Fracture Surfaces of Fatigue Case Number 11 Anomaly

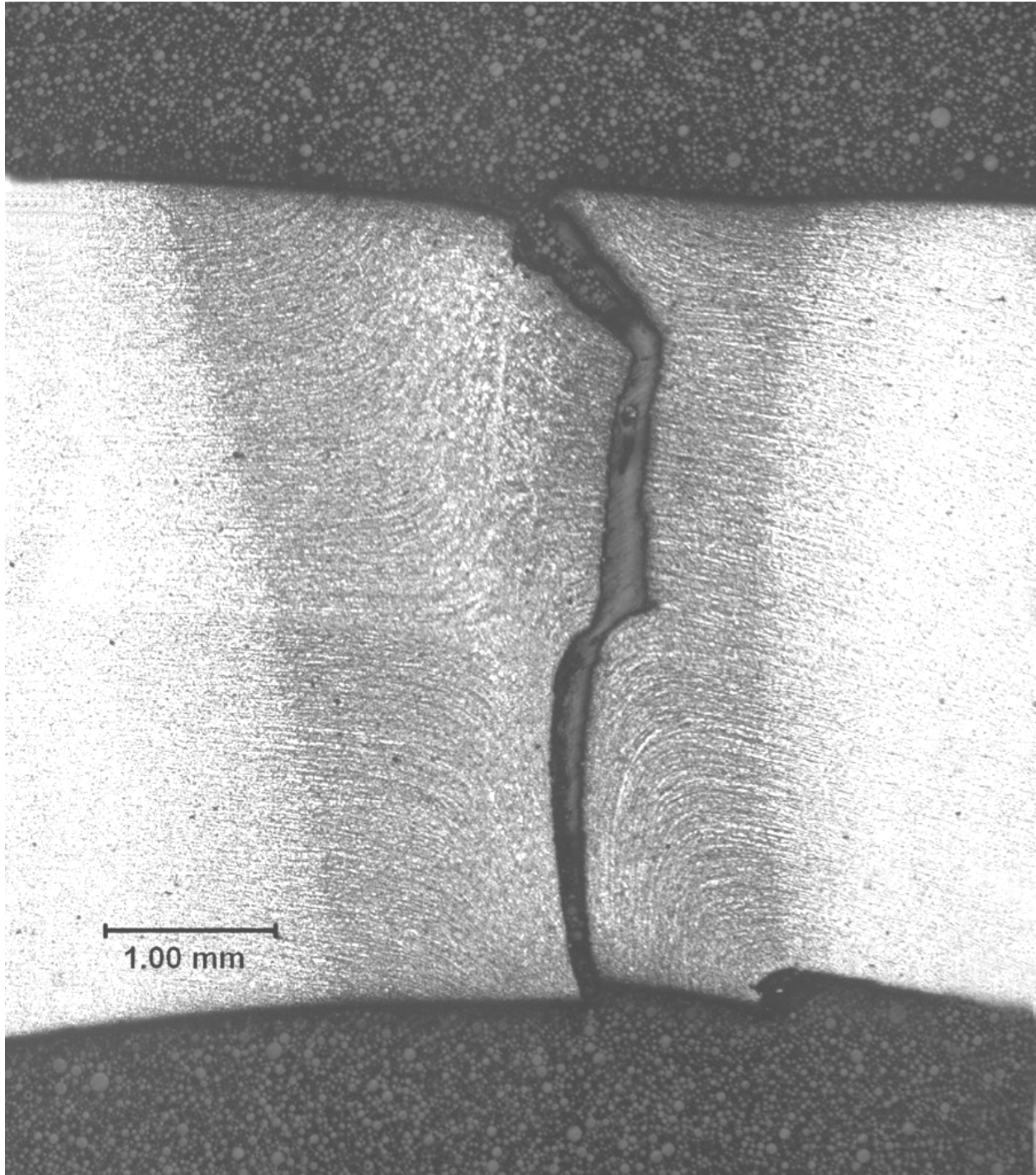


Figure 83. Cross Section of Fatigue Case Number 11 Anomaly

Using the Modified RECTANG model with the hook crack length of 9.5 inches and depth of 49 percent of the wall, a flow stress of 63,000 psi, and the base metal full-size Charpy upper shelf energy of 49 ft lb, one would predict the failure stress of the hook crack by itself to be 66 percent of SMYS. This suggests that the hook crack itself would not have survived the prior hydrostatic test to 82.1 percent of SMYS or the mill test to 85 percent of SMYS. A benchmark for the actual

properties in the zone where the hook crack existed (heat-affected material near the seam) is that if the flow stress is assumed to be 85,000 psi, the Modified Ln-Sec RECTANG model would predict that the hook crack would have survived the mill hydrostatic test.

If one applies this flow stress to the fatigue cracks and utilizes their apparent lengths, the results are as follows.

Using the Modified Ln-Sec Elliptical C-equivalent model with the flaw length of 6 inches and depth of 60 percent of the wall for the combined hook crack and Stage 1 fatigue crack depth, a flow stress of 85,000 psi, and the base metal full-size Charpy upper shelf energy of 49 ft lb, one would predict the failure stress of the anomaly to be 84.1 percent of SMYS. This level is consistent with the flaw have survived the test to 82.1 percent of SMYS 9 years prior to the failure.

Using the Modified Ln-Sec Elliptical C-equivalent model with the flaw length of 4 inches and the total depth of 80 percent of the wall, a flow stress of 85,000 psi, and the base metal full-size Charpy upper shelf energy of 49 ft lb, one would predict the failure stress of the anomaly to be 57.2 percent of SMYS. That is pretty close to the actual failure stress of 59.8 percent of SMYS.

Fatigue Case Number 12

Fatigue Case Number 12 involved a hydrostatic test rupture in a 16-inch-OD, 0.250-inch-wall, X52, DC-welded ERW seam. The rupture occurred at a hoop stress level of 81.6 percent of SMYS. The initiator was a 4.5-inch-long ID-surface-connected hook crack that penetrated about 1/3 of the way through the wall thickness. The fatigue crack plus the hook crack penetrated 70 percent through the wall (see Figure 84).

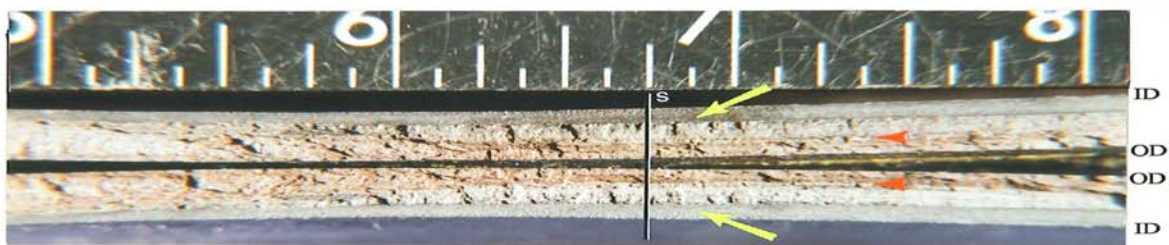


Figure 84. Fracture Surfaces of Fatigue Case Number 12 Anomaly

Fatigue Case Number 13

Fatigue Case Number 13 involved a hydrostatic test rupture in a 16-inch-OD, 0.250-inch-wall, X52 DC-welded ERW seam. The rupture occurred at a hoop stress level of 81.8 percent of SMYS. The initiator was a 9-inch-long ID-surface-connected hook crack that penetrated about

40 percent the wall thickness. A 3-inch-long fatigue crack had grown to a total depth (hook crack plus fatigue crack) of 60 percent through the wall. The contributor calculated a predicted failure stress for the hook crack by itself representing the depth profile over its 9-inch length as a semi-ellipse with a maximum through-wall depth of 0.102-inches, and CVN of 15 ft-lbs (as measured in the seam). Predicted failure stress levels for the hook crack as calculated by the contributor were 70.3 percent of SMYS using CorLAS, 66.5 percent using KAPA, and 68.1 percent of SMYS using PFC40. All three values indicate that the hook cracking should have failed during prior hydrostatic tests including the manufacturer's test to 85 percent of SMYS. The contributor offered the observation that predicting burst pressures for hook cracking with these methodologies produces conservative estimates of the likely failure pressure.

Using the Modified Ln-Sec Elliptical C-equivalent model with the hook crack length of 9 inches and the total depth of 41 percent of the wall, a flow stress of 65,000 psi, and the base metal full-size Charpy upper shelf energy of 30 ft lb, one would predict the failure stress of the anomaly to be 81.2 percent of SMYS also suggesting that the hook crack should have failed in prior tests including the mill test.

Fatigue Case Number 14

Fatigue Case Number 14 involved an in-service rupture in a 20-inch-OD, 0.312-inch-wall, X52 pipe with a flash-welded seam. The failure occurred at a hoop stress level of 55.3 percent of SMYS. The initial defect appears to have been a 3.5-inch-long, 40-percent-through area involving what looked like two hook cracks separated by a region of inclusion-filled metal that appears to have been torn apart while the material was still hot after welding, joining the hook cracks to make a continuous defect. This defect was ID-surface-connected. Fatigue cracking occurred in two stages. Stage 1, which had probably occurred before but did not cause failure in a hydrostatic test to 90.0 percent of SMYS 22 years prior to the failure, took the depth to 55 percent of the wall thickness. The second stage took the total crack depth to 79 percent of the wall thickness.

Using the Modified RECTANG model with the length of 3.5 inches and depth of 40 percent of the wall of the compound initial defect, a flow stress of 67,000 psi, and the base metal full-size Charpy upper shelf energy of 25 ft lb (assumed because no Charpy data were available), one would predict the failure stress of the hook crack by itself to be about 95 percent of SMYS. This suggests that the compound initial defect by itself would have survived the prior hydrostatic test to 90 percent of SMYS and the mill test to 85 percent of SMYS.

Using the Modified Ln-Sec Elliptical C-equivalent model with the flaw length of 3.5 inches and depth of 55 percent of the wall for the combined initial defect and Stage 1 fatigue crack depth, a

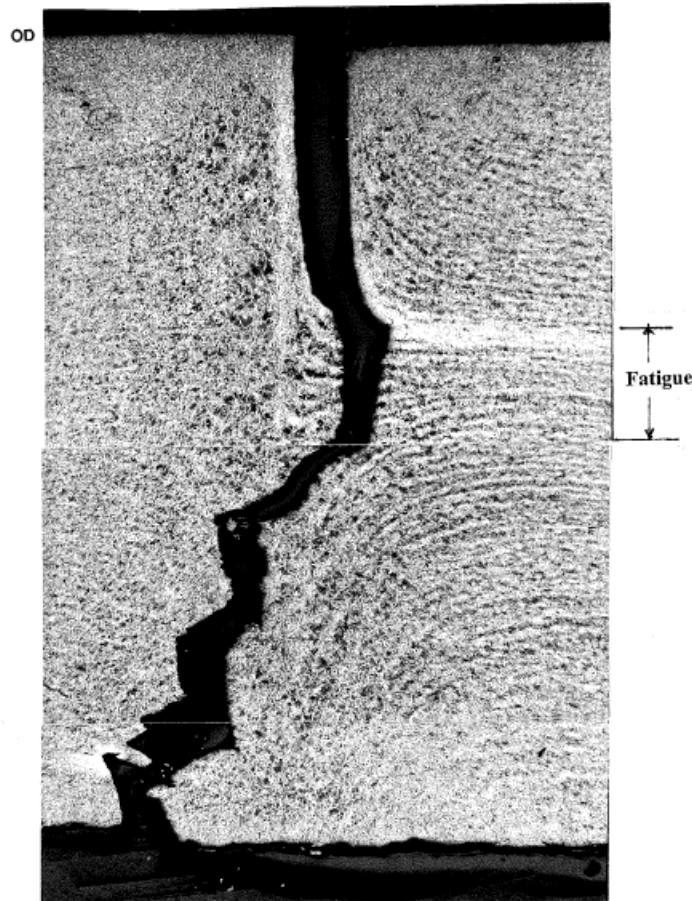
flow stress of 67,000 psi, and the base metal full-size Charpy upper shelf energy of 25 ft lb, one would predict the failure stress of the anomaly to be more than 90 percent of SMYS. This level is consistent with the flaw having survived the test to 90 percent of SMYS 22 years prior to the failure.

Using the Modified Ln-Sec Elliptical C-equivalent model with the flaw length of 3.5 inches and the total depth of 79 percent of the wall, a flow stress of 67,000 psi, and the base metal full-size Charpy upper shelf energy of 25 ft lb, one would predict the failure stress of the anomaly to be about 66 percent of SMYS. That is more than the actual failure stress of 55.3 percent of SMYS, so either the effective toughness was less than assumed or the model does not give a lower bound prediction.

Fatigue Case Number 15

Fatigue Case Number 15 involved a rupture in a 12.75-inch-OD, 0.250-inch-wall, X46 pipe with a low-frequency welded ERW seam. The seam failed during a hydrostatic test at a hoop stress level of 97 percent of SMYS. The initiating anomaly was an OD-surface-connected hook crack that had a length of 2.4 inches and a through-thickness depth that was 34 percent of the wall thickness. By itself this anomaly would be predicted to fail at a stress level of 128 percent of SMYS based on a calculation using the Modified Ln-Sec EllipticalCEQ model with a flow stress of 66,000 psi and a full-size-equivalent Charpy upper shelf energy of 28 ft lb.

Figure 85 shows that a fatigue crack had propagated from the tip of the relatively deep OD-surface-connected hook crack to a total depth of 50 percent of the wall thickness. On the basis of the Modified Ln-Sec EllipticalCEQ model with a flow stress of 66,000 psi and a full-size-equivalent Charpy upper shelf energy of 28 ft lb, one predicts that the combined defect would fail at a stress level of 116 percent of SMYS. The actual failure stress was 97 percent of SMYS, so the actual failure stress was only 83 percent of the predicted failure stress.



(d) Enlargement of section at fracture showing zone of fatigue

Figure 85. Cross Section of Fatigue Case Number 15 Anomaly

Fatigue Case Number 18

Fatigue Case Number 18 involved a rupture in a 22-inch-OD, 0.344-inch-wall, X46 pipe with a DC-welded seam. The rupture of this defect occurred during a hydrostatic test at a hoop stress level of 85.9 percent of SMYS. No information on a prior hydrostatic test was available, but the anomaly failed 55 years after installation. Therefore, the initiating anomaly had at least survived the mill hydrostatic test to 85 percent of SMYS.

The existence of fatigue crack growth at this defect is not certain. What is known is that the failure initiated at an OD-connected hook crack that was 4 inches long and 30 percent through the wall. At the same location there was also an ID-connected hook crack that was only about an inch long and 30 percent through the wall. The remaining ligament of material between the two hook cracks failed as shown in Figure 86 but whether or not crack growth took place before the test is not known. The failure stress of the defect was not calculated because of the confounding effect of two interacting defects. A calculation based on the longer hook crack alone results in a

predicted failure stress level of 119 percent of SMYS, a level well above the actual failure stress level of 85.9 percent of SMYS.



Figure 86. Cross Section of Fatigue Case Number 18 Anomaly

Fatigue Case Number 19

Fatigue Case Number 19 involved a rupture in a 22-inch-OD, 0.312-inch-wall, X46 pipe with a DC-welded seam. The rupture of this defect occurred during a hydrostatic test at a hoop stress level of 78.0 percent of SMYS. The defect had survived a prior hydrostatic test to 81.2 percent of SMYS apparently 13 years before it failed in another hydrostatic test.

The initiating defect was a 3.6-inch-long, 37-percent-through-wall ID-surface-connected hook crack. By itself this anomaly would be predicted to fail at a stress level of 116 percent of SMYS based on a calculation using the Modified Ln-Sec EllipticalCEQ model with a flow stress of 59,600 psi and a full-size-equivalent Charpy upper shelf energy of 34 ft lb.

As can be seen in Figure 87, there was evidence of fatigue crack growth at the tip of the hook crack on the fracture surfaces of the ruptured pipe (see arrows). It appears that there is a crack arrest mark even deeper than the apparent fatigue region. Perhaps the two regions represent fatigue crack growth before and after the test conducted 13 years prior to the failure. A metallographic section across the failure origin is shown in Figure 88. It shows the initiating hook crack, the apparent fatigue crack growth to a total depth of about 55 percent of the wall thickness, and some apparent ductile tearing that joins the crack to an embedded hook crack. On the basis of the Modified Ln-Sec EllipticalCEQ model with a flow stress of 59,600 psi and a full-size-equivalent Charpy upper shelf energy of 34 ft lb, one predicts that the hook crack plus fatigue crack would fail at 96.4 percent of SMYS. The actual failure stress was only 81 percent of this predicted value. The effect of the embedded hook crack was not taken into account in the calculation.

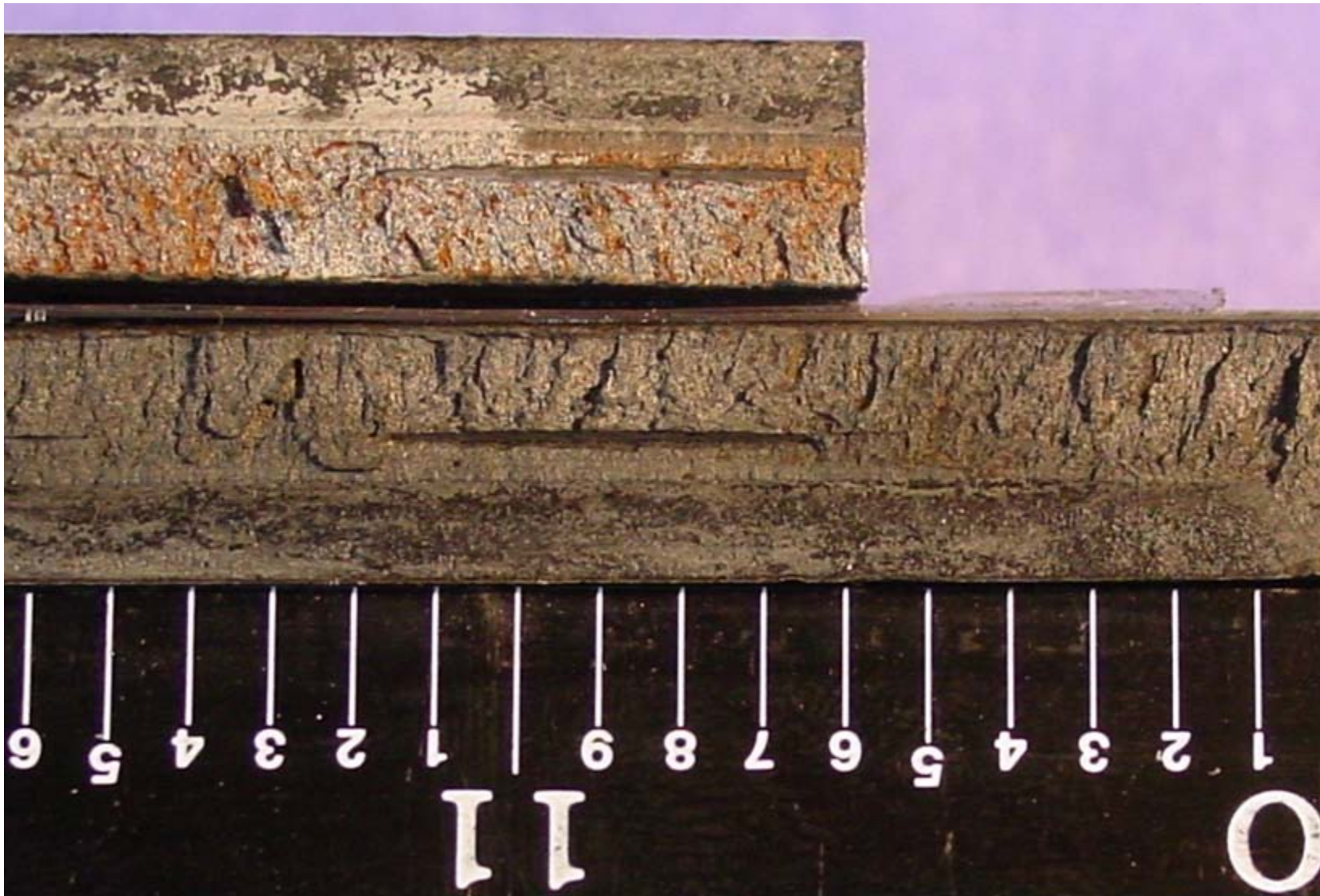


Figure 87. Fracture Surfaces of Fatigue Case Number 19 Anomaly



Figure 88. Cross Section of Fatigue Case Number 19 Anomaly

Fatigue Case Number 20

Fatigue Case Number 20 involved an in-service leak in an 8.625-inch-OD, 0.203-inch-wall, Grade B pipe with a flash-welded seam. The hoop stress level at the time the leak was discovered is uncertain, but the pipeline was normally operated at 69.8 percent of SMYS. The leak initiated at a location of mismatched and misaligned edges where some amount of lack of fusion may have been present as well. The length of the anomaly was about 1.4 inches. The

fracture surface was too corroded to permit identification of nature of the cracking, but fatigue is suspected to have occurred.

Fatigue Case Number 23

Fatigue Case Number 23 involved a hydrostatic test rupture in a 26-inch-OD, 0.281-inch-wall, X52 pipe with a flash-welded seam. The rupture occurred at a hoop stress level of 87.8 percent of SMYS. The initiating defect was an OD-connected hook crack several inches long that penetrated 50 percent of the wall thickness as shown in Figure 89. Other figures (Figure 90 and Figure 91 provided in the contributed report suggest that while the hook crack was indeed the primary cause of failure, the crack growth mechanism was probably stress corrosion cracking rather than fatigue.

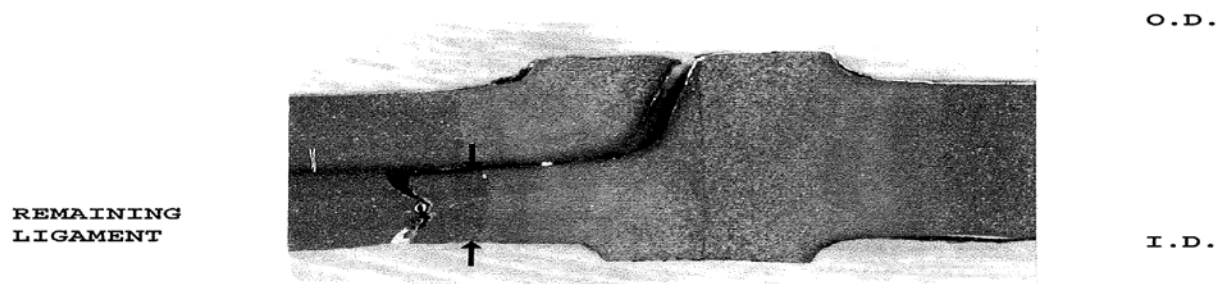


Figure 89. Cross Section of Fatigue Case Number 23 Anomaly



Figure 90. One Fracture Surface of the Anomaly that Raises Doubts about Fatigue Being the Crack Growth Mechanism

**SURFACE
CRACKS**

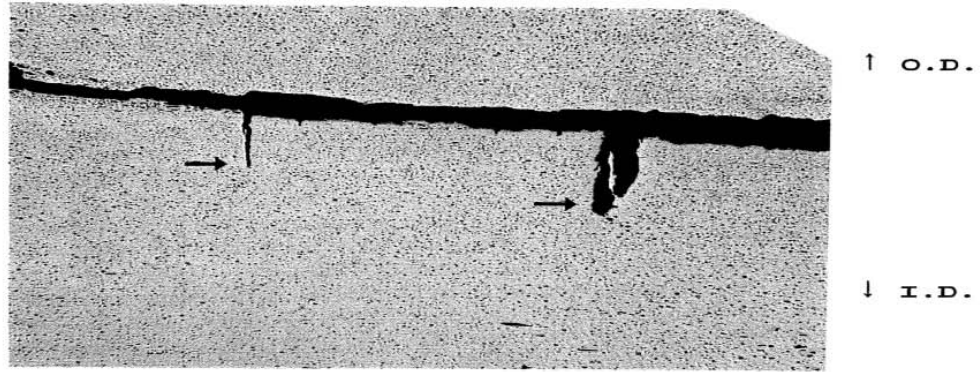


Figure 91. A Metallographic Section that Raises Doubts about Fatigue Being the Crack Growth Mechanism

Fatigue Case Number 24

Fatigue Case Number 24 involved an in-service leak in a 26-inch-OD, 0.281-inch-wall, X52 pipe with a flash-welded seam. The hoop stress level at the time the leak was discovered was 55.7 percent of SMYS. The initiator was an ID-surface-connected hook crack. This hook crack was about three inches long and penetrated less than 25 percent of the wall thickness. However, hook cracks on different planes over-lapped both ends of the hook crack that leaked, probably facilitating the fatigue crack growth (see Figure 92). Five years prior to the leak, the location of the leak had been subjected to a hydrostatic test to 87.6 percent of SMYS.

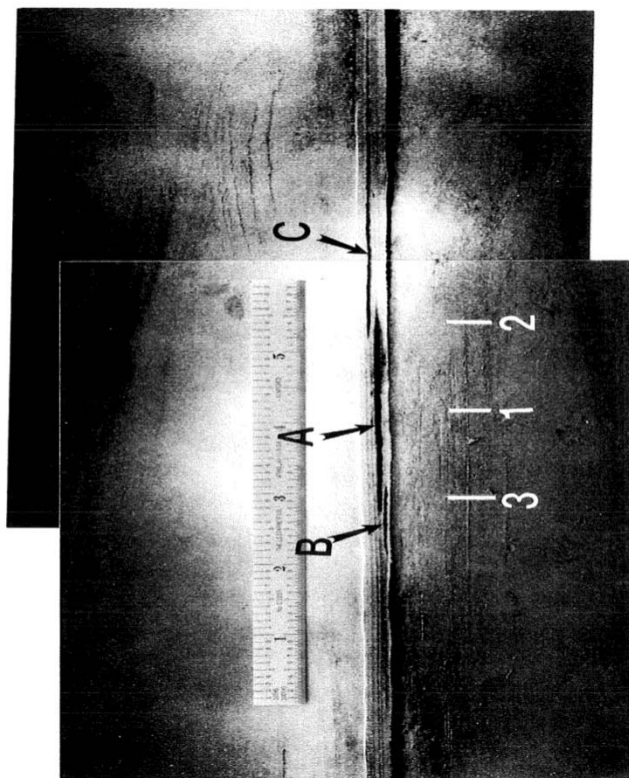


Figure 92. Pipe Surface Showing Anomalies in the Flash-Welded Seam of the Pipe in Fatigue Case Number 24

Fatigue Case Number 25

Fatigue Case Number 25 involved an in-service leak in a 34-inch-OD, 0.281-inch-wall, X52 pipe with a flash-welded seam. The hoop stress level at the time the leak was discovered was only 12.8 percent of SMYS. However, the location had experienced stress levels as high as 72 percent of SMYS. Twenty-eight years prior to the leak, the pipe had experienced a hydrostatic test to a stress level of 94 percent of SMYS.

The fracture surfaces of the leak, after they had been exposed by chilling and breaking the sample revealed an ID-surface connected hook crack which initiated fatigue crack growth. Ratchet marks and beachmarks typical of fatigue crack growth were clearly visible on the fracture. The hook crack and the fatigue crack were within the raised flash of the seam but not in the centerline of the seam.

The initiating hook crack has an overall length of 4.5 inches and penetrates 33 percent of the 0.355-inch thickness of the flash at the deepest point. Using the Modified Ln-Sec RECTANG model with a flow stress of 66,500 psi and the base metal full-size Charpy upper shelf energy of 43 ft lb, one would predict the failure pressure of the hook crack by itself to be 1200 psig. This

pressure level corresponds to 140 percent of SMYS for the nominal 0.281-inch-thick pipe. So, the initiating hook crack would easily have survived any feasible level of hydrostatic testing.

Fatigue Case Number 26

Fatigue Case Number 26 involved an in-service rupture in a 20-inch-OD, 0.219-inch-wall, X52 pipe with a high-frequency-welded seam. The rupture of this defect occurred at a hoop stress level of 54.3 percent of SMYS. The initiating defect was a hook crack with a length of 9 inches that penetrated 30 percent of the wall thickness at the deepest point. The hook crack had survived a prior hydrostatic test to 91.1 percent of SMYS 34 years before it failed in service.

Using the Modified Ln-Sec RECTANG model with a flow stress of 69,500 psi and the base metal full-size Charpy upper shelf energy of 32 ft lb, one would predict the failure stress for the hook crack by itself to be 94.4 percent of SMYS. So, the initiating hook crack could have survived the 1974 hydrostatic test.

The fatigue portion of the defect grew over a length of 4.5 inches along the hook crack to a final depth of 95 percent of the wall thickness. On the basis of the Modified Ln-Sec EllipticalCEQ model with a flow stress of 69,500 psi and a full-size-equivalent Charpy upper shelf energy of 32 ft lb, one predicts that the hook crack plus fatigue crack would fail at 15.5 percent of SMYS. The actual failure stress of 54.3 percent of SMYS is 3.5 times this predicted value.

Fatigue Case Number 27

Fatigue Case Number 27 involved an in-service rupture in an 18-inch-OD, 0.219-inch-wall, X52 pipe with a DC-welded seam. The rupture of this defect occurred at a hoop stress level of 60.9 percent of SMYS. The defect had survived a prior hydrostatic test to 90.1 percent of SMYS 21 years before it failed in service. The initiator of the fatigue crack was a 27-inch-long damaged edge that left 46 percent of the wall thickness missing. The nature of the missing metal is shown in Figure 93. An 8.5-inch-long fatigue crack had propagated to a total depth (missing metal plus crack) of 86 percent of the wall thickness. This anomaly apparently was not identified as a serious anomaly during an ultrasonic crack-detection tool run a few months before the failure.

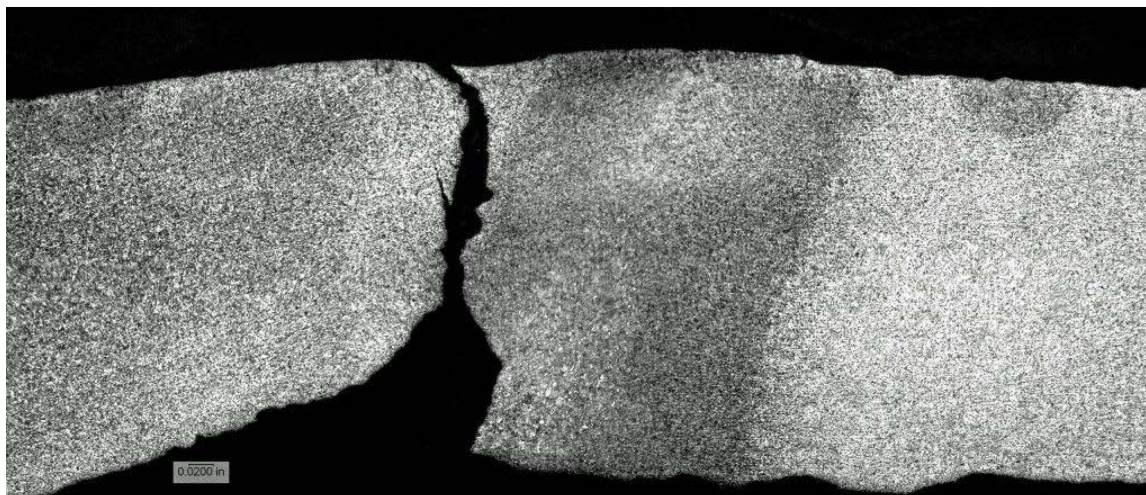


Figure 93. Cross Section of Fatigue Case Number 27 Anomaly

Using the Modified RECTANG model with the missing metal length of 27 inches and depth of 46 percent of the wall, a flow stress of 70,000 psi, and the base metal full-size Charpy upper shelf energy of 44 ft lb, one would predict the failure stress of the missing metal to be 71 percent of SMYS. This suggests that the initial mill anomaly would not have survived the mill test to 85 percent of SMYS. A benchmark for the actual properties in the zone where the missing metal existed (heat-affected material near the seam) is that if the flow stress is assumed to be 90,000 psi, the Modified Ln-Sec RECTANG model would predict that the hook crack would have survived the mill hydrostatic test.

If one applies this flow stress to the fatigue crack and utilizes its length, the results are as follows.

Using the Modified Ln-Sec Elliptical C-equivalent model with the flaw length of 8.5 inches and depth of 86 percent of the wall for the combined missing metal and fatigue crack depth, a flow stress of 90,000 psi, and the base metal full-size Charpy upper shelf energy of 44 ft lb, one would predict the failure stress of the anomaly to be 31.9 percent of SMYS. This level is quite a bit below the actual failure stress level of 60.9 percent of SMYS.

Fatigue Case Number 30

Fatigue Case Number 30 involved an in-service rupture in a 24-inch-OD, 0.328-inch-wall, X70 pipe with a high-frequency-welded seam. The rupture of this defect occurred at a hoop stress level of 69.6 percent of SMYS. The defect had survived a pre-service hydrostatic test to 96 percent of SMYS 9 years before it failed in service. The initiator of the fatigue crack was a lack of fusion defect, the original dimensions of which were unavailable. This case is significant for two reasons. First, it is the only fatigue case in the database where a lack of fusion (i.e., cold

weld) served as a fatigue initiator. Second, the material was of recent vintage, having been manufactured in 1998. The base metal was a micro-alloyed X70 material with a full-size-equivalent Charpy upper shelf energy of 116 ft lb. The measured full-size equivalent Charpy upper shelf energy for the weld metal was 137 ft lb.

Fatigue Case Number 36

Fatigue Case Number 36 involved a leak during a hydrostatic test of a 26-inch-OD, 0.281-inch-wall, X52 pipe with a flashed-welded seam. The leak was detected at a hoop stress level of 100.0 percent of SMYS. The leak developed as the result of fatigue crack growth from a 2-inch-long, ID-surface-connected hook crack that penetrated about 27 percent of the 0.355-inch-thick raised portion of the flash-welded seam. The leak was broken open to reveal classic macro characteristics of fatigue crack propagation (ratchet marks and beach marks). These features are shown in Figure 94 and Figure 95. The propagation path through the raised flash is shown in Figure 96.

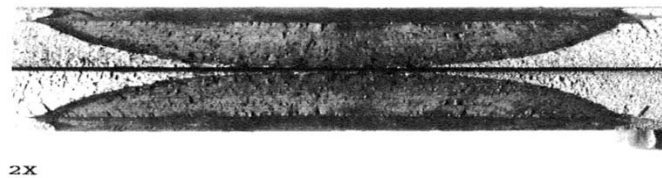


Figure 94. Fracture Surface of Fatigue Case Number 36 Anomaly

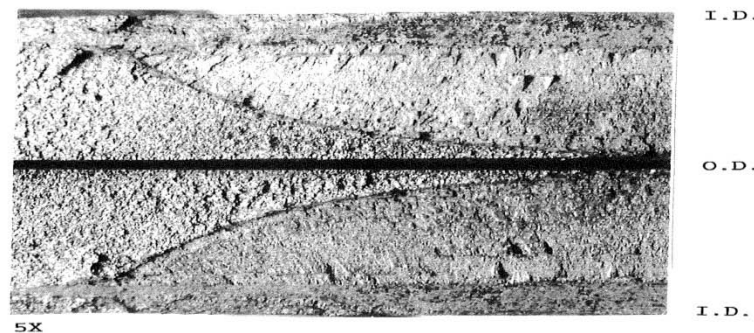


Figure 95. Close-up of Fracture Surface Showing Ratchet Marks and Beach Marks

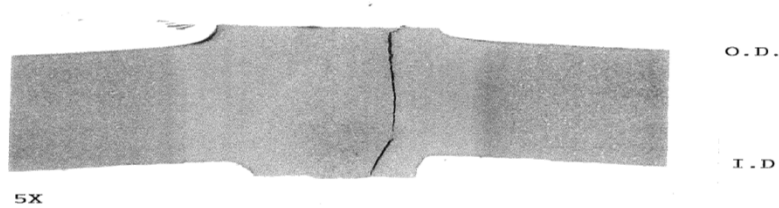


Figure 96. Cross Section of Fatigue Case Number 36 Anomaly

Fatigue Case Number 37

Fatigue Case Number 37 involved an in-service rupture in a 20-inch-OD, 0.230-inch-wall, X52 pipe with a DC-welded seam. The rupture of this defect occurred at a hoop stress level of 70.8 percent of SMYS. The defect had survived the pre-service hydrostatic test to 92.8 percent of SMYS 25 years before it failed in-service. The initiator of the fatigue crack growth was a mismatched edge that left as little as 62 percent of wall thickness remaining in places. The overall length of the mismatch was 12 inches, but the net wall thickness of the pipe was affected significantly over a distance of about 6.5 inches. A 3.40-inch-long fatigue crack had propagated to a total depth (mismatched edge plus fatigue) of 86 percent of the wall thickness.

Using the Modified Ln-Sec Elliptical C-equivalent model with the initial mismatch length of 6.5 inches and depth of 38 percent of the wall thickness, a flow stress of 67,000 psi, and the base metal full-size Charpy upper shelf energy of 36 ft lb, one would predict the failure stress of the pipe with the mismatched edge by itself to be 95.5 percent of SMYS. Thus, the mismatch would have been expected to survive the pre-service test to 92.8 percent of SMYS.

Using the Modified Ln-Sec Elliptical C-equivalent model with the fatigue crack length of 3.4 inches and depth of 86 percent of the wall for the combined missing metal and fatigue crack depth, a flow stress of 67,000 psi, and the base metal full-size Charpy upper shelf energy of 36 ft lb, one would predict the failure stress of the anomaly to be 46.4 percent of SMYS. This level is quite a bit below the actual failure stress level of 70.8 percent of SMYS.

Summary of Fatigue Failures

The fatigue failure cases show that fatigue-enlargement of various ERW and flash-welded seam manufacturing defects is a threat to the integrity of some liquid pipelines. The threat is believed to arise from the aggressive pressure cycling experienced in liquid pipelines that does not exist in gas pipelines. Addressing this threat by either using ILI crack-detection tools or hydrostatic testing seems possible, but there are problems associated with these integrity assessment tools. In the case of ILI, two in-service failures (Cases 11 and 25) occurred in spite of quite recent ILI crack-tool runs. The reliability of ILI crack-tools needs to be assessed and improved if

necessary. The state of the art in ILI crack-tool assessment is to be discussed in the Subtask 1.3 report.

In the case of hydrostatic testing, in-service failures have occurred after a test at surprisingly short times (within 3 years in Case 7, within 5 years in Case 22). The use of hydrostatic testing to address pressure-cycle-induced fatigue requires that the retest interval be short enough to prevent such occurrences. As stated previously, the Fessler-Rapp model for predicting retest intervals is suitable for use with crack growth mechanisms such as SCC and selective seam weld corrosion where it is reasonable to assume that crack growth rates are constant. However, the Fessler-Rapp model is not appropriate for predicting retest intervals for fatigue crack growth because fatigue crack growth is non-linear with time (the crack depth increases at an accelerating rate). Instead, Paris-Law⁵ crack growth modeling is typically used to determine retest or re-inspection intervals for fatigue crack growth because it does account for the accelerating growth. The success of this modeling depends on knowledge of starting flaw sizes, the effective flow stress and toughness of the material local to the crack initiator, applicable pressure-cycle-spectra, and accurate fatigue crack growth rates. Operators do use such modeling with success in many cases as will be seen in the Subtask 1.2 report.

Other Cracking

Examples of three causes of ERW seam failures resulting from cracking other than fatigue crack growth appear in the database. These other causes include a hook crack where sulfide stress cracking took place, hook cracks where SCC had taken place, and a hook crack where a failure from hydrogen induced cracking occurred. In fact, another case of failure from a hook crack where SCC had taken place was identified previously under Fatigue Case Number 21. The report of the contributor identified the cracking as fatigue, but pictures of the cracks shown in Figure 89 through Figure 91 strongly suggest that SCC, not fatigue, was the cause of the crack growth in-service.

The cases of other cracking (OC) in the database are discussed individually below.

OC Case Number 1 (Hook Crack + Sulfide Stress Cracking)

The pipe in which the leak occurred is 22-inch-OD, 0.250-inch-wall, Grade X45 line pipe manufactured with a flash-welded longitudinal seam. The pipeline carried natural gas throughout its time in service. The pipe was manufactured just prior to the first tentative standard for X-grade pipe, Tentative Standard API STD 5LX, First Edition, February 1948. However, it was common practice for manufacturers in the period just prior to the issuance of the first standard for X-graded pipe to follow the requirements of the planned-for tentative STD 5LX when manufacturing an X-grade material. So, it is assumed that with respect to the tensile

strength, chemical content, and mill test pressure requirements, this X-grade line pipe material made in 1947 would have been expected to conform to the requirements of Tentative Standard API STD 5LX, First Edition, February 1948. According to the latter, the minimum hydrostatic test for each piece of pipe of this size would have been carried out at a stress level not less than 85 percent of SMYS.

This leak appears to have been caused by sulfide-stress crack growth that started from a hook crack. A picture of the hook crack and the sulfide-stress crack as they appeared when the sample was chilled and broken is shown in Figure 97. A metallographic section across the leak is shown in Figure 98.

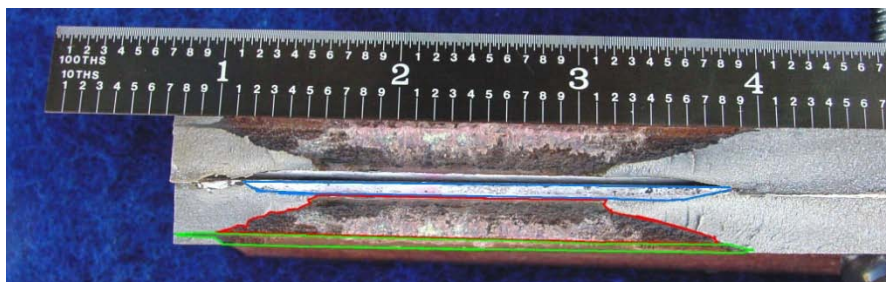


Figure 97. Fracture Surfaces of the Sulfide Stress Cracking that Took Place at an ID-Surface-Connected Hook Crack

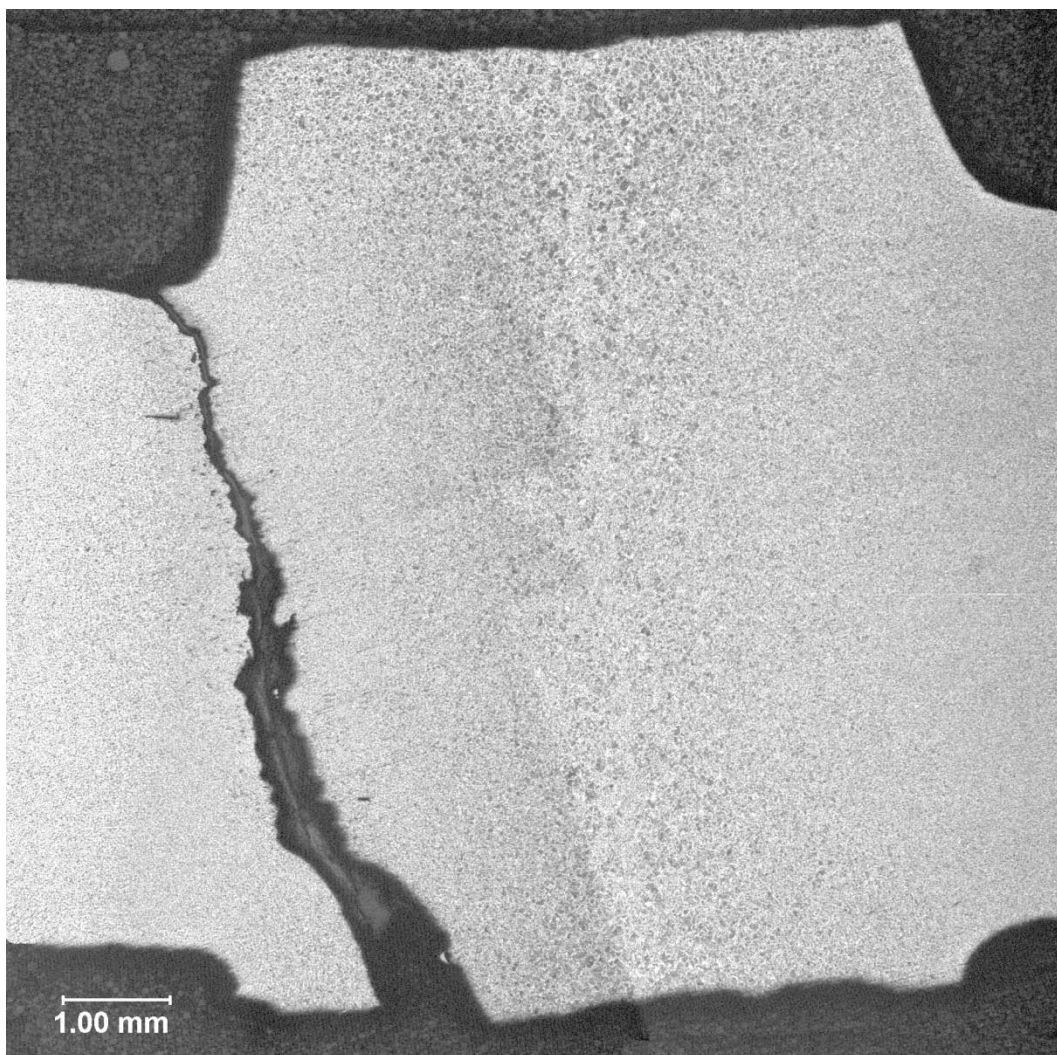


Figure 98. Metallographic section across the weld showing the various stages of cracking

The original hook crack, though relatively small, was large enough to have warranted rejection according to the workmanship standards of API Specification 5L. However, it likely was not detected because it was too small to have caused a failure during the manufacturer's hydrostatic test. Visual inspection clearly could not have detected the hook crack either, because the hook crack was ID-surface connected. The hook crack likely would not have failed in a pre-service hydrostatic test even if that test had been carried out at a pressure level corresponding to 100 percent of SMYS because of its relatively small size.

The sulfide-stress cracking was facilitated by the microstructural properties of the heat-affected zone of the flash-welded seam (i.e., microstructural morphology and microhardness) and the internal environment of the pipeline. Sulfide-stress cracking in line pipe typically occurs near welds where unfavorable microstructures are sometimes present in the heat-affected zones, if and when there is hydrogen sulfide present in the flowing medium.⁶ Without knowing the gas

composition that existed over the years, one cannot say how that hydrogen sulfide came to be present. It could have arisen from wet, sour gas or from natural or intentionally added mercaptans. In any case, the presence of a deposit of what appears to be elemental sulfur within the crack and the presence of a corrosion product on the crack surfaces and the ID surface of the pipe strongly suggest that the required crack-inducing environment existed at some time in the past.

OC Case Number 2 (HC+SCC)

OC Case Number 2 involved a 6.625-inch-OD, 0.125-inch-wall, X60, high-frequency-welded pipe manufactured by Tex-Tube in 1982. The pipeline was in liquid service. The failure mode was a rupture that occurred during a hydrostatic test at a hoop stress level of 83.9 percent of SMYS. The anomaly had survived a hydrostatic test to 99.8 percent of SMYS 24 years prior to the hydrostatic test rupture. The OD surface of the pipe was clearly affected by SCC. A metallographic section across the origin of the failure is shown in Figure 99. The failure appears to have begun at an SCC crack and propagated through the thickness apparently by ductile tearing toward a large embedded hook crack. The hook crack apparently raised the hoop stress sufficiently to promote the SCC at that particular location.

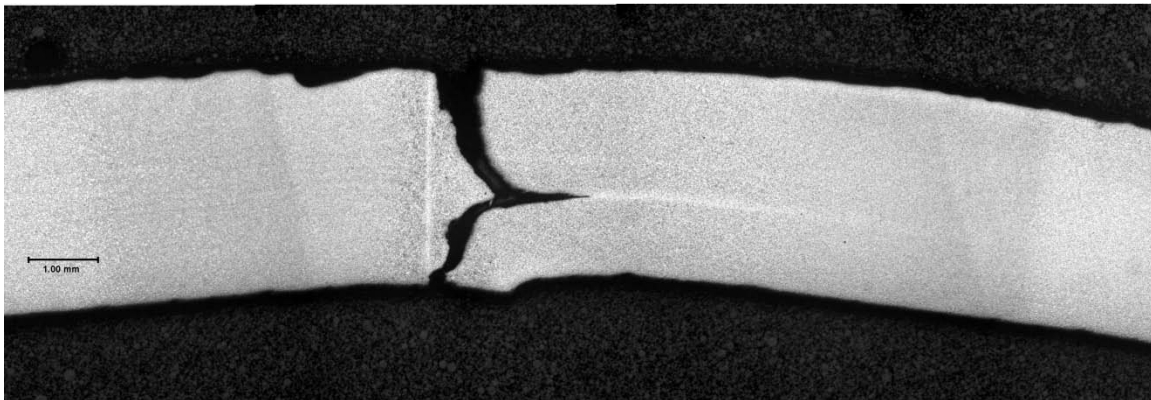


Figure 99. Combination of SCC and Hook Crack the Caused a Hydrostatic Test Rupture

OC Case Number 3 (Hook Crack + SCC)

OC Case Number 3 involved a 10.75-inch-OD, 0.188-inch-wall, X52 high-frequency-welded pipe manufactured by Republic in 1970. The failure mode was a leak in-service discovered while the pipeline was being operated at a hoop stress level of 40 percent of SMYS. The anomaly had survived a hydrostatic test to 90 percent of SMYS 7 years prior to the discovery of the leak, and it had survived a mill test to a stress level of 85 percent of SMYS. The through-wall anomaly was about 0.5 inch long. A picture of the fracture surfaces of the leak after it had been chilled and broken open is shown in Figure 100. The leakage path exists between an OD-surface-connected hook crack and an ID-surface-connected hook crack and is coated with rust.

The irregular black-coated cracks nearby that penetrated from the OD hook crack are believed to have been caused by SCC, and by inference, the cracking that joined the OD and ID hook cracks is believed to have been SCC.



Figure 100. Fracture Surface Showing SCC on the Same Plane as Hook Cracks

OC Case Number 4 (Hydrogen Induced Cracking)

OC Case Number 4 involved a 22-inch-OD, 0.344-inch-wall, X46, DC-welded pipe manufactured by Youngtown in 1949. The failure mode was a rupture that occurred in-service at a hoop stress level of 57.5 percent of SMYS. The anomaly had survived a hydrostatic test to 82 percent of SMYS 11 years prior to the failure, and it had survived a mill test to a stress level of 85 percent of SMYS in 1949. The failure origin coincided with a hook crack that was about 0.6-inch long and penetrated about 16 percent of the wall thickness. The fracture surfaces are shown in Figure 101 and a metallographic section prepared through the origin is shown in Figure 102.

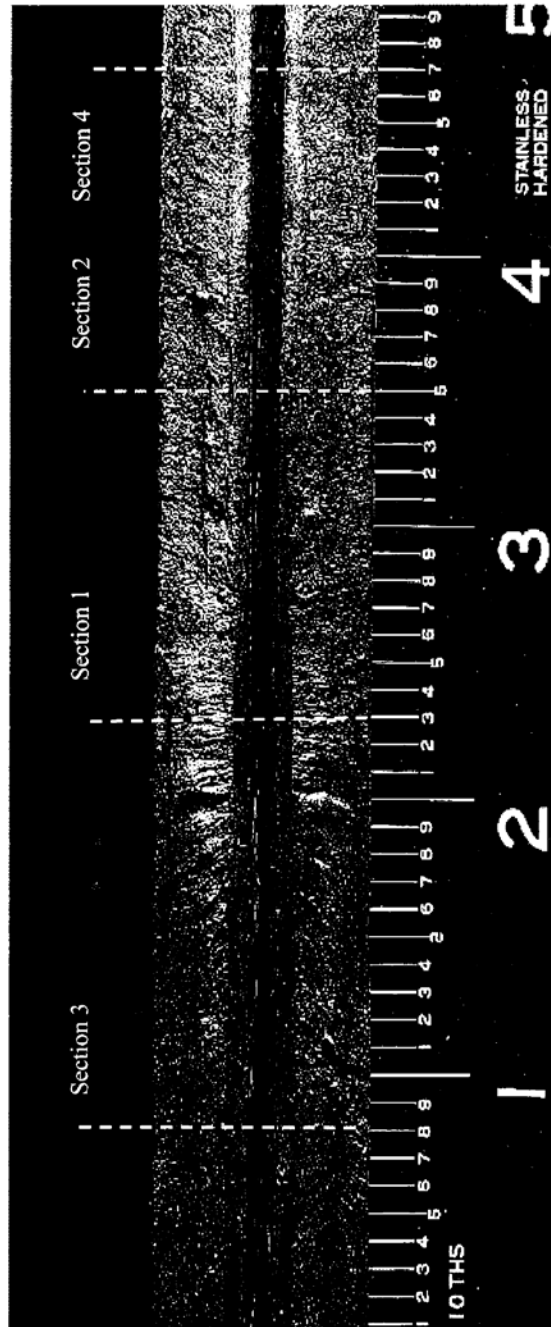


Figure 101. Fracture Surface Showing Markings Indicating the Origin to be a Small Hook Crack

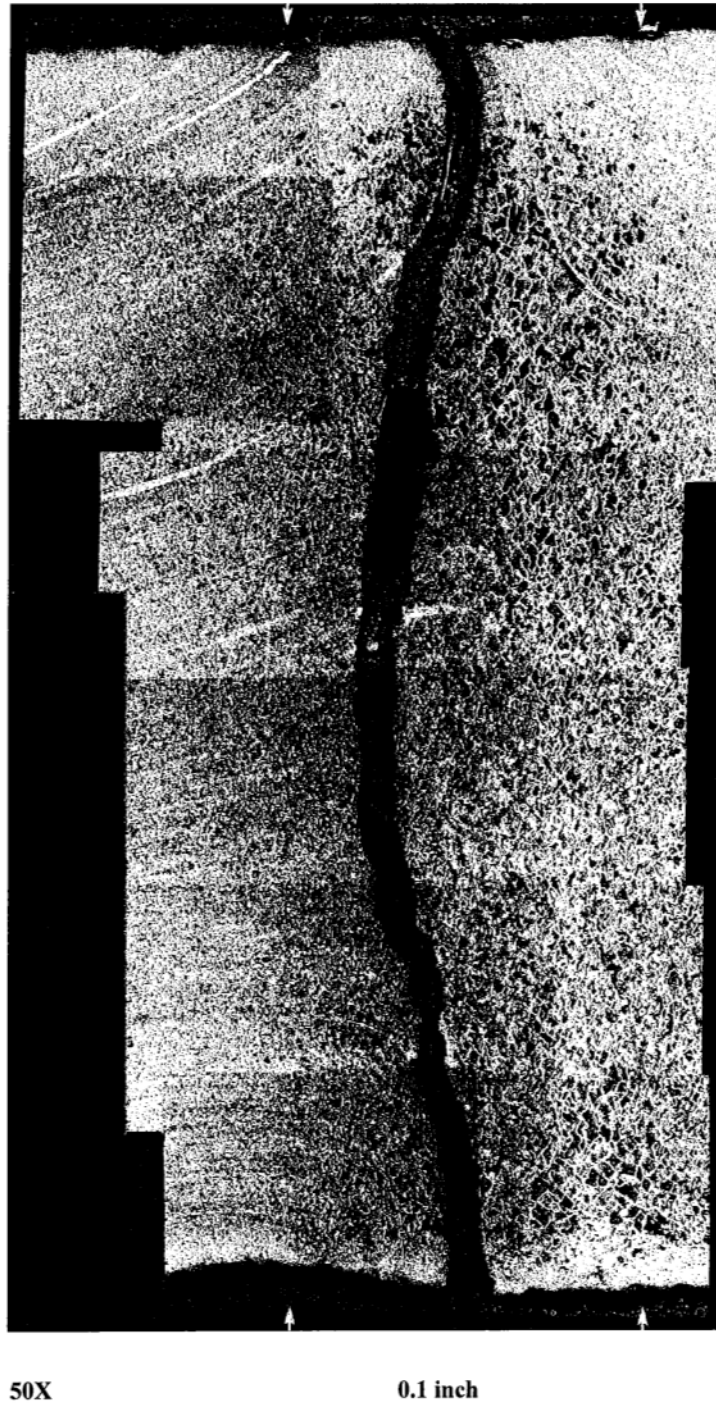


Figure 102. Metallographic Section across the Fracture

The small hook crack by itself probably would not have caused a fracture let alone a ductile fracture at a hoop stress level of 57.5 percent of SMYS. The hook crack resides, however, in a zone of material with hardness measured in the range of 35 to 45 Rockwell C. This situation is not unusual for 1949-vintage X-grade Youngtown pipe. What is believed to have happened here is the occurrence of a sudden hydrogen embrittlement failure with the hook crack providing the

stress concentration needed for the cracking to occur. Another clue that it was a hydrogen cracking phenomenon comes from the SEM image shown in Figure 103. This image shows the type of into-the-plane cracks that often characterize a hydrogen cracking failure.

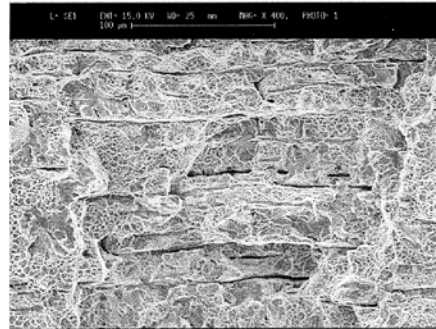


Figure 103. 400X SEM Image of Fracture Surface Showing Into-the-Plane Cracks often Associated with Hydrogen Embrittlement Cracking

Summary of Other Cracking Failures

The examples of other cracking shown herein represent fairly unique circumstances.. The combination of hook cracks and SCC can be worse than SCC alone, but if an SCC threat exists, that threat needs to be addressed in any case. The sulfide stress cracking in hard weld zones apparently happens only rarely, as there was only one case in the database. Lastly, the risk of hard heat-affected zone cracking associated with late 1940s through the 1950s Youngstown pipe has been known for some time. Operators who have that vintage of Youngstown pipe have to take steps to minimize the chances of atomic hydrogen being generated at the ID surface of the pipe from internal sour components or from excess cathodic protection at the OD surface. It is noted that neither hydrostatic testing nor ILI would be of any use in preventing such failures. Neither technique will find the very small flaws of the type that initiated the observed failure. The hydrogen cracking itself can occur suddenly and unpredictably, so rational timing of tests or inspections is impossible.

Miscellaneous Causes

Fourteen failures of ERW and flash-welded seams were attributed to various causes that apparently did not involve defect growth in-service. All fourteen occurred during hydrostatic tests. None were in-service failures. The pipe attributes associated with the failures from Miscellaneous Causes are listed in Table 23. The failure stress levels and test histories associated with these failures are shown in Table 24.

Table 23. Pipe Attributes and Primary Causes of Failure for Miscellaneous Causes

Miscellaneous Case Number	Database Number	Liquid/Gas	Pipe OD, inches	Pipe WT, inch	SMYS, psi	Type of Seam	Manufacturer	Primary Failure Cause
1	39	HVL	12.75	0.25	52,000	ERW - LF	Lone Star	Unbonded layer
2	56	Liquid	6.625	0.125	60,000	ERW - HF	TexTube Pipe Corp.	Weld inclusions
3	59	Liquid	20	0.312	42,000	ERW - DC	Youngstown	Hot Tear Cracks
4	60	Liquid	20	0.312	42,000	ERW - DC	Youngstown	Weld Flash
5	62	Liquid	20	0.312	42,000	ERW - DC	Youngstown	Weld inclusions
6	74	Liquid	16	0.25	52,000	ERW - DC	Youngstown	Contact Burn
7	106	Liquid	12.75	0.25	46,000	ERW - LF	Republic	Lamination + Hook Crack +Cold Weld
8	194	Liquid	12.75	0.25	52,000	ERW - LF	Lone Star	Weak Plane
9	196	Liquid	12.75	0.25	52,000	ERW - LF	Lone Star	Weak Plane
10	226	Liquid	5.564	0.25	35,000	ERW - LF		LOF defect SW, HAC RW
11	232	Gas	12.75	0.219	52,000	ERW - HF	Tenaris Prudential	foreign material in weld
12	233	Gas	12.75	0.219	52,000	ERW - HF	Tenaris Prudential	foreign material in weld
13	262	Liquid	20	0.312	52,000	Flash-weld	A.O. Smith	Dent and Hook crack

Table 24. Failure Stress Levels and Test Histories Associated with Miscellaneous Causes

Miscellaneous Case Number	Primary Failure Cause	Failure Mode	Failure Pressure, %SMYS	Pressure in last hydrostatic test, % SMYS	Date_last_hydro	Pipe Vintage	Mill Test Pressure, SMYS	Failure Pressure less than Mill Test Pressure
1	Unbonded layer	Rupture	89.8			1961	85	no
2	Weld inclusions	Rupture	101.1	99.8	1983	1983	100	no
3	Hot Tear Cracks	Rupture	85.9	74.4	1991	1944	85	no
4	Weld Flash	Rupture	92.0	76.6	1991	1944	85	no
5	Weld inclusions	Rupture	78.7	73.0	1991	1944	85	yes
6	Contact Burn	Rupture	96.2	85.4	1991	1954	85	no
7	Lamination + Hook Crack +Cold Weld	Leak	94.4	94.2	1999	1958	85	no
8	Weak Plane	Rupture	97.0	91.8	2004	1961	85	no
9	Weak Plane	Rupture	91.1	91.6	2004	1961	85	no
10	LOF defect SW, HAC RW	Leak	68.8			1938	45.7	no
11	foreign material in weld	Leak	0.0			2009	85	yes
12	foreign material in weld	Leak	61.6			2009	85	yes
13	Dent and Hook crack	Leak	138.7			1950s	90	no

Failures occurred at low stresses in only three cases: Cases 5, 10, 11 and 12. In Cases 5, 11, and 12 the failures occurred at stress levels below the mill test stress levels. Note that the leaks in Cases 11 and 12 occurred in one lot of new pipe at the time it was subjected to a pre-service hydrostatic test. The cause in both cases was foreign material in the seam. These anomalies probably passed the mill test because of its short duration. The anomaly associated with Case 11 apparently was leaking even before the field test started. The Case 10 anomaly involved a repair weld apparently made by the pipe mill which many operators do not permit and have never permitted for ERW seams.

The contributor's report on the Case 5 failure reveals that the fracture was quite brittle and that the origin was confined by chevron marks possibly pointing to a cold weld region near the ID surface with a length and depth considerably less than the thickness of the pipe. As mentioned under the discussion on cold welds, large pressure reversals seem more probable when brittle fracture initiation is involved. So this case appears to belong in the category of cold welds.

Case 13 involved a dent and a hook crack that failed at 138.7 percent of SMYS. This does not seem like a circumstance worthy of a lot of concern.

Case 6, the contact burn is the only failure of its type in the database. The pipe was Youngstown pipe which is known for having contact burns with deep rounded grooves created by melting. In this case the burn ran at least 7 inches along the axis and penetrated to a depth of more than 15 percent of the wall thickness. Its failure during a test at 96.2 percent of SMYS is not a cause for concern.

The remainder of the miscellaneous anomalies failed at sufficiently high stress levels that they should not be of much concern.

DISCUSSION

Analysis of the 280 seam failures in the database produced the following findings. The types of ERW and flash weld anomalies that have caused failures in-service and/or during hydrostatic tests are:

- Cold Welds (99 cases)
- Penetrators (8 cases)
- Hook Cracks (76 cases)
- Cold Weld, Hook Crack Combinations (5 cases)
- Stitching (7 cases)
- Woody Fracture (6 cases)
- Selective Seam Weld Corrosion (24 cases)
- Fatigue Enlargement of Seam Defects (37 cases)
- Other Cracking (4 cases)
- Miscellaneous (14 cases)

The failure circumstances of some of these types of anomalies have important implications for pipeline integrity, and for the manner in which the remaining strength of the pipe is calculated. The failure circumstances of other types of anomalies suggest that they can be expected to have little or no impact on pipeline integrity. The details of these findings are as follows.

Cold Welds and Penetrators

The failure circumstances of 99 cold welds and 8 penetrators (essentially a short, through-wall cold weld) were examined. These anomalies were characterized by no apparent crack extension from in-service pressure cycles or from tearing during a hydrostatic test. In fact, however, it can be inferred from the circumstances of some of the failures that some of these anomalies had sustained damage either from in-service pressure cycles or from hydrostatic tests conducted prior to their failing. The findings regarding these kinds of anomalies are as follows.

In-Service Leaks

Sixteen cold welds and five penetrators that caused leaks in operating pipelines within their normal operating pressure ranges were through-wall defects as-manufactured. All had survived manufacturers' hydrostatic tests and, in some cases, even higher-stress levels during in-situ hydrostatic tests. Two scenarios are presented to explain how these defects became leaks.. The first scenario is that the leak path was initially plugged with the oxide formed at high-temperatures immediately after welding (Fe_3O_4). As long as this oxide remained competent and bonded to the metal, the leakage path was blocked. The oxide could have been degraded by oxidation to a less-competent oxide or, more likely, a hydrostatic test stretched the anomaly open sufficiently to break the bond between the oxide and the metal allowing leakage.

The second scenario is that leakage only occurred at a threshold stress level, below which residual compressive stresses kept the crack faces leak-tight. Very small leaks may not be detected during a hydrostatic test, and if a change in operation occurred such that the threshold stress level is met as result of increasing operating pressure, then a slow leak may eventually be detected.

In either case, the hydrostatic tests were applied at insufficient stress levels to cause these anomalies to be detected even though the tests in most cases were to stress levels above 85 percent of SMYS. It can be argued in some cases that the tests actually contributed to the formation of the leaks. Since test stress levels are inherently limited by the need to avoid expanding or bursting sound pipe, it is possible for small cold welds or penetrators to remain after a test even to a level of 100% of SMYS. While the rupture of such a defect at stress levels at or near an operating stress as high as 72% of SMYS is practically inconceivable following a test to a stress level in the 90 to 100% of SMYS range, there is no guarantee that such an anomaly will not leak. So, hydrostatic testing cannot be relied upon to eliminate this threat. Within the current state of the art in ILI crack detection, it is likely that these kinds of anomalies are too short to be reliably detected and repaired.

In-Service Ruptures

Seven cold welds caused ruptures at stress levels in the range of 51 to 71 percent of SMYS. These anomalies had previously survived manufacturers' hydrostatic tests at stress levels of 75 or 85 percent of SMYS. No evidence of crack growth had been identified in conjunction with these anomalies. An explanation for these failures is that they represent pressure reversals. Pressure reversals arise from some form of damage to an anomaly, if not physical crack extension, during a previous exposure to a stress level higher than the observed failure stress level. Another explanation is that an upset condition occurred and a pressure surge was sent through the pipeline but the pressure-recording equipment was not capable of responding fast enough to document the pressure excursion.

Ruptures and Leaks at Stress Levels above Operating Stress Ranges

Thirty-five of the 99 cold weld anomalies leaked or ruptured at hoop stress levels ranging from 85 to 100 percent of SMYS. A useful implication of these results is that hydrostatic testing to stress levels of 90 percent of SMYS or more can eliminate many cold weld defects that have not ever experienced stress levels that high. That implies that pipelines that have been tested to such levels are less likely to exhibit an in-service rupture from a cold weld anomaly. That does not change the fact discussed above that hydrostatic testing is not expected to prevent leaks from short through-wall cold welds or penetrators.

Failure Stress Prediction

Where dimensions of non-through-wall cold welds were determinable, predictions of the failure stress levels using a ductile crack initiation model (the Modified Ln-Sec model) gave unsatisfactory estimations of the actual failure pressures of most of the anomalies. In 16 of 27 cases the actual failure stress levels were less than 80 percent of the model-predicted failure stress levels. It should be noted that the other widely-used ductile fracture initiation models, API 579 Level II, PAFFC and CorLAS would be expected to produce predictions similar to that of the Modified Ln-Sec model, so it is not likely that these methods would give reliable predictions of the failure stress levels of most cold weld anomalies.

It is speculated that the reason for the inability of ductile fracture initiation models to reliably predict the failure stresses of cold welds is that most of the cold weld anomalies failed in a brittle manner. There was one case of a high-toughness, recent-vintage pipe (CW Case Number 15) that failed in a ductile manner. In this case the model appeared to give a good prediction of the actual failure stress when used in its rectangular shape mode. It predicted a failure stress of 49 percent of SMYS compared to the actual failure stress of 51 percent of SMYS.

The implication of the inability to predict the failure stress levels for most cold weld anomalies is that even if an ILI crack tool arises that can reliably find and characterize these types of anomalies, a reliable algorithm for calculating anomaly failure stress levels would have to be developed based on the seam-weld characteristics of the particular pipeline which would most likely entail small and full-scale testing. It is possible that a brittle fracture initiation model can do a better job of estimating failure stresses of cold weld anomalies in brittle ERW and flash welded seams, but that will depend on the ability to determine the effective toughness levels of the seams. These possibilities will be addressed under Subtasks 2.3 and 2.4.

Hook Cracks

The failure circumstances of 76 hook crack anomalies located adjacent to but not in the ERW and flash-weld bondlines were examined. Hook cracks were also implicated in 27 fatigue-related failures in the database. However, the ones identified only as hook cracks were characterized by no apparent crack extension from in-service pressure cycles or from tearing during a hydrostatic test. In fact, however, it can be inferred from the circumstances of the failures that some of these anomalies had sustained some damage either from in-service pressure cycles or from prior hydrostatic tests. The findings regarding these kinds of anomalies are as follows.

In-Service Ruptures

All but one of the 76 hook crack failures occurred during hydrostatic tests. As to whether the remaining hook crack failure was an in-service failure or a test failure was not stated by the contributor. However, because it failed at a hoop stress level of 56.6 percent of SMYS, it is reasonable to assume that it failed in-service. The information provided by the contributor suggests that the failure of the defect most likely was the result of crack extension from several large pressure applications leading to a pressure reversal. Hence, one could just as easily have placed this anomaly in the category of a seam defect having been enlarged by pressure-cycle-induced fatigue.

Hydrostatic Test Failures

Of the 75 hook cracks that failed in hydrostatic tests, 74 failed as ruptures, and only one failed as a leak. This was most likely the result of the hook cracks having been relatively long in order to fail at a stress level below 90 percent of SMYS. First, two-thirds of the hook cracks where depth was provided by the contributor had depths of 40 percent of the wall thickness or less. Secondly, the deepest part of a hook crack usually is the farthest from the bondline. Consequently, the tip of a hook crack resides in a material that tends to have properties more like the base metal than those of the bondline. These circumstances favor hook cracks failing at higher stress levels,

exhibiting more ductility in the process of failing than cold weld defects, and failing as ruptures rather than as leaks.

A few of the hook cracks failed in hydrostatic tests at stress levels more than 5 percent below those of the manufacturers' hydrostatic tests. Because the manufacturers' tests were of only 5 to 10-second duration, it is not a stretch to believe that a 5-percent pressure reversal would be fairly common for an anomaly that barely survives the mill test. When the failure stress level of a seam manufacturing defect is more than 5 percent below that of the mill test, it is reasonable to suspect that some factor in its test or service history has had an influence on its failure stress level even if direct evidence of such influence cannot be found. One such anomaly failed at 68 percent of SMYS (about 80 percent of the mill test pressure). This hook crack had undergone some ductile tearing before failing, but its final failure path involved a sideways jump from the ductile tearing to a brittle fracture in the bondline. It is considered significant that this behavior was similar to the fracture behavior of the hook crack that is believed by many to have been the origin of the November 1, 2007 failure of the Dixie Pipeline at Carmichael MS. The latter defect, if it was indeed the origin of the failure, failed at a hoop stress level of 80 percent of that of the hydrostatic test it had survived 23 years prior to its failing in service. The implication is that something changed in both situations over the period between the tests and the subsequent failures at much lower stress levels. Growth of the defects either by ductile tearing or pressure-cycle-induced fatigue is assumed to have occurred, and that growth may have facilitated the abrupt failure of the bondline in a brittle manner in both cases. Two additional hook cracks failed in hydrostatic tests at hoop stress levels more than 5 percent below those applied in previous hydrostatic tests (79 percent and 93 percent of the levels in previous tests). Except for the fact that both of these cases were associated with liquid pipelines, no additional information was provided about these anomalies. It is reasonable to speculate that some growth of these defects had taken place either as the result of pressure-cycle-induced fatigue or ductile tearing in a prior test possibly leading to the failure of the bondline via a sideways jump as was evident in the case described previously.

Twelve hook cracks failed in hydrostatic tests at stress levels ranging from 80.8 to 83.8 percent of SMYS, all at stress levels below their 85-percent-of-SMYS mill test levels and in two cases at stress levels below 85.2 and 88.3 percent of SMYS applied during in-situ hydrostatic tests. It is reasonable to speculate that these occurrences are attributable to pressure-cycle-induced fatigue or pressure reversals. Only one of these cases involved a gas pipeline, the other eleven cases involved liquid pipelines.

Ruptures at Stress Levels above the Mill Test Stress Levels

Fifty-nine of the 76 hook cracks failed at stress levels above the mill test stress levels. Most of these failed at the highest stress levels they had ever experienced. For the five that failed at stress levels below those of prior in-situ hydrostatic tests, the stress levels at failure ranged from 0.7 to 2.8 percent less than that of the previous test, all within the range commonly seen for pressure reversals during hydrostatic testing of existing ERW or flash-welded pipelines. A useful implication of these results is that hydrostatic testing to stress levels of 90 percent of SMYS or more can eliminate many hook cracks that have not ever experienced stress levels that high. That implies that pipelines that have been tested to such levels are less likely to exhibit an in-service rupture from a hook crack anomaly unless that anomaly becomes enlarged in service via pressure-cycle-induced fatigue.

Failure Stress Prediction

Where dimensions of hook cracks were determinable, predictions of the failure stress levels using a ductile crack initiation model (the Modified Ln-Sec model) with base metal strength and toughness were made. Calculations were made for 61 of the hook cracks. In 23 cases the predictions underestimated the actual failure stresses by factors ranging from 1.03 to 1.8 (unlike the predictions for cold welds). In these cases, especially for the large-ratio ones, the problem may be that the hook cracks were partly bonded in places and the defect size was overestimated. In 22 cases the actual failure stresses ranged from 0.57 to 0.94 percent of the predicted values. These cases are attributable to a variety of reasons including the failure involving a brittle region such as the bondline or a region of low toughness arising from clusters of inclusions. In any case, there was essentially no correlation between the predicted and the actual failure stress levels using the flow stresses and Charpy energy levels of the base metal. It should be noted that the other widely-used ductile fracture initiation models, API 579 Level II, PAFFC and CorLAS would be expected to produce predictions similar to that of the Modified Ln-Sec model, so it is not likely that these methods would give reliable predictions of the failure pressures of most hook crack anomalies.

The implication of the inability to predict the failure stress levels for hook crack anomalies is that even if an ILI crack tool arises that can reliably find and characterize these types of anomalies, a reliable algorithm for calculating anomaly failure stress levels would have to be developed based on the seam-weld characteristics of the particular pipeline which would most likely entail small and full-scale testing. It is possible that a brittle fracture initiation model can do a better job of estimating or at least providing a lower bound for the failure stresses of hook crack anomalies, but that will depend on the ability to determine the effective toughness levels of the materials in which hook cracks reside. These possibilities will be addressed under Subtasks .2.3 and 2.4.

Cold Weld + Hook Crack

The five cases involving a combination of a cold weld and a hook crack illustrate that such combinations constitute risks to pipeline integrity that are about the same as those posed by cold welds and hook cracks separately. Those risks include possible leaks and ruptures in service from service or test-induced defect growth, the inability to apply ductile fracture initiation models to the prediction of failure stress levels, and the possibility that brittle fracture initiation in the bondline will result in failures at relatively low stress levels associated with large pressure reversals. As with cold welds and hook cracks it would appear that hydrostatic testing to stress levels of 90 percent of SMYS or more can eliminate cold weld/hook crack combinations that have not ever experienced stress levels that high. This implies that pipelines that have been tested to such levels are less likely to exhibit an in-service rupture from a cold weld/hook crack anomaly unless that anomaly becomes enlarged in-service via pressure-cycle-induced fatigue.

Stitching

Seven failures in the database were said to have been caused by stitching. All 7 occurred at stress levels of 89.5 percent of SMYS or more. Stitching is a phenomenon associated with the fracture of low-frequency-welded ERW seams where the fracture surfaces exhibit a repetitive “stitch-like” pattern. The presence of stitching on a fracture surface is indicative of sub-optimum bonding. In the cases examined herein, it was not a threat to seam integrity. However, it is believed that stitching on occasion has been so severe as to have caused failures at stress levels below those of the stitched weld failures discussed herein.

Woody Fracture

Six failures in the database were said to have been caused by woody fracture. A woody fracture is indicative of an ERW seam region that is affected by clusters of inclusions and/or small discontinuous hook cracks. It describes the appearance of a fracture created in such a material. In the absence of some other defect such as a hook crack or a cold weld, woody fractures appeared in the database only in conjunction with hydrostatic test failures at stress levels of 94.7 percent of SMYS or more. Hence, woody fractures are not a threat to seam integrity.

Selective Seam Corrosion

Twenty-four failures in the database were caused by selective seam weld corrosion. Selective seam weld corrosion is a phenomenon where corrosion occurs at a higher rate in the bondline region of an ERW or flash-welded seam than in the surrounding base metal. Fourteen of the failures occurred in service, and the stress level in one case was only 7.3 percent of SMYS. Selective seam weld corrosion failures occurred in both gas and liquid pipelines. The ability of ILI tools to detect and characterize selective seam corrosion anomalies is currently not as reliable

as the detection and characterization of pipe body metal loss anomalies.. Therefore, if ILI is used to assess a potential selective seam weld corrosion problem, an adequate number of anomalies should be examined and characterized to establish confidence in the particular ILI tool. The use of ILI is complicated by the fact that neither the models normally used to predict the remaining strength of corroded pipe nor the models used to predict failure stress levels of cracks in ductile materials can be used to predict the failure stress levels of selective seam weld corrosion anomalies.

Hydrostatic testing, if used on a periodic basis, could prevent failures from selective seam weld corrosion, but the times to failure observed for some of the anomalies in the database suggest that the maximum rate of corrosion must be known for testing to be done at the required interval to be effective. The Fessler-Rapp approach to scheduling retests for controlling SCC is probably applicable for scheduling retests for selective seam weld corrosion because both SCC and selective seam weld corrosion are believed to occur at constant rates of growth.

Fatigue Enlargement of Seam Defects

Thirty-seven cases of failures from fatigue enlargement of ERW and flash-weld seam defects are represented in the database. All of these occurred in liquid pipelines; none occurred in a gas pipeline. Thirteen of the failures occurred in-service; 24 occurred in hydrostatic tests. Most of the fatigue cracks initiated at hook cracks (28 cases). Other fatigue initiators included mismatched edges (6 cases), one case of lack of fusion (a cold weld in a high-frequency-welded pipe), one case of a damaged edge, and one case where the initiator was referred to simply as an ID feature.

Pipeline operators who have identified fatigue enlargement of ERW seam defects as a threat to pipeline integrity manage the threat either by means of periodically running an appropriate ILI crack-detection tool or by conducting period hydrostatic tests. Scheduling of re-assessment for a fatigue threat is typically done using a “Paris-Law” model of fatigue crack growth where the fatigue crack growth rate is based on constants provided in API RP 579 or BS 7910 using actual pressure-cycle histories for the relevant pipeline. If the re-assessment technique chosen is ILI, failure stresses for the anomalies are routinely calculated based on the defect dimensions provided by the ILI vendor using a ductile fracture initiation model. The operator then responds accordingly if the calculated remaining strength endangers the pipeline immediately. The fact that the actual values of failure stress for the anomalies in the database were higher in most cases and sometimes much higher than the predicted failure stress levels suggests that this approach is reasonable. If hydrostatic testing is chosen as the re-assessment technique, a ductile fracture initiation model is typically used to predict the remaining life of the family of defects that could

barely have survived the test. That approach seems reasonable as well, given the fact the actual values of failure stress for the anomalies in the database were higher in most cases.

It was noted in the cases of two of the failures by fatigue enlargement, that ILI crack tools failed to identify the relevant anomalies as being significant. The reliability of ILI crack-tools needs to be assessed and improved if necessary. It was also seen that some of the fatigue-enlargement failures occurred at relatively short times (3 and 5 years) after a hydrostatic test. Therefore, it is necessary to determine and use the correct crack growth rate constants, the effective level of flow stress and toughness for the material, and representative pressure cycles in the analysis to determine the time at which the next test should be scheduled to prevent an in-service failure.

Other Cracking

Causes of failures categorized as “other cracking” included sulfide stress cracking starting at a hook crack in a flash-welded seam in a gas pipeline, two cases of SCC starting at hook cracks in ERW seams, and a case of hydrogen stress cracking starting at a small hook crack in the excessively hard heat-affected zone of a 1949-vintage Youngstown pipe. The sulfide-stress cracking incident was one of a kind. It occurred in a flash weld that had a slightly harder microstructure than normal. There is no reason to believe that this is a significant threat to pipeline integrity. Regarding the SCC/hook crack combinations, SCC was the dominant threat. Both of the pipelines in which these incidents occurred are known to be at risk from SCC. Therefore, these incidents should not be viewed as indicative of a new category of an ERW seam threat. Lastly, the hydrogen cracking risk with the Youngstown pipe of a certain vintage is a known risk. Failures of this type have occurred in the past, and the operators of pipelines with this type of pipe are usually alert to the need to mitigate atomic hydrogen generation.

Miscellaneous Causes

Thirteen (13) failures in the database were attributed to miscellaneous causes. Some, such as “unbonded layer”, “weld inclusions”, “hot tear cracks”, “lamination+hook crack+cold weld”, “LOF defect” and “weak planes” accounting for 8 of the failure,s can be expected to have effects similar to those of cold welds or hook cracks and can be classified as such for the purpose of seam integrity assessment. The fact that only 2 of these 7 anomalies failed at a stress level below the mill test pressure suggests that at least 5 of them were probably not significant anomalies in any case. Not enough information was available of the other two to warrant any assessment of their significance.

Neither the contact burn that failed at a hoop stress level of 96.2 percent of SMYS nor the “weld flash” the failed at a stress level of 92 percent of SMYS nor the dent plus hook crack that failed in a burst test at a stress level of 138.7 percent of SMYS can be considered as significant causes

of failure. The two cases of foreign material in the weld involved leaks in a pre-service hydrostatic test of 2009-vintage pipe. This is a pipe quality control issue, not an on-going seam integrity issue.

Significance of the Pipe Vintages Involved in the Failures

As discussed previously, the failure circumstances of four types of ERW and flash weld seam anomalies, cold welds, hook cracks, selective seam weld corrosion, and fatigue enlargement of seam defects are important from the standpoint of pipeline seam integrity. It is also important to look at the vintages of pipe involved in each of these types of failures because improvements in manufacturing processes over the years have had a significant influence on level of risk associated with particular vintages of pipe. Shown below are plots of year of manufacture for each of the four main causes of failure. Cold weld failures are shown in Figure 104, hook crack failures are shown in Figure 105, selective seam weld corrosion failures are shown in Figure 106, and failures of fatigue-enlarged ERW seam defects are shown in Figure 107. Note that the numbers of failures in the cold weld chart is less than the total number of cold weld failures because the vintage of the pipe was not given in three cases.

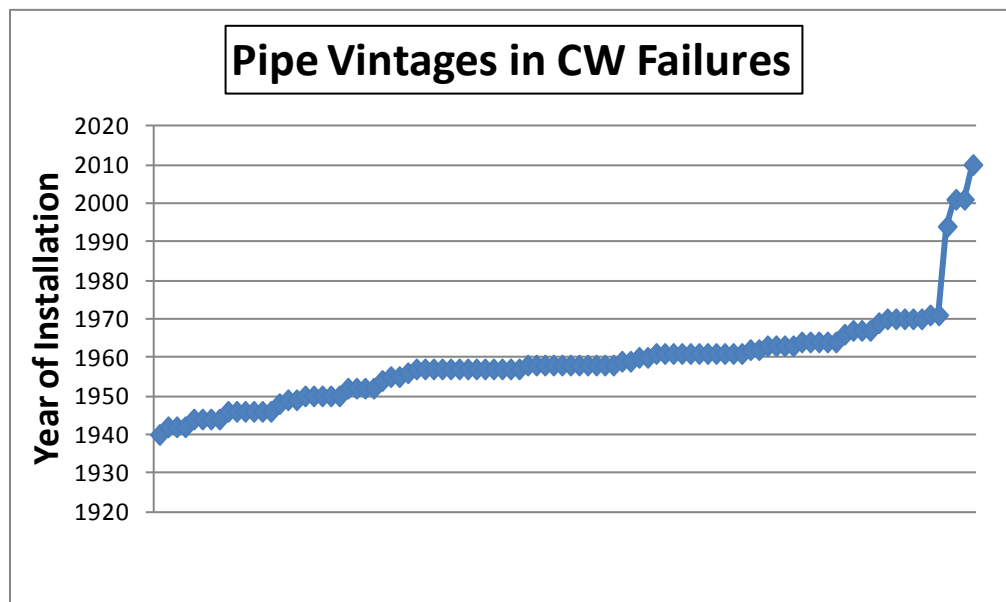


Figure 104. Pipe Vintages in Failures of Cold Welds

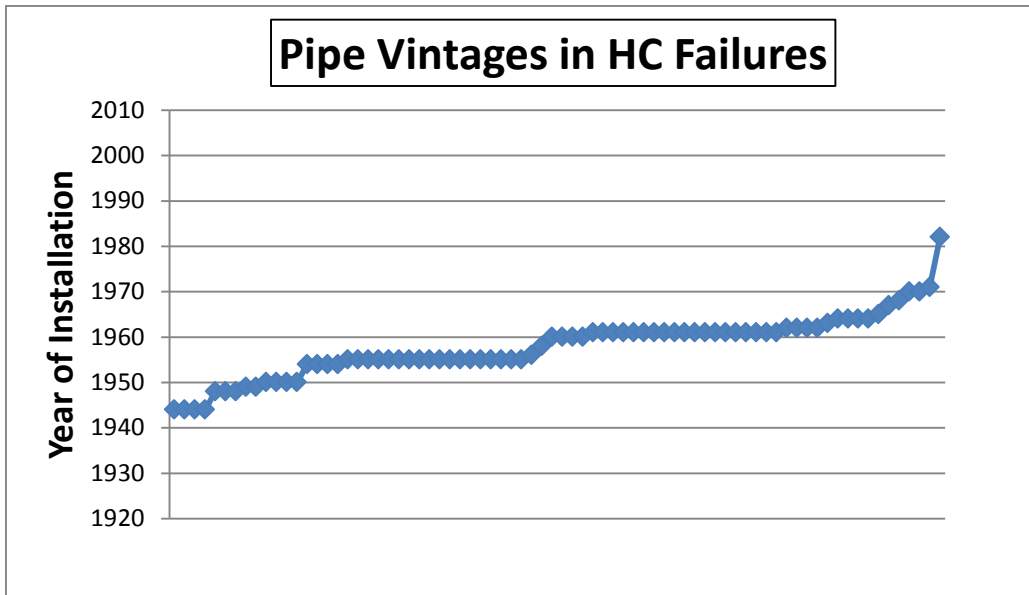


Figure 105. Pipe Vintages in Failures of Hook Cracks

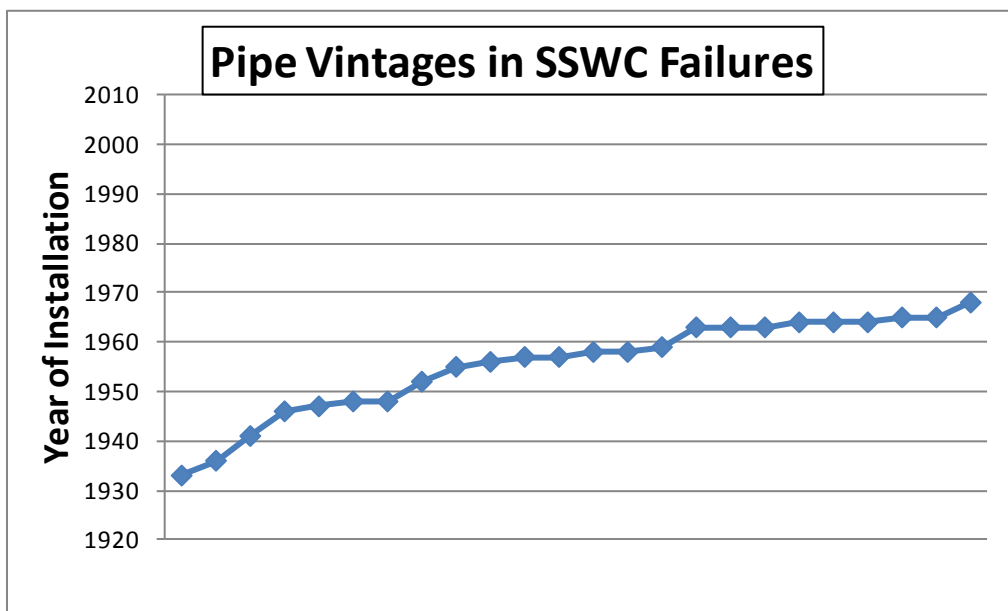


Figure 106. Pipe Vintages in Failures of Selective Seam Weld Corrosion

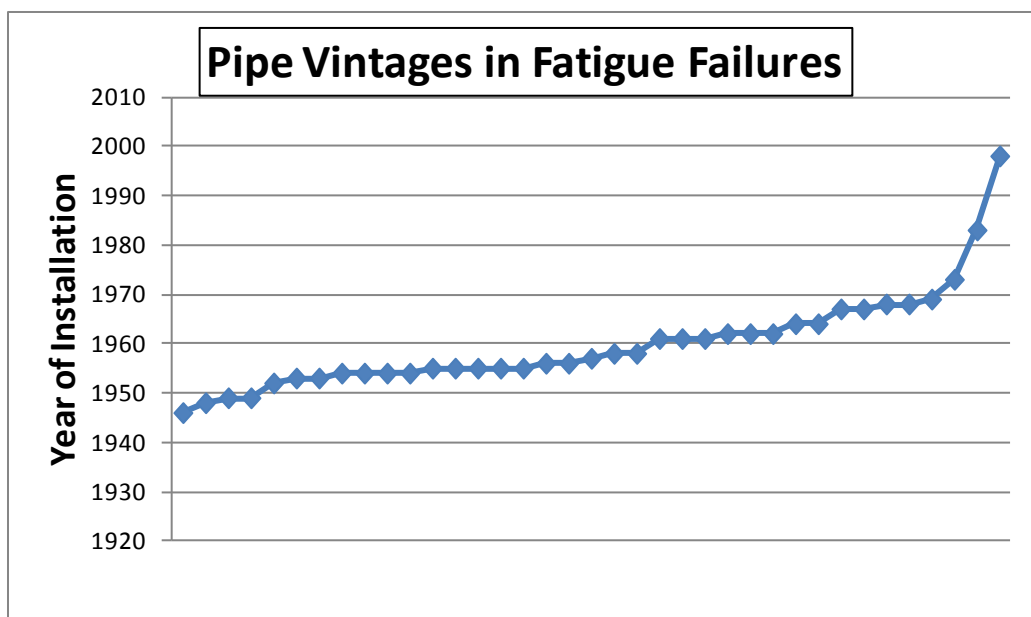


Figure 107. Pipe Vintages in Fatigue Failures

The year 1970 is seen to be significant. Only 6 of 96 cold weld failures occurred in pipe manufactured after 1970. Only two hook crack failures out of 77 occurred in pipe manufactured after 1970. None of the 24 selective seam weld failures occurred in pipe manufactured after 1970, and only 3 of 37 fatigue failures occurred in pipe manufactured after 1970. While it is true that somewhere around 80 percent of the pipelines in the U.S. were installed prior to 1970, the track record of failures involving pipe of pre-1970 vintage is clearly not as good as that of pipe manufactured after 1970. The reasons for the improved track record of pipe manufactured after 1970 are many.

Between 1960 and 1970 all of the major ERW pipe manufacturers switched from low-frequency seam welding to high-frequency seam welding. Flash-welding of seams was terminated in 1968. As has been noted, the fracture resistance of high-frequency-welded seams is superior to that of low-frequency-welded seams because high-frequency welding is not accompanied by the grain-coarsening that facilitates brittle fracture in the bondline regions of low-frequency-welded seams.

In 1962, the use of non-destructive inspection of seams by ultrasonic or electromagnetic means was made mandatory in API Specification 5LX. Undoubtedly, this led to the rejection of many more anomalies than would have been found during the mill hydrostatic tests alone.

The advent of U.S. federal pipeline safety regulations in 1970 resulted in the requirement that most pipelines installed after 1970 be subjected to a pre-service hydrostatic test to a minimum

pressure level of 1.25 times their maximum operating pressure⁴. Pre-service tests to this level tended to screen out additional anomalies that were not eliminated by the mill hydrostatic tests. The federal regulations also made mandatory the use of external coating and cathodic protection to mitigate the threat of external corrosion.

These findings do not mean that seam integrity is not an issue for ERW pipe made after 1970, but they certainly indicate that the focus should be on pre-1970 pipe in order to gain significant improvements in seam integrity.

⁴ The federal regulations still permit the gas testing of natural gas pipelines to a level of 1.1 times their maximum operating pressure. However, it is believed that this exception to the 1.25-times-MAOP requirement is seldom utilized anymore.

REFERENCES

¹ Kiefner, J. F., Maxey, W. A., Eiber, R. J., and Duffy, A. R., “Failure Stress Levels of Flaws in Pressurized Cylinders”, *Progress in Flaw Growth and Fracture Toughness Testing*, ASTM STP 536, American Society for Testing and Materials, pp. 461-481 (1973).

² Groeneveld, T. P. and Fessler, R. R., “Hydrogen Stress Cracking Overview and Controls”, *6th Symposium on Line Pipe Research*, American Gas Association, Catalog No. L30175 (1979).

³ Fessler, Raymond R., and Rapp, Steve, “*Method for Establishing Hydrostatic Re-Test Intervals for Pipelines with Stress-Corrosion Cracking*”, Paper No. IPC2006-10163, Proceedings of IPC 2006, 6th International Pipeline Conference, September 25-29, 2006, Calgary, Alberta, Canada

⁴ Sen, Millan, and Kariyawasam, Shahani, “*Analytical Approach to Determine Hydrotect Intervals*”, Paper No. IPC2008-64537, Proceedings of the 7th International Pipeline Conference, IPC08, September 29 – October 3, 2008, Calgary, Alberta, Canada

⁵ Paris, P.C., and Erdogan, F., “*A Critical Analysis of Crack Propagation Laws*”, Transactions of ASME, Journal of Basis Engineering, Series D, Volume 85, No. 5, (1963) pp 405-09

⁶ Bruno, T. V., “SSC Resistance of Pipeline Welds”, NACE Task Group T-IF-23, *Materials Performance* (January 1993).